

1997

Azo Dyes Based on 1,10-Phenanthroline

Minchong Mao

Eastern Illinois University

This research is a product of the graduate program in [Chemistry](#) at Eastern Illinois University. [Find out more](#) about the program.

Recommended Citation

Mao, Minchong, "Azo Dyes Based on 1,10-Phenanthroline" (1997). *Masters Theses*. 1814.
<https://thekeep.eiu.edu/theses/1814>

This is brought to you for free and open access by the Student Theses & Publications at The Keep. It has been accepted for inclusion in Masters Theses by an authorized administrator of The Keep. For more information, please contact tabruns@eiu.edu.

THESIS REPRODUCTION CERTIFICATE

TO: Graduate Degree Candidates (who have written formal theses)

SUBJECT: Permission to Reproduce Theses

The University Library is receiving a number of requests from other institutions asking permission to reproduce dissertations for inclusion in their library holdings. Although no copyright laws are involved, we feel that professional courtesy demands that permission be obtained from the author before we allow theses to be copied.

PLEASE SIGN ONE OF THE FOLLOWING STATEMENTS:

Booth Library of Eastern Illinois University has my permission to lend my thesis to a reputable college or university for the purpose of copying it for inclusion in that institution's library or research holdings.

[Redacted Signature]

Author

[Redacted Signature]

Date

I respectfully request Booth Library of Eastern Illinois University not allow my thesis to be reproduced because:

Author

Date

Azo Dyes Based on 1,10-Phenanthroline

(TITLE)

BY

Minchong Mao

THESIS

SUBMITTED IN PARTIAL FULFILLMENT OF THE REQUIREMENTS
FOR THE DEGREE OF

Master of Science in Chemistry

IN THE GRADUATE SCHOOL, EASTERN ILLINOIS UNIVERSITY
CHARLESTON, ILLINOIS

1997

YEAR

I HEREBY RECOMMEND THIS THESIS BE ACCEPTED AS FULFILLING
THIS PART OF THE GRADUATE DEGREE CITED ABOVE



Azo Dyes Based on 1,10-Phenanthroline

Approved by Thesis Committee:



Dr. Mark E. McGuire



Date



Dr. Ellen A. Keiter



Date




Dr. Richard L. Keiter



Date



Dr. Jerry W. Ellis



Abstract

Title of Thesis: Azo Dyes Based on 1,10-Phenanthroline.

Name: Minchong Mao

Thesis directed by: Dr. Mark E. McGuire

A series of new phenanthroline based azo-dye ligands, produced by diazotizing 5-amino-1,10-phenanthroline (5-NH₂-phen) and then coupling this intermediate to a variety of coupling components, has been synthesized and characterized. The coupling components used were β -naphthol, phenol, and 2,6-dimethylphenol, and the three dye ligands were named phen-azo- β -naphthol, phen-azo-p-phenol, and phen-azo-2,6-dimethylphenol, respectively. ¹H-NMR and IR spectra showed that the dyes exist primarily in the azo form in DMSO solution and as solids. UV-Vis spectra (in MeOH) showed intense ($\epsilon \cong 10^4 \text{ M}^{-1} \text{ cm}^{-1}$) absorptions ranging from 380 nm to 500 nm for these ligands.

The ligand phen-azo-p-phenol has been coordinated to a Re(I) metal center through the phenanthroline linkage to form a stable polypyridyl complex, *fac*-Re^I(CO)₃(phen-azo-p-phenol)Cl. When compared to the well-known complex *fac*-Re^I(CO)₃(phen)Cl, the new Re(I)-dye complex shows a greatly enhanced visible absorption band in the 370 - 400 nm range. This absorption is primarily due to a ligand-centered transition in the coordinated phen-dye ligand. Preliminary emission spectra (in MeOH) reveal that *fac*-Re^I(CO)₃(phen-azo-p-phenol)Cl, unlike its Re(I)-phen analog, does not emit.

Acknowledgments

I would like to express my sincere and deep appreciation to Dr. Mark E. McGuire, my research advisor, for his knowledgeable guidance, great patience, and kind encouragement.

I wish to thank Dr. Ellen A. Keiter for her help in instruction of operating the QE-300 NMR spectrometer.

Also, I would like to thank the faculty and staff of the Chemistry Department and the other members of our research group for their assistance.

Table of Contents

Abstract	i
Acknowledgments	ii
Table of Contents	iii
List of Tables	v
List of Figures	vi

Chapter	page
1. Introduction	1
2. Experimental	
Materials	14
Synthesis	14
Methods	23
3. Results and Discussion	
Synthesis and Purification of Phenanthroline-Based Dyes	24
(1) A possible self-coupling reaction of 5-NH ₂ -phen	24
(2) Coupling temperature and pH value	26
(3) Starting materials / chromatographic materials	28
(4) Elemental analysis	28
¹ H-NMR Spectra	29
(1) Starting materials	29
(2) Phen-azo-β-naphthol	29
(3) Phen-azo-p-phenol	32
(4) Phen-azo-2,6-dimethylphenol	33
(5) Re(I) complexes	34

Table of Contents (contd)

IR Spectra	35
(1) Phen-dye ligands	35
(2) Re(I) complexes	36
 UV-Vis Spectra	 37
(1) Phen-dye ligands	37
(2) Re(I) complexes	39
 Summary	 42
 4. References	 98

List of Tables

Table	page
3-1	$^1\text{H-NMR}$ for 5- NO_2 -phen, phen, and 5- NH_2 -phen 43
3-2	$^1\text{H-NMR}$ for 2,3,4,5,6-d phenyl-azo- β -naphthol and phenyl-azo- β -naphthol 44
3-3	$^1\text{H-NMR}$ for phen-azo- β -naphthol and related compounds 45
3-4	$^1\text{H-NMR}$ for phen-azo-p-phenol and related compounds 46
3-5	$^1\text{H-NMR}$ for phen-azo-2,6-dimethylphenol and related compounds 47
3-6	$^1\text{H-NMR}$ for $\text{Re}^{\text{I}}(\text{CO})_3(\text{phen})\text{Cl}$, $\text{Re}^{\text{I}}(\text{CO})_3(\text{phen-azo-p-phenol})\text{Cl}$ and related compounds 48
3-7	Carbonyl Stretching Frequencies in IR spectra 49
3-8	UV-Vis data for phen-azo dye ligands and related compounds 50

List of Figures

Figures	page
1-1	bpy and phen 1
1-2	Relative disposition of metal and ligand orbitals and possible electronic transitions in an octahedral ligand field of a transition metal complex 2
1-3	Schematic representation of various orbital disposition in strong-field (nd^6) complexes $[M(LL)_3]^{n+}$; LL = bpy 4
1-4	Overall process of an individual molecule capturing a photon of sunlight. 5
1-5	Examples of multidentate polypyridyl ligands used in the synthesis of multimetallic polypyridyl complexes 6
1-6	Molecular orbital diagram for monometallic and bimetallic Ru(II) complexes 6
1-7	Synthesis of phen-azo-dyes 9
1-8	Preparation of 5-NH ₂ -Phen 10
1-9	Mechanism of Diazotization 11
1-10	Mechanism of coupling reaction 12
1-11	Synthesis of Re(I) complexes containing phen and phen-azo phenol 13
3-1	Self coupling reaction of amine 24
3-2	The structure of phen-azo-phen 25
3-3	The decomposition of diazonium ions 27
3-4 a	Model reaction using 2,3,4,5,6-d-aniline as starting material 30
3-4 b	Model reaction using aniline as starting material 30
3-5	The tautomerization and intramolecular hydrogen bond of phen-azo-2-naphthol 32
3-6	The structure of <i>trans</i> -azobenzene 38
3-7	¹ H-NMR spectrum of 5-NH ₂ phen 52
3-8	¹ H-NMR spectrum of 5-NO ₂ phen 53
3-9	¹ H-NMR spectrum of phen 54

3-10 a	¹ H-NMR spectrum of phenyl-azo-β-naphthol (16.0-6.5 ppm) (product of model reaction)	55
3-10 b	¹ H-NMR spectrum of phenyl-azo-β-naphthol (9.0-6.5 ppm) (product of model reaction)	56
3-11 a	¹ H-NMR spectrum of phenyl-azo-β-naphthol (16.0-6.5 ppm) (97%, from Aldrich)	57
3-11 b	¹ H-NMR spectrum of phenyl-azo-β-naphthol (9.0-6.5 ppm) (97%, from Aldrich)	58
3-12 a	¹ H-NMR spectrum of 2,3,4,5,6-d-phenyl-azo-β-naphthol (16.0-6.5 ppm)	59
3-12 b	¹ H-NMR spectrum of 2,3,4,5,6-d-phenyl-azo-β-naphthol (9.0-6.5 ppm)	60
3-13 a	¹ H-NMR spectrum of phen-azo-β-naphthol (17.3 - 6.5 ppm)	61
3-13 b	¹ H-NMR spectrum of phen-azo-β-naphthol (10.0 - 6.5 ppm)	62
3-14	¹ H-NMR spectrum of β-naphthol	63
3-15	¹ H-NMR spectrum of phen-azo-p-phenol	64
3-16	¹ H-NMR spectrum of phenol	65
3-17 a	¹ H-NMR spectrum of phen-azo-2,6-dimethylphenol (in DMSO) (10.0 - 0.5 ppm)	66
3-17 b	¹ H-NMR spectrum of phen-azo-2,6-dimethylphenol (in DMSO) (10.0 - 7.0 ppm)	67
3-18 a	¹ H-NMR spectrum of phen-azo-2,6-dimethylphenol (in CDCl ₃) (10.0 - 2.0 ppm)	68
3-18 b	¹ H-NMR spectrum of phen-azo-2,6-dimethylphenol (in CDCl ₃) (9.5 - 5.0 ppm)	69
3-19 a	¹ H-NMR spectrum of 2,6-dimethylphenol (in DMSO) (9 - -0.5 ppm)	70
3-19 b	¹ H-NMR spectrum of 2,6-dimethylphenol (in DMSO) (8.5 - 6.0 ppm)	71
3-20 a	¹ H-NMR spectrum of 2,6-dimethylphenol (in CDCl ₃) (9 - -0.5 ppm)	72
3-20 b	¹ H-NMR spectrum of 2,6-dimethylphenol (in CDCl ₃) (7.5 - 4.0 ppm)	73
3-21	¹ H-NMR spectrum of phen-azo-phen	74
3-22	¹ H-NMR spectrum of <i>fac</i> -Re ^I (CO) ₃ (phen)Cl	75

3-23	$^1\text{H-NMR}$ spectrum of <i>fac</i> - $\text{Re}^{\text{I}}(\text{CO})_3(\text{phen-azo-p-phenol})\text{Cl}$	76
3-24	IR spectrum of phen-azo- β -naphthol	77
3-25	IR spectrum of phen-azo-p-phenol	78
3-26	IR spectrum of phen-azo-2,6-dimethylphenol	79
3-27	IR spectrum of phen-azo-phen	80
3-28	IR spectrum of <i>fac</i> - $\text{Re}^{\text{I}}(\text{CO})_3(\text{phen})\text{Cl}$	81
3-29	IR spectrum of <i>fac</i> - $\text{Re}^{\text{I}}(\text{CO})_3(\text{phen-azo-p-phenol})\text{Cl}$	82
3-30	UV-Vis spectrum of 5- NH_2 -phen	83
3-31	UV-Vis spectrum of phen	84
3-32	UV-Vis spectrum of phen-azo- β -naphthol	85
3-33	Beer-Lambert plot of phen-azo- β -naphthol	86
3-34	UV-Vis spectrum of β -naphthol	87
3-35	UV-Vis spectrum of phen-azo-p-phenol	88
3-36	Beer-Lambert plot of phen-azo-p-phenol	89
3-37	UV-Vis spectrum of phenol	90
3-38	UV-Vis spectrum of phen-azo-2,6-dimethylphenol	91
3-39	Beer-Lambert plot of phen-azo-2,6-dimethylphenol	92
3-40	UV-Vis spectrum of 2,6-dimethylphenol	93
3-41	UV-Vis spectrum of <i>fac</i> - $\text{Re}^{\text{I}}(\text{CO})_3(\text{phen})\text{Cl}$	94
3-42	UV-Vis spectrum of <i>fac</i> - $\text{Re}^{\text{I}}(\text{CO})_3(\text{phen-azo-p-phenol})\text{Cl}$	95
3-43	Emission Spectrum of <i>fac</i> - $\text{Re}^{\text{I}}(\text{CO})_3(\text{phen})\text{Cl}$ ($\lambda_{\text{excit}} = 365 \text{ nm}$)	96
3-44	Emission Spectrum of <i>fac</i> - $\text{Re}^{\text{I}}(\text{CO})_3(\text{phen-azo-p-phenol})\text{Cl}$ ($\lambda_{\text{excit}} = 389 \text{ nm}$) ..	97

Chapter 1: Introduction

Polypyridyl transition metal complexes, especially those including d^6 and d^3 metal ions (e.g. Ru(II), Os(II), Re(I), Cr(III), Ir(III)), have been extensively studied by inorganic and physical chemists over the past two decades. Interest in the photochemistry of polypyridyl metal complexes can be traced to their potential practical applications in areas such as solar energy conversion.¹⁻⁴ For example, the electronic excited states of $[\text{Ru}^{\text{II}}(\text{bpy})_3]^{2+}$ and $[\text{Ru}^{\text{II}}(\text{phen})_3]^{2+}$ (bpy = 2, 2'-bipyridine; phen = 1,10-phenanthroline, see Fig. 1-1) can participate in redox processes in fluid solution.^{5,6} It was also discovered that both $[\text{Ru}^{\text{II}}(\text{bpy})_3]^{2+}$ and $[\text{Ru}^{\text{II}}(\text{phen})_3]^{2+}$ could function as photocatalysts for the decomposition of water into hydrogen and oxygen.⁷ Systems based on $[\text{Ru}^{\text{II}}(\text{bpy})_3]^{2+}$ and $[\text{Re}^{\text{I}}(\text{CO})_3(\text{LL})\text{X}]$ (LL = polypyridyl ligand) have been used as sensitizers and redox catalysts in the reduction of CO_2 to CO.^{8,9} Moreover, the applications of polypyridyl transition metal complexes can be extended to the design of molecular-level electronic devices¹⁰ and DNA probes.¹¹⁻¹³

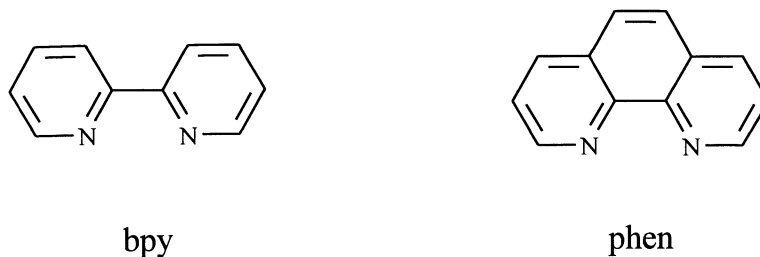


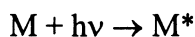
Fig. 1-1 bpy and phen

A common feature of polypyridine ligands such as bpy and phen is the presence of a vacant π^* orbital that can accept electron density from the metal ion to form a type of π bonding (π -back bonding) that supplements the σ bonding arising from the donation of lone pairs of electrons from the ligand (in this case from the N-atoms). The π -back bonding stabilizes the resulting metal complexes, especially those with metal ions in low

oxidation states. High electron density on the metal (of necessity in low oxidation states) can thus be delocalized onto the ligands.

A general framework to analyze the bonding interactions between the metal ion and the ligands during the formation of the metal complex is shown in Fig. 1-2. Conceptually, the metal orbital diagram is combined with the ligand orbital diagram to arrive at a composite model for the entire system.

Absorption of a photon of energy in the visible or ultraviolet (UV) region of the spectrum by a metal complex M leads to its transformation to an electronically excited state M*.



The types of electronic transitions have been classified as follows: ¹⁴

Charge transfer(CT) – these transitions may arise from promotion of an electron from a metal-based MO to a ligand-based MO (metal-to-ligand charge transfer; MLCT, labeled as ③) or vice versa (ligand-to-metal charge transfer; LMCT, labeled as ④).

Metal-centered (MC) – essentially metal-localized dd transitions (labeled as ①).

Ligand-centered (LC) – these arise from $(\pi-\pi^*)$ transitions involving ligand-localized orbitals (labeled as ②).

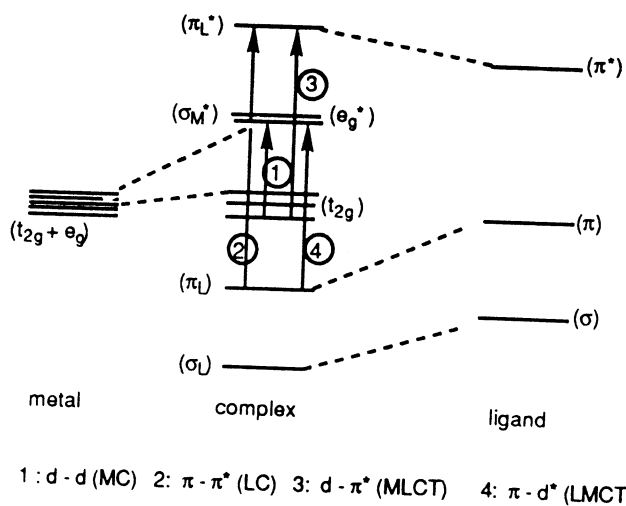
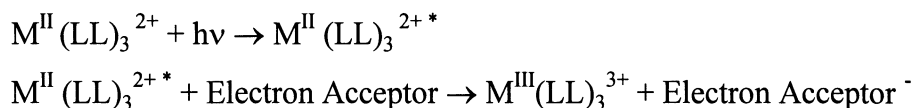


Fig. 1-2 Relative disposition of metal and ligand orbitals and possible electronic transitions in an octahedral ligand field of a transition metal complex (taken from ref. 14).

After initial electronic excitation, a complex in an upper excited state relaxes rapidly (in a few picoseconds or less) to the lowest energy excited state. Interesting electron or energy transfer processes typically occur from the lowest energy excited states in polypyridyl transition metal complexes.¹⁴ For example:



The identities of the lowest energy excited states in polypyridyl transition metal complexes can often be identified from an examination of their electronic absorption and electronic emission spectra. For the emission measurements it has been found that:¹⁴

1. Emission from MLCT transitions is usually intense and highly structured. It can be observed at both room temperature and 77 K. Lifetimes are typically 10-1000 ns at room temperature and 1-10 μ s at 77 K.
2. Emission from LC transitions can seldom be observed in fluid solutions at room temperature. Emission at 77 K usually occurs at energies close (within $\sim 1000 \text{ cm}^{-1}$) to that observed for the free ligand. In addition, the lifetimes are fairly long (ms range). The band shapes can be similar in appearance to MLCT bands.
3. Emission from MC transitions is broad and structureless and is usually relatively solvent independent. Emission at room temperature is rarely observed. Lifetimes at 77 K typically range from 10 to 500 μ s.

The nature of the lowest energy excited state can be altered through appropriate synthetic modifications (variation of metal and/or ligands). This is because the extent of crystal field splitting along with the relative disposition of the metal d orbitals with respect to ligand π orbitals vary with the nature of the metal ion and the ligands, leading to complexes having different types of lowest energy excited states and photochemical reactivity. Fig. 1-3 shows schematically the orbital disposition for a series of transition metal tris (bipyridine) complexes. The lowest energy excited state of $[Fe^{II}(bpy)_3]^{2+}$ is

assigned as metal-centered (MC), those of Ru(II) and Os(II) as metal-to-ligand charge transfer (MLCT) and those of Rh(III) and Ir(III) as ligand centered (LC).¹⁴ For the first row transition metal ion Fe²⁺, the ligand field splitting Δ is small, so the MC transitions are of relatively low energy. For Ru(II) and Os(II) complexes, the ligand field splitting Δ is larger, and the LUMO (lowest unoccupied molecular orbital) is a bpy π^* orbital. Therefore, the lowest energy excited states are MLCT for [Ru^{II}(bpy)₃]²⁺ and [Os^{II}(bpy)₃]²⁺. For metal ions such as Rh(III) and Ir(III), the crystal field is so large that the HOMO and LUMO orbitals are bpy π and π^* , respectively. Therefore, the lowest energy excited state is LC. Moreover, Balzani et al^{15,16} showed that for another series of complexes [Ru^{II}(i-biq)₂(LL)]²⁺ (i-biq = isobiquinoline), the lowest energy excited state is LC when LL = i-biq, and MLCT when LL = bpy.

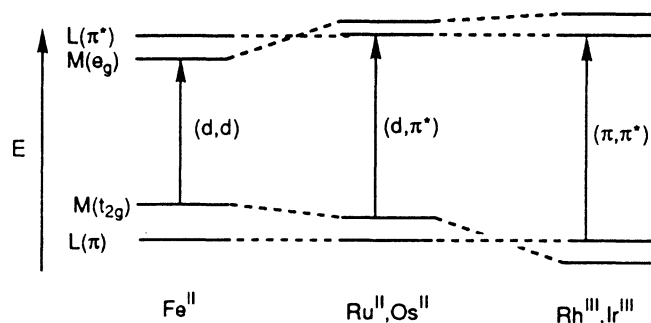


Fig. 1-3 Schematic representation of various orbital disposition in strong-field (nd^6) complexes $[M(LL)_3]^{n+}$; LL = bpy (taken from ref. 14).

Chemical solar energy conversion schemes depend on the synthesis of particular compounds that strongly absorb visible light. Figure 1-4 represents the overall process of an individual molecule capturing a photon of sunlight.

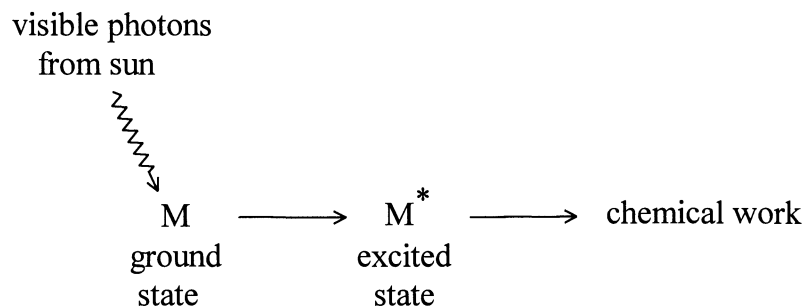


Fig. 1-4 Overall process of an individual molecule capturing a photon of sunlight.

The design and synthesis of molecules (M) that strongly absorb sunlight over a broad spectrum of wavelengths would increase the probability of successfully harnessing the sun's energy. Three ways to approach this problem are:

1. *Construction of multimetallic complexes using bridging ligands that allow for significant metal-metal interactions.* Ligands such as 2,2'-bipyrimidine (bpym) and 2,3-bis(2-pyridyl)pyrazine (dpp) serve as templates for building multimetallic complexes. The structures of some of the bridging polypyridyl ligands commonly used for the synthesis of multimetallic complexes are shown in Fig. 1-5.

Multimetallic systems often show CT transitions well into the visible spectrum.¹⁷ For example, the electronic spectroscopy of the monometallic complex $[(\text{NH}_3)_4\text{Ru}^{\text{II}}(\text{bpym})]^{2+}$ shows an intense MLCT band in the visible region centered at 402 nm while the bimetallic complex $[(\text{NH}_3)_4\text{Ru}^{\text{II}}]_2(\text{bpym})^{4+}$ has intense MLCT absorption bands at 424 and 697 nm.^{18a} The bimetallic absorption maxima for $[(\text{NH}_3)_4\text{Ru}^{\text{II}}]_2(\text{bpym})^{4+}$ are at lower energy than the $[(\text{NH}_3)_4\text{Ru}^{\text{II}}(\text{bpym})]^{2+}$ monometallic absorption maxima. The reason for this shift is that coupling of two Ru(II) orbitals with the ligand π^* LUMO orbital creates a set of bonding (ψ_b), nonbonding (ψ_n) and antibonding (ψ_a) orbitals. (Fig. 1-6) The presence of the nonbonding (ψ_n) HOMO in the bimetallic complexes gives rise to a lower energy transition than in the corresponding monometallic complex. A similar trend for a series of Ru(II) polypyridyl complexes was demonstrated by Rillema.^{18b} Specifically, for series of monometallic, bimetallic, trimetallic, and tetrametallic complexes, there was increasing absorption out in the red portion of the spectrum.

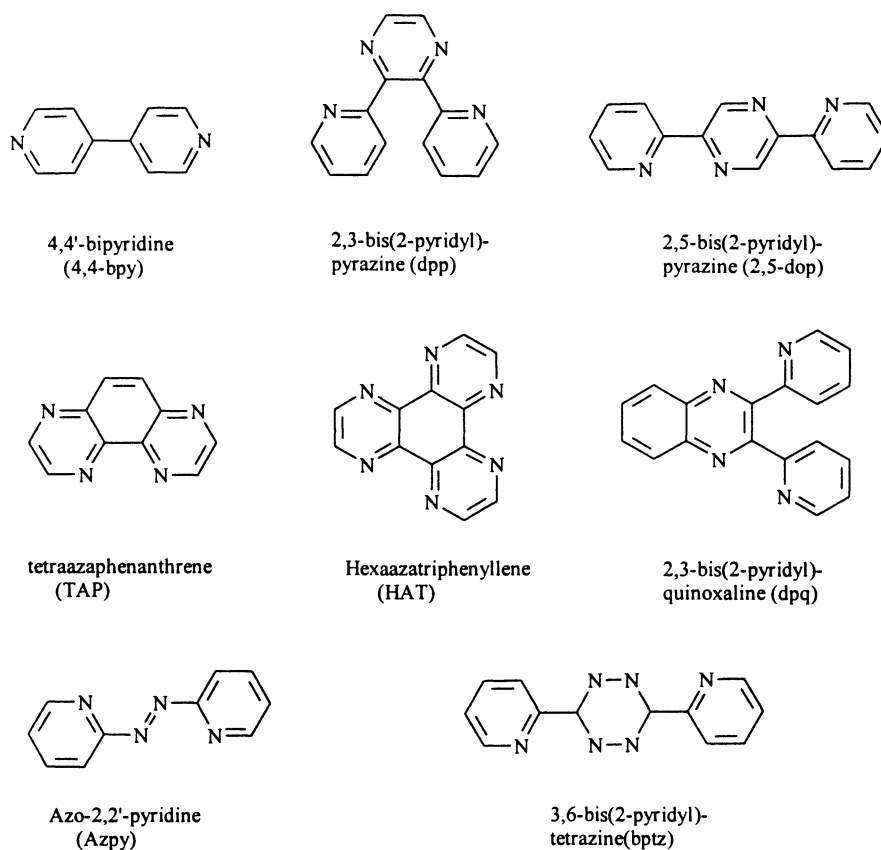


Fig. 1-5 Examples of multidentate polypyridyl ligands used in the synthesis of multimetallic polypyridyl complexes (taken from ref. 14).

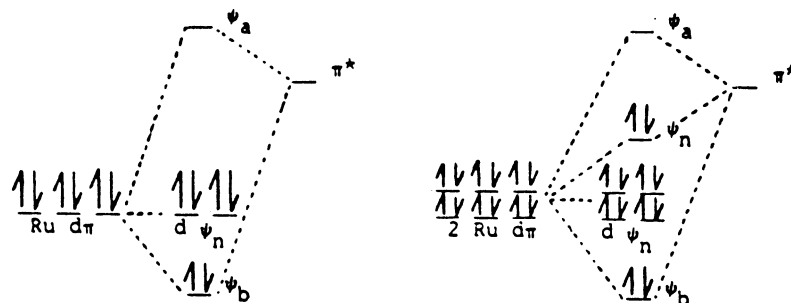


Fig. 1-6 Molecular orbital diagram for monometallic and bimetallic Ru(II) complexes (taken from ref. 18a).

2. *Attachment of several different ligands on the same metal center.* Attempts have been made to make use of substituent effects and extensions of the ligand π system.^{19,20} For example, tris(heteroleptic) complexes which contain three different bidentate ligands (e.g. $[\text{Ru}^{\text{II}}(\text{bpy})(\text{Me}_2\text{bpy})\{(\text{EtCO}_2)_2\text{bpy}\}]^{2+}$ (bpy is 2,2'-bipyridine, Me_2bpy is 4,4'-dimethyl-2,2'-bipyridine, and $(\text{EtCO}_2)_2\text{bpy}$ is 4,4'-bis(carboxyethyl)-2,2'-bipyridine)) show enhanced MLCT absorptions throughout the UV and visible spectral region (200-700 nm), which are sufficiently long-lived to undergo efficient electron and energy transfer.

3. *Utilization of ligands that strongly absorb in the visible region.*

The work described in this thesis focuses on this third approach. This approach involves the synthesis of three highly-colored phenanthroline-based azo dyes (phen-azo-dyes). Azo dyes are compounds containing azo groups ($\text{—N}=\text{N—}$) which are linked to sp^2 -hybridized carbon atoms. Azo dyes represent the largest group of colorants used as dyes and pigments. They are usually synthesized by diazotization of aromatic amines followed by azo coupling at higher pH with coupling components. The use of various aromatic and heterocyclic amines and variation in the coupling components provide a rich array of azo dyes and absorption properties. Phen-azo dye ligands in polypyridyl transition metal complexes might offer the following advantages:

1. *More efficient use of visible light for population of low lying excited states.*

As previously stated, important photophysical and photochemical processes occur from the lowest energy excited states of polypyridyl transition metal complexes. Absorption of photons of higher energies typically results in rapid internal decays to the lowest energy excited state. Since most phen and bpy derivatives do not absorb strongly at $\lambda > 400 \text{ nm}^{21-23}$, the presence of phen-azo dye ligands might provide “antennas” for collection of visible photons. The idea is to absorb visible light photons at a highly absorbing but unreactive phen-

azo dye ligands (“antenna fragment”), and then transfer the energy to the lowest energy excited state of the complex.

2. *Increased flexibility in “tuning” the nature of lowest energy excited states.*

For example, Re(I) complexes with the general formula $\text{Re}^{\text{I}}(\text{CO})_3\text{Cl}(\text{LL})$ (LL = bpy, phen or derivatives) typically show strong MLCT - based emission in the 550 nm to 650 nm range.^{24,25} Appropriate choice of LL (e.g. phen-azo dye ligand; $\lambda_{\text{em}} \sim 600$ nm) would lead to a complex where the LC and MLCT transitions were very close in energy. The lowest energy excited states for these complexes would thus be MLCT, LC, or a mixture of the two depending on subtle variations in LL, temperature, or medium.

The first part of this thesis describes the synthesis and characterization of three phenanthroline-based azo dye ligands: phen-azo- β -naphthol, phen-azo-p-phenol and phen-azo-2,6-dimethylphenol. These syntheses were carried out by diazotizing 5-amino-1,10-phenanthroline (5-NH₂-phen) and then coupling this intermediate to a variety of coupling components (Fig. 1-7). Coordination of transition metals through the 1,10-phen N-atoms of the phen-azo dye ligands should produce complexes that are expected to retain the stability and redox properties of traditional polypyridyl complexes while possessing enhanced abilities to absorb visible light due to the presence of the dye moieties.

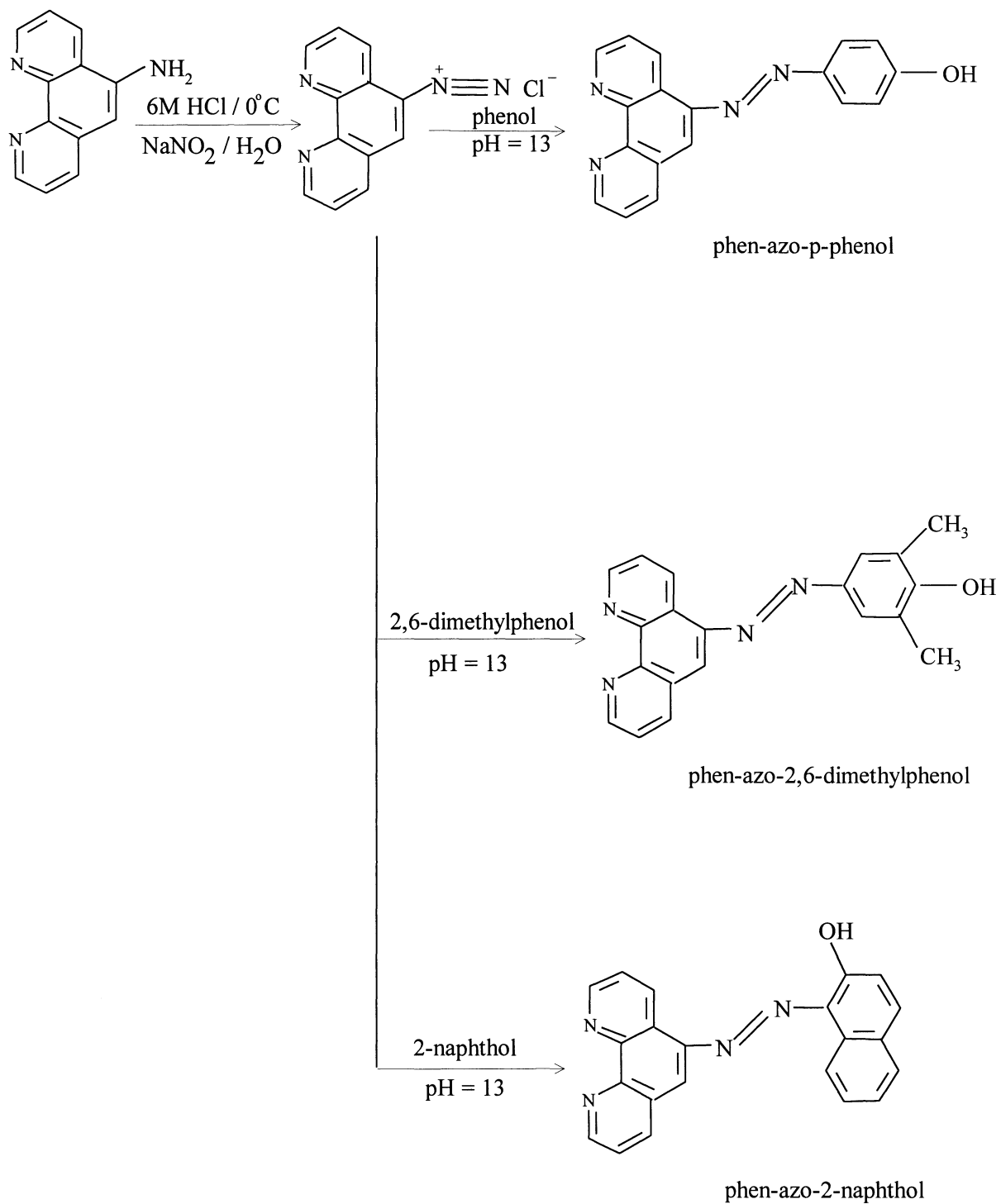


Fig. 1-7 Synthesis of phen-azo-dyes.

The 5-NH₂-phen starting material can be produced (~90% yield) by reduction of 5-NO₂-1,10-phenanthroline with hydrazine in absolute ethanol (Pd/C catalyst) using a procedure similar to that outlined by Nasielski–Hinkens et al.²⁶ (Fig. 1-8)

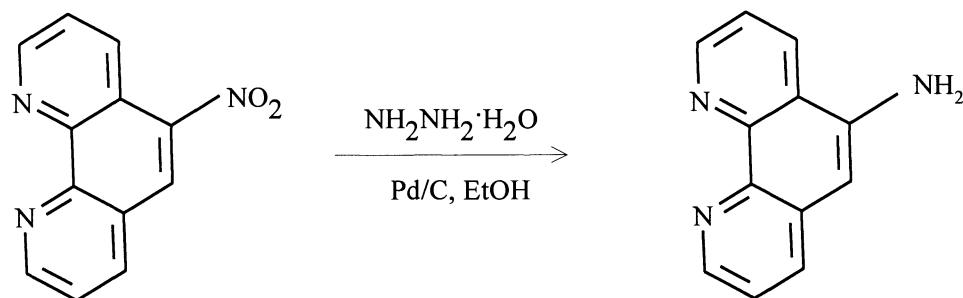


Fig. 1-8 Preparation of 5-NH₂-Phen.

The synthesis of phenanthroline-based azo dyes is a two-step process. The first step is the diazotization of 5-NH₂-phen. In this step, an aqueous solution of 5-NH₂-phen is converted into the diazonium ion at a temperature of about 0° C by the action of sodium nitrite in the presence of HCl. The mechanism of this reaction is outlined in Fig. 1-9.^{27, 28} Under very acidic conditions, the amine group is protonated, and the ammonium ion Ar-N⁺H₃ is attacked by the nitrosating reagent. The nitrosamine is quickly transformed into the diazonium ion via the diazo hydroxide.

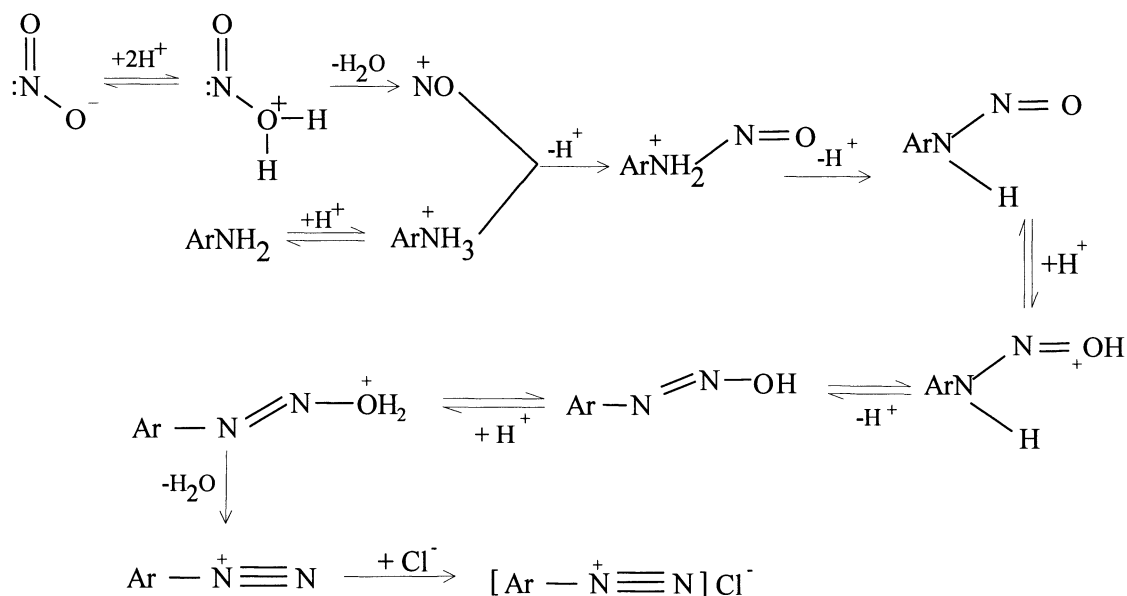


Fig. 1-9 Mechanism of Diazotization (taken from ref. 28).

The second step is the azo coupling reaction. The diazonium ion formed during diazotization can react with a variety of "coupling components" in a subsequent electrophilic aromatic substitution of a nucleophilic substrate in the so-called "azo coupling" reactions. As diazonium ions are relatively weak electrophilic reagents, only aromatic compounds that carry electron donor substituents (-OH, -NH₂, -NHR, etc.) can normally be used as coupling compounds. The reactions follow an S_E2 mechanism in which in a first step the electrophilic reagent forms a covalent bond to the carbon at the reacting site of the coupling component. The intermediate formed is called a σ-complex because of the covalent σ bond between the reaction partners. In a subsequent step, the proton is transferred to a proton acceptor (i.e. a base). Fig. 1-10 outlines the coupling reaction starting with an aromatic diazonium ion and using 2-naphtholate anion as the coupling component. Phenol and 2,6-dimethylphenol were also used as coupling reagents, and synthesis of the corresponding azo dyes was successful. (Fig. 1-7)

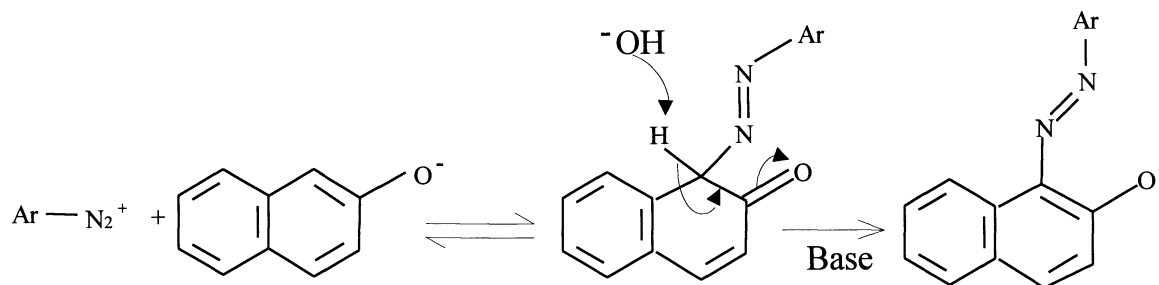


Fig. 1-10 Mechanism of coupling reaction (taken from ref. 28).

The second part of this thesis involves the synthesis and characterization of a d^6 metal complex of one of the phen-azo-dye ligands (phen-azo-p-phenol). A phenol derivative was chosen over the naphthol derivative to reduce the chance of the metal ion binding to a site other than the 1,10-phenanthroline portion of the ligand. (For example, the azo-ortho-hydroxy position of phen-azo- β -naphthol might offer a reasonable alternate binding site.)

The target metal complex was $fac\text{-Re}^I(\text{CO})_3$ (phen-azo-p-phenol) Cl. This was chosen for several reasons:

- 1) The complex $fac\text{-Re}^I(\text{CO})_3$ (phen) Cl is easily synthesized and well characterized in the literature,^{29,30} and can serve as a basis of comparison. For example, electrochemical and IR data could be used to verify coordination through the 1,10-phenanthroline linkage in $fac\text{-Re}^I(\text{CO})_3$ (phen-azo-p-phenol) Cl.
- 2) $fac\text{-Re}^I(\text{CO})_3(\text{LL})\text{Cl}$ complexes typically show MLCT absorptions in the 350-400 nm range, and emission in the 550-600 nm range. The emission is from an MLCT-based lowest energy excited state. When LL = phen-azo-p-phenol, absorption around 400 nm should be greatly enhanced. The lowest energy excited state, however, would still be expected to have MLCT character, and population of this state (and thus emission at 550-600 nm) might be significantly enhanced.

Fig. 1-10 outlines the proposed syntheses of both $fac\text{-Re}^I(\text{CO})_3$ (phen) Cl and $fac\text{-Re}^I(\text{CO})_3$ (phen-azo-p-phenol) Cl. The syntheses are based on literature precedents.^{29,30}

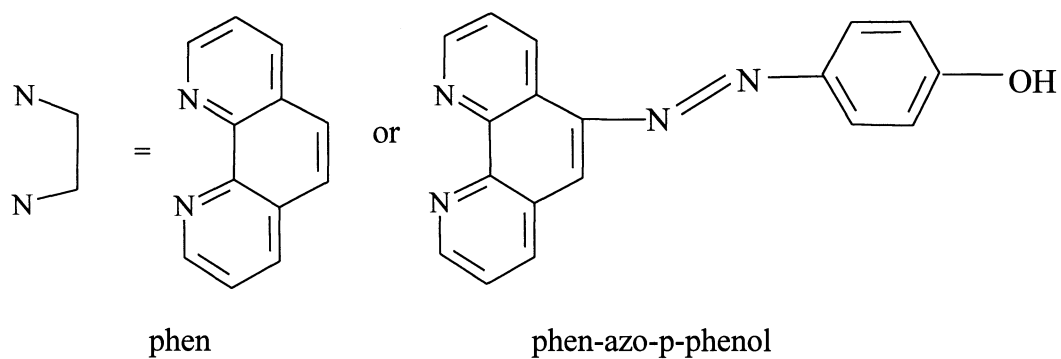
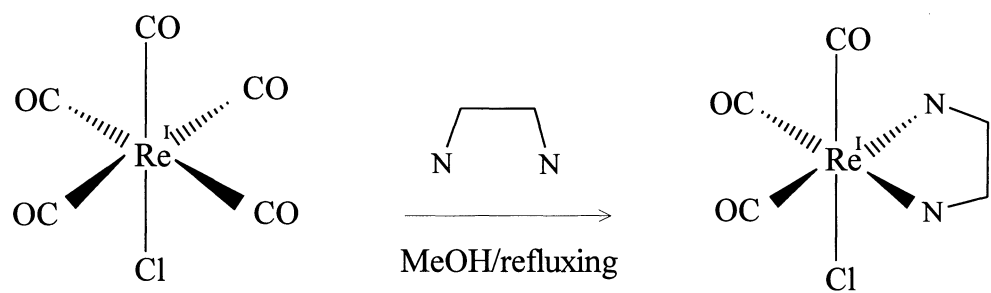


Fig. 1-11 Synthesis of Re(I) complexes containing phen and phen-azo-p-phenol.

Chapter 2: Experimental

Materials: 5-Nitro-1,10-phenanthroline (5-NO₂-phen) was available from previously studies⁴⁵ and used without further purification. Aniline, 2,3,4,5,6-d-aniline, 1,10-phenanthroline monohydrate, pentacarbonylchlororhenium(I) (Re^I(CO)₅Cl), phenol (C₆H₅OH, 99%), hydrazine monohydrate (N₂H₄·H₂O, 99%), 10% Pd/C, and sodium nitrite (NaNO₂) were purchased from Aldrich Chemical Co. and used without further purification. β-naphthol (99%) was purchased from Aldrich Chemical Co. and was either used as received or was recrystallized from 25:75 ethanol:H₂O and sublimed before use. 2,6-Dimethylphenol was purchased from Eastman Kodak Co. and used as received. Glacial acetic acid (99.7%) and diethyl ether (99.9%) were reagent grade and purchased from Fisher Chemical Co. and used as received. Acetone, chloroform, methanol, 2,2',4-trimethylpentane, and 95% ethanol were purchased from E.M. Science and used as received. Dichloromethane was purchased from Mallinckrodt and used as received. Absolute ethanol was purchased from Midwest Grain Products and used as received. Aluminum oxide (Brockman activity I, neutral, 150 mesh) was purchased from Aldrich Chemical Co. and used as received. Silica gel (60-200 mesh) was purchased from Fisher Chemical Co. and used as received. The deuterated solvents CDCl₃ (99.8 atom% D), D₂O (99.9 atom% D) and d₆-DMSO (99.9 atom% D) were purchased from Cambridge Isotope Laboratories and used as received. The trifluoroacetic acid-d (CF₃COOD, 99.5 atom% D) was purchased from Aldrich and used as received. All water used for reactions and solutions was purified from a Millipore “Milli-Q” water system fed by house deionized water.

Synthesis: 5-NH₂-1,10-phenanthroline (5-NH₂-phen): The starting material 5-NH₂-phen was prepared by reduction of 5-NO₂-1,10-phen with hydrazine in absolute ethanol (Pd/C catalyst) using a procedure similar to that outlined by Nasielski-Hinkens et al.²⁶ In a 500-mL 3-neck flask, 0.4004 g (1.778 mmol) of 5-NO₂-phen was added with stirring to 300 mL of absolute ethanol. The yellow 5-NO₂-phen dissolved to form a light yellow

solution, and then 0.3658 g of 10% Pd/C was added slowly with stirring, forming a black suspension. Meanwhile, a solution of 1.082 mL of $\text{N}_2\text{H}_4 \cdot \text{H}_2\text{O}$ in 30 mL of absolute ethanol was prepared in a separate 100-mL beaker. The N_2H_4 /ethanol solution was added to the 5- NO_2 -phen mixture drop by drop from a separatory funnel over a 1 h time period. The reaction mixture was heated to reflux for 2 h, and then it was cooled to room temperature in a water bath. The dark green-black mixture was filtered using Whatman #1 filter paper. The green-yellow filtrate was evaporated in the hood and the solid was vacuum dried for 3 h. Yield: 0.3089 g (89% based on 5- NO_2 -phen). Purity was checked by $^1\text{H-NMR}$.

Phenyl-azo-2-naphthol: This compound was synthesized using a method analogous to that described by Hart and Craine³¹ for the preparation of phenyl-azo-2-naphthol. In a typical preparation, 1.5 mL of H_2O and 2.0 mL of cooled 6 M HCl were added slowly with stirring and cooling to 0.500 mL (5.49 mmol) of aniline in a 25-mL beaker (kept at 0 °C in an ice bath). The light yellow aniline dissolved in the HCl to form a colorless solution. Stirring was continued for 3 min. Meanwhile, a solution of 0.25 g of NaNO_2 (3.6 mmol) in 2.5 mL of H_2O was prepared in a separate 6-dram vial and cooled to 0 °C in an ice bath. The NaNO_2 solution was added slowly to the aniline/HCl solution, and the color gradually turned to light yellow. No precipitate was formed in this step. Stirring and cooling were continued for another 3 min.

In a 40-mL beaker, 0.103 g (0.708 mmol) of β -naphthol was dissolved in 2 mL of 10% NaOH solution at room temperature. Water (5 mL) was added to the beaker, and then 2 mL of the diazotized aniline (1.688 mmol) mixture was transferred into the β -naphthol solution all at once with stirring. A dark orange precipitate formed immediately, and the stirring was continued for 2 min. The pH of the mixture was >13 at this time. The reaction mixture was then transferred to a 15-mL Buchner funnel containing a glass frit filter (F).^a The mixture filtered slowly. The dark orange solid in the frit was thoroughly washed with water and the filtrate was light orange. The solid

^a Glass frit properties: C - coarse M - medium F - fine

was dried under vacuum for 3 h. Yield of crude phenyl-azo-2-naphthol: 0.1678 g (95.4% based on β -naphthol). Purity was checked by $^1\text{H-NMR}$.

2,3,4,5,6-d₅-Phenyl-azo-2-naphthol: This compound was synthesized by using a method analogous to the preparation of phenyl-azo-2-naphthol. In a typical preparation, 0.5 mL of H₂O and 0.667 mL of cooled 6 M HCl were added slowly with stirring and cooling to 0.167 mL (1.832 mmol) of 2,3,4,5,6-d₅-aniline in a 25-mL beaker (kept at 0 °C in an ice bath). The light yellow 2,3,4,5,6-d₅-aniline dissolved in the HCl to form a colorless solution. Stirring was continued for 3 min. Meanwhile, a solution of 0.083 g of NaNO₂ (1.2 mmol) in 0.830 mL of H₂O was prepared in a separate 6-dram vial and cooled to 0 °C in an ice bath. The NaNO₂ solution was added slowly to the aniline/HCl solution, and the color gradually turned to light yellow. No precipitate was formed in this step. Stirring and cooling were continued for another 3 min.

In a 40-mL beaker, 0.103 g (0.708 mmol) of β -naphthol was dissolved in 2 mL of 10% NaOH solution at room temperature. Water (5 mL) was added to the beaker, and then 2 mL of the diazotized 2,3,4,5,6-d₅-aniline (1.688 mmol) mixture was transferred into the β -naphthol solution all at once with stirring. A dark orange precipitate formed immediately, and the stirring was continued for 2 min. The pH of the mixture was >13 at this time. The reaction mixture was then transferred to a 15-mL Buchner funnel containing a glass frit filter (F). The mixture filtered slowly. The dark orange solid in the frit was thoroughly washed with water and the filtrate was light orange. The solid was dried under vacuum for 3 h. Yield of crude 2,3,4,5,6-d₅-phenyl-azo-2-naphthol: 0.1778 g (99.1% based on β -naphthol). Purity was checked by $^1\text{H-NMR}$.

Phen-azo-2-naphthol: This compound was synthesized by using a method analogous to that used for the preparation of phenyl-azo-2-naphthol. In a typical preparation, 1.5 mL of cooled 6 M HCl was added slowly with stirring and cooling to 0.0610 g (0.3125 mmol) of 5-NH₂-phen in a 6-dram vial (kept at 0 °C in an ice bath). The yellow-green 5-NH₂-phen dissolved in the HCl to form a red solution. Stirring was continued for 3 min.

Meanwhile, a solution of 0.0220 g of NaNO_2 (0.3188 mmol) in 0.836 mL of H_2O was prepared in a separate 4-dram vial and cooled to 0 °C in an ice bath. The NaNO_2 solution was added all at once to the 5- NH_2 -phen/ HCl solution, and the color turned to dark orange. No precipitate was formed in this step. Stirring and cooling were continued for another 3 min.

In a 40-mL beaker, 0.0451 g (0.3125 mmol) of β -naphthol was dissolved in 4 mL of 10% NaOH solution at room temperature. Water (10 mL) was then added to the beaker. The diazotized phenathroline mixture was then transferred into the β -naphthol solution all at once with stirring. A dark red precipitate formed immediately, and the stirring was continued for 2 min. The pH of the mixture was >13 at this time. The reaction mixture was then transferred to a 15-mL Buchner funnel containing a glass frit filter (F). The mixture filtered very slowly. The dark red solid in the frit was thoroughly washed with water and the filtrate was dark red-purple. The solid was dried under vacuum for 3 h. The dried solid was rinsed with 25 mL of diethyl ether (to remove any remaining β -naphthol), the resulting suspension was filtered, and the solid was dried under vacuum for 3 h. Yield of crude phen-azo-2-naphthol: 0.0650 g (55.8% based on 5- NH_2 -phen).

The crude phen-azo-2-naphthol was purified by silica gel chromatography. A 20-mg sample of solid was dissolved in 1.5 mL of 85:15 acetic acid:methanol and loaded onto a silica gel column which was 20 cm long and 1.1 cm wide. The column was developed with 85:15 acetic acid:methanol with a flow rate of 20 drops/min. Over a 20-min time period, four different bands developed from bottom to top: light yellow, light pink, red and dark purple. Based on the results of TLC, the desired compound was thought to be the red fraction. About 30 mL of the red fraction was collected from the column, and this solution was filtered through a 30-mL F-frit to remove small silica particles. The solution was evaporated in the hood and the solid was vacuum dried at 100 °C for 5 h. Yield: 10 mg (28% based on 5- NH_2 -phen). Mp: 225-230 °C. Elemental analysis: Calcd for $\text{C}_{22}\text{H}_{14}\text{N}_4\text{O}\cdot\text{H}_2\text{O}\cdot 0.2\text{HC}_2\text{H}_3\text{O}_2$: %C 70.72, %H 4.45, %N 14.73. Found: %C 70.84, %H 4.13, %N 14.78.

Alumina chromatography was also employed to purify the crude phen-azo-2-naphthol. In this procedure, 20 mg of crude product was dissolved in 1.5 mL of 95% ethanol and loaded onto an alumina column which was 26 cm long and 1.1 cm wide. The column was developed using 50:50 EtOH:CHCl₃ with a flow rate of 20 drops/min. Over a 30-min time period, three different bands developed from bottom to top: red, pink and dark purple. Based on the results of TLC, the desired fraction (red fraction) was eluted first and the impurities formed the pink and dark purple bands. About 20 mL of desired fraction was collected, and it was filtered through a 30-mL F-frit to remove small alumina particles. The red solution was evaporated in the hood and the product was vacuum dried at 120 °C for 8 h. Yield: 8.0 mg (22% based on 5-NH₂-phen). Purity was checked by ¹H-NMR.

Phen-azo-p-phenol: In a typical preparation, 1.5 mL of cooled 6 M HCl was added slowly with stirring and cooling to 0.0610 g (0.3125 mmol) of 5-NH₂-phen in a 6-dram vial (kept at 0 °C in an ice bath). The yellow-green 5-NH₂-phen dissolved in the HCl to form a red solution. Stirring was continued for 3 min. Meanwhile, a solution of 0.0220 g of NaNO₂ (0.3188 mmol) in 0.836 mL of H₂O was prepared in a separate 4-dram vial and cooled to 0 °C in an ice bath. The NaNO₂ solution was added all at once to the 5-NH₂-phen/HCl solution, and the color turned to dark orange. No precipitate was formed in this step. Stirring and cooling were continued for another 3 min.

In a 40-mL beaker, 0.0294 g (0.3125 mmol) of phenol was dissolved in 4 mL of 10% NaOH solution at room temperature. Water (10 mL) was then added to the beaker. The diazotized phenathroline mixture was then transferred into the phenol solution all at once with stirring. A dark brown precipitate formed immediately, and the stirring was continued for 2 min. The pH of the mixture was >13 at this time. The reaction mixture was then transferred to a 15-mL Buchner funnel containing a glass frit filter (F). The mixture filtered very slowly. The dark red solid in the frit was thoroughly washed with water and the filtrate was dark brown-purple. The solid was dried under vacuum for 3 h. The dried solid was rinsed with 25 mL of diethyl ether (to remove any remaining phenol),

the resulting suspension was filtered, and the solid was dried under vacuum for 3 h.

Yield of crude phen-azo-p-phenol: 0.0503 g (53.3% based on 5-NH₂-phen).

Alumina chromatography was employed to purify the crude phen-azo-p-phenol. In this procedure, 20 mg of crude product was dissolved in 1.5 mL of 95% ethanol and loaded onto an alumina column which was 26 cm long and 1.1 cm wide. The column was developed using 60:40 EtOH:CHCl₃ with a flow rate of 20 drops/min. Over a 30-min time period, three different bands developed from bottom to top: pink, yellow and dark purple. Based on the results of TLC, the yellow fraction was thought to be the target compound, and this fraction was eluted right after the pink impurity. Another impurity formed a dark purple band which barely moved and remained at the top of the column. About 20 mL of the desired fraction was collected, and it was filtered through a 30-mL F-frit to remove small alumina particles. The yellow solution was evaporated in the hood and the product was vacuum dried at 120 °C for 8 h. Yield: 7.0 mg (19% based on 5-NH₂-phen). Mp: 280-282 °C. Elemental analysis: Calcd for C₁₈H₁₂N₄O·1H₂O: %C 67.91, %H 4.43, %N 17.60. Found: %C 68.28, %H 4.28, %N 17.36.

The crude phen-azo-p-phenol could also be purified by silica gel chromatography. A 20-mg sample of solid was dissolved in 1.5 mL of 90:10 acetic acid:methanol and loaded onto a silica gel column which was 20 cm long and 1.1 cm wide. The column was developed with 90:10 acetic acid:methanol with a flow rate of 20 drops/min. Over a 20-min time period, three different bands developed from bottom to top: light yellow, purple and dark purple. Based on the results of TLC, the desired compound was thought to be the yellow fraction. About 30 mL of the yellow-orange fraction was collected from the column, and this solution was filtered through a 30-mL F-frit to remove small silica particles. The solution was evaporated in the hood and the solid was vacuum dried at 120 °C for 8 h. Yield: 8.1 mg (22% based on 5-NH₂-phen). Purity was checked by ¹H-NMR.

Phen-azo-2,6-dimethylphenol: In a typical preparation, 1.5 mL of cooled 6 M HCl was added slowly with stirring and cooling to 0.0610 g (0.3125 mmol) of 5-NH₂-phen in a 6-

dram vial (kept at 0 °C in an ice bath). The yellow-green 5-NH₂-phen dissolved in the HCl to form a red solution. Stirring was continued for 3 min. Meanwhile, a solution of 0.0220 g of NaNO₂ (0.3188 mmol) in 0.836 mL of H₂O was prepared in a separate 4-dram vial and cooled to 0 °C in an ice bath. The NaNO₂ solution was added all at once to the 5-NH₂-phen/HCl solution, and the color turned to dark orange. No precipitate was formed in this step. Stirring and cooling were continued for another 3 min.

In a 40-mL beaker, 0.0380 g (0.3125 mmol) of 2,6-dimethylphenol was dissolved in 4 mL of 10% NaOH solution at room temperature. Water (10 mL) was then added to the beaker. The diazotized phenanthroline mixture was then transferred into the 2,6-dimethylphenol solution all at once with stirring. A dark brown precipitate formed immediately, and the stirring was continued for 2 min. The pH of the mixture was >13 at this time. The reaction mixture was then transferred to a 15-mL Buchner funnel containing a glass frit filter (F). The mixture filtered very slowly. The dark red solid in the frit was thoroughly washed with water and the filtrate was dark purple. The solid was dried under vacuum for 3 h. The dried solid was rinsed with 25 mL of diethyl ether (to remove any remaining 2,6-dimethylphenol), the resulting suspension was filtered, and the solid was dried under vacuum for 3 h. Yield of crude phen-azo-2,6-dimethylphenol: 0.0786 mg (76.6% based on 5-NH₂-phen).

Alumina chromatography was employed to purify the crude phen-azo-2,6-dimethylphenol. In this procedure, 20 mg of crude product was dissolved in 1.5 mL of 95% ethanol and loaded onto an alumina column which was 26 cm long and 1.1 cm wide. The column was developed using 90:10 EtOH:CHCl₃ with a flow rate of 20 drops/min. Over a 30-min time period, three different bands developed from bottom to top: yellow, pink and dark purple. The desired (based on TLC) yellow fraction was eluted first, and the impurities formed pink and dark purple bands. About 20 mL of the desired fraction was collected, and it was filtered through a 30-mL F-frit to remove small alumina particles. The yellow solution was evaporated in the hood and the product was vacuum dried at 120 °C for 8 h. Yield: 7.8 mg (31% based on 5-NH₂-phen). Mp: 272-276 °C.

Elemental analysis: Calcd for $C_{20}H_{16}N_4O \cdot 1H_2O$: %C 69.35, %H 5.24, %N 16.17. Found: %C 69.85, %H 4.90, %N 15.98.

The crude phen-azo-2,6-dimethylphenol could also be purified by silica gel chromatography. A 20-mg sample of solid was dissolved in 1.5 mL of 90:10 acetic acid:methanol and loaded onto a silica gel column which was 20 cm long and 1.1 cm wide. The column was developed with 90:10 acetic acid:methanol with a flow rate of 20 drops/min. Over a 20-min time period, three different bands developed from bottom to top: light yellow, purple and dark purple. Based on the results of TLC, the desired compound was thought to be the yellow fraction. About 30 mL of the yellow fraction was collected from the column, and this solution was filtered through a 30-mL F-frit to remove small silica particles. The solution was evaporated in the hood and the solid was vacuum dried at 120 °C for 8 h. Yield: 8.8 mg (35% based on 5-NH₂-phen).

***fac*-Re^I(CO)₃(phen)Cl** This compound was synthesized by using a method analogous to that reported by Guarr et al^{29,30} for the preparation of *fac*-[(Mebpy-Mebpy)Re^I(CO)₃Cl]. Methanol (80 mL) was added to a 250-mL 3-neck RB flask that was equipped with a reflux column and a stirring bar, and the methanol was deoxygenated with N₂ for 25 min. Re^I(CO)₅Cl (0.1000 g, 0.2764 mmole) was added with stirring, followed by 0.0548 g (0.2764 mmole) of 1,10-phenanthroline monohydrate. The mixture was refluxed under N₂. The solution was clear and colorless when the ligand was added, but became light yellow after 20 min. After 1 h, some yellow solid precipitated. Refluxing and stirring were continued under N₂ for 6 h. The reaction mixture was cooled to room temperature, resulting in the precipitation of more yellow solid. The reaction mixture was then transferred to a 15-mL Buchner funnel containing a glass frit filter(F). The yellow solid in the frit was thoroughly washed with 5 mL methanol and the filtrate was light yellow. The solid was dried under vacuum for 3 h. Yield of crude *fac*-Re^I(CO)₃(phen)Cl: 0.0971 g (72.3% based on phen).

The crude *fac*-Re^I(CO)₃(phen)Cl was purified by recrystallization. The yellow solid was dissolved in 80 mL of CH₂Cl₂ in a 500-mL beaker, and then 160 mL of 2,2',4-

trimethylpentane was dripped into this solution causing precipitation. The mixture was filtered on a 15-mL F frit. The solid was washed with a few drops of methanol, and then dried under vacuum for 3 hr. Yield of purified *fac*-Re^I(CO)₃(phen)Cl: 0.0825 g (61.4% based on phen). Mp: 343-348 °C. Elemental analysis: Calcd for C₁₅H₈ClN₂O₃Re: %C 37.08, %H 1.66, %N 5.77. Found: %C 36.95, %H 1.73, %N 5.73.

***fac*-Re^I(CO)₃(phen-azo-p-phenol)Cl** This compound was synthesized by using a method analogous to the preparation of Re^I(CO)₃(phen)Cl. Methanol (120 mL) was added to a 250-mL 3-neck RB flask that was equipped with a reflux column and a stirring bar, and the methanol was deoxygenated with N₂ for 25 min. Re^I(CO)₅Cl (0.0454 g, 0.126 mmole) was added with stirring, followed by 0.0400 g (0.126 mmole) of phen-azo-p-phenol. The mixture was brought to reflux under N₂. The resulting solution was clear and dark orange when the ligand was added, but became very bright orange after 2 h. Refluxing and stirring were continued under N₂ for 21 h. Reaction progress was monitored by TLC using EtOH as solvent. The solution was cooled to room temperature, and the solvent was then removed by roto-evaporation. The resulting brown-yellow solid was dried under vacuum for 3 h. Yield of crude *fac*-Re^I(CO)₃(phen-azo-p-phenol)Cl: 0.0802 g (93.9% based on phen-azo-p-phenol).

The crude *fac*-Re^I(CO)₃(phen-azo-p-phenol)Cl was washed with 10 mL of 2,2',4-trimethylpentane to remove unreacted Re^I(CO)₅Cl. The resulting suspension was filtered, and the brown-yellow solid was dried under vacuum for 3 h. The solid was added to 10 mL of methanol in a 25-mL RB flask equipped with a reflux column and a stirring bar. The dark orange suspension was refluxed for 25 min, and the hot mixture was filtered on a 15-mL F frit. The dark yellow solid was washed with a few drops of cold methanol, and the filtrate was dark orange. The solid obtained was dried under vacuum for 3 hr. Yield of purified *fac*-Re^I(CO)₃(phen-azo-p-phenol)Cl: 0.0501 g (58.7% based on phen-azo-p-phenol). Mp: 316-320 °C. Elemental analysis: Calcd for C₂₁H₁₂ClN₄O₄Re: %C 41.62, %H 2.00, %N 9.25. Found: %C 42.50, %H 2.48, %N 8.63.

Methods: Melting point measurements were performed on a Laboratory Devices MEL-TEMP. $^1\text{H-NMR}$ spectra were obtained using a General Electric QE-300 FT-NMR spectrometer. UV-Vis spectra were recorded on a Shimadzu UV-3100 spectrophotometer. FT-IR spectra were recorded using a Nicolet 20-DXB instrument. Elemental analyses were carried out by Atlantic Microlabs, Norcross, GA.

Chapter 3: Results and Discussion

Synthesis and Purification of Phenanthroline-Based Dyes

(1) A possible self-coupling reaction of 5-NH₂-phen:

In traditional azo coupling reactions, the diazotization step needs to be carried out at as low a temperature as possible (generally 0-5 °C) in order to prevent the decomposition of the diazonium ion.²⁸ Since diazotization is an exothermic reaction, the NaNO₂ solution is usually added slowly to prevent the temperature from rising too rapidly. Adding the NaNO₂ solution slowly will always result in the temporary coexistence of diazonium ion and unreacted amine in the solution, which generates the possibility of self coupling(Fig. 3-1). The self-coupling reaction should not be favored, however, because under the acidic conditions employed (pH < 1), any free amine would be protonated to form the ammonium ion (Ar-NH₃⁺). The protonated amine should not react readily as a coupling component because the added proton depletes the electron density of the amine, greatly lowering the coupling reactivity. Consistent with this reasoning, the model reactions using aniline as the starting material were carried out successfully, with no apparent self-coupling of the aniline.

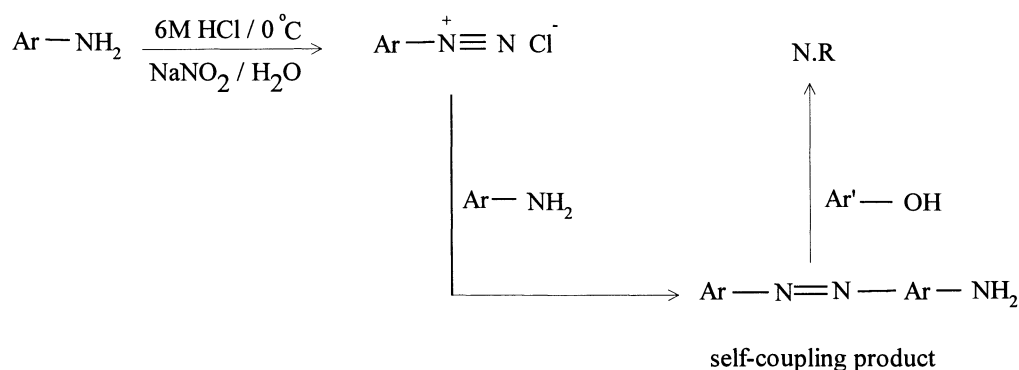
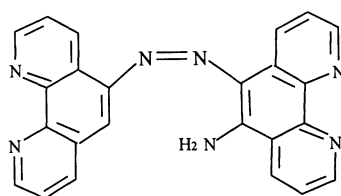


Fig. 3-1 Self-coupling reaction of amine

Initially, the diazotization of 5-NH₂-phen was carried out using the same procedure as used for aniline. However, when the NaNO₂ solution was added slowly to the acidified 5-NH₂-phen, a dark red precipitate (not solution) formed immediately. When this mixture was added to a basic β-naphthol solution (the coupling component), no coupling reaction occurred. This was confirmed by performing a control experiment. In this experiment, diazotized 5-NH₂-phen was mixed with the basic solution used to dissolve the β-naphthol (i.e. no β-naphthol present). The solid product obtained from this control experiment had a ¹H-NMR spectrum identical to the product obtained with β-naphthol. This indicated that the product resulted from a reaction that did not involve β-naphthol. The dark red product generated from this reaction did not dissolve in typical organic solvents, such as CDCl₃, acetone, or DMSO. The ¹H-NMR spectrum taken in trifluoroacetic acid-d (Fig. 3-21) shows four sets of multiplets between 8.0 and 8.6 ppm. It is typical for a phenanthroline that is asymmetrically substituted at the 5,6 positions to have two sets of multiplets (two sets of 4 peaks) in the aromatic region of its ¹H-NMR spectrum. For example, 5-NH₂-phen shows these two multiplets at around 7.50 ppm and 7.75 ppm (Fig. 3-7), while these peaks overlap slightly in 5-NO₂-phen at around 7.95 ppm (Fig. 3-8). The four sets of multiplets in Fig. 3-21 imply the presence of two different unsymmetrically substituted phenanthrolines. On the basis of the insolubility of the product and the ¹H-NMR spectra, a tentative "self-coupling" structure can be deduced as shown in Fig. 3-2. The upfield pair of multiplets could be assigned to the phen containing the -NH₂ group. The -NH₂ signal itself can not be observed in trifluoroacetic acid because of H/D exchange.



phen-azo-phen

Fig. 3-2 Self coupling product of 5-NH₂-phen

Additional evidence for self-coupling of phen can be observed in the IR spectrum (Fig. 3-27). The characteristic azo stretching vibration band can be observed at 1449 cm^{-1} . This frequency is consistent with the literature value³² of 1450 cm^{-1} . Moreover, a strong broad absorption at 3256 cm^{-1} can be assigned to the N-H stretching vibration.³⁴ Usually, primary aromatic amines display strong C-N stretching absorption in the $1340\text{--}1250\text{ cm}^{-1}$ region, and a medium peak can be observed at 1323 cm^{-1} in Fig. 3-27. A band at 737 cm^{-1} can be assigned to the C-H out of plane bending of three adjacent H atoms in each ring of the phenanthroline. This is a typical absorption of 5,6-substituted phenanthroline derivatives. The 737 cm^{-1} band was abnormally strong in Fig. 3-27 compared to that of phen-azo-2-naphthol (Fig. 3-24), phen-azo-p-phenol (Fig. 3-25), and phen-azo-2,6-dimethylphenol (Fig. 3-26). This is probably because of the existence of two phen rings.

Since the phenanthroline self-coupling product was not the target compound, no attempts were made on final purification. However, a crude sample was sent out for elemental analysis. The result was: Calcd for $\text{C}_{24}\text{H}_{15}\text{N}_7 \cdot 1\text{H}_2\text{O}$: %C 68.71, %H 4.08, %N 23.38. Found: %C 70.55, %H 4.18, %N 23.38.

In subsequent diazotizations of phen, the NaNO_2 was kept in slight excess (phen: $\text{NaNO}_2 = 1:1.1$) and it was added to the acidified phen solution all at once in an attempt to discourage self-coupling. This method appeared to give satisfactory results and yields in subsequent coupling reactions with phenols.

(2) Coupling temperature and pH value:

The aromatic and heteroaromatic diazonium ions formed in Fig. 1-9 are subject to irreversible decomposition reactions. (Fig. 3-3) The C-N bond of the diazonium ion may dissociate heterolytically or homolytically, depending on the structure of the diazonium ion and the reaction conditions.²⁸ Since the diazo decomposition reactions have larger activation energies than the desired coupling reactions, diazotization and the subsequent coupling reactions (theoretically) need to be carried out at as low a temperature as possible. For the preparation of phen-azo-2-naphthol, phen-azo-p-phenol, and phen-azo-

2,6-dimethylphenol, diazotization of the phenanthroline was always done at low temperature. The subsequent coupling reactions were attempted at both room temperature and at 0-5 °C. It was found that low-temperature coupling seemed to improve the yield slightly, but the purity of the products (as checked by $^1\text{H-NMR}$) was not improved. For phen-azo-p-phenol, more impurities showed up in the $^1\text{H-NMR}$ spectra when the coupling reaction was carried out at low temperature.

The coupling reaction is base catalyzed.²⁸ Basic conditions shift the equilibrium of the phenolic coupling component to favor the deprotonated form (Ar-O^-). The deprotonated form is much more reactive towards electrophilic attack by the diazonium ion. Therefore, after carrying out diazotization of the phenanthroline under strongly acidic conditions, the coupling reactions must be performed at pH values greater than the pKa's of the phenols. The pKa's of phenol, 2,6-dimethylphenol and β -naphthol are 9.99, 10.59, and 9.57, respectively.³² These phenols were dissolved in aqueous NaOH before coupling and the final pH values after the coupling reactions were measured to be > 13 .

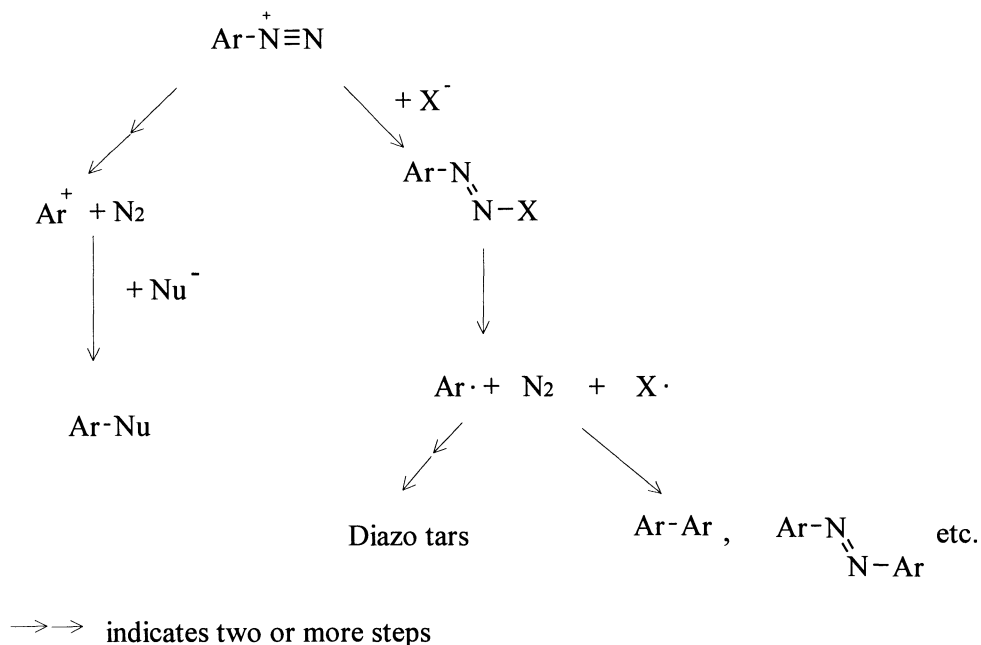


Fig. 3-3 The decomposition of diazonium ion (taken from ref. 28).

(3) Starting materials / chromatographic materials

β -Naphthol (99%) was purchased from Aldrich Chemical Co. and was used as received or was recrystallized from 25:75 ethanol:H₂O. The ¹H-NMR spectra of the crude coupling product of diazotized phenanthroline and β -naphthol showed that it did not appear to make any difference whether or not the purified β -naphthol was used in the reaction. Also, the yield was about the same when using purified β -naphthol. Moreover, the ¹H-NMR spectra of crude and purified β -naphthol were very similar.

Two different lots of Aldrich aluminum oxide (both ~150 mesh, Brockman I, neutral) were used for chromatographic separation. The eluant of Lot# 09009KT alumina was very cloudy. Apparently, some small particles of alumina were washed out by the solvents and passed through either the glass wool plug or coarse glass frit in the columns. The particle size of the Aldrich alumina was ~ 0.105 mm. The pore size of the coarse glass frit ranged from 0.04 mm to 0.06 mm. Therefore, no alumina particles should have come through, at least not in the columns using glass frits. The reason for this problem was not clear. Interestingly, a different lot of the same material (Lot# 06405DW) worked better, as the eluants from columns made of this material were much clearer (but were still filtered through fine glass frits with pore sizes of 0.0040 mm- 0.0055 mm).

(4) Elemental analysis.

The phen-azo dyes were vacuum dried at 120 °C before being sent out for elemental analyses but still appeared to be approximately monohydrates in all cases. The ¹H-NMR spectra of all three phen-azo dyes showed significantly increased water peaks at 3.4 ppm as compared to that of DMSO blank spectra. This result is common for azo dyes.⁴⁰

The sample of phen-azo-2-naphthol (for elemental analysis) was purified by silica gel chromatography using a combination solvent of acetic acid and MeOH. Acetic acid proved to be quite difficult to remove completely. In the ¹H-NMR of the purified solid, a small peak at 1.90 ppm (-CH₃ from acetic acid) integrated to ~0.5 H, equivalent to ~ 0.2 HC₂H₃O₂. Therefore, 0.2 HC₂H₃O₂ was included in the elemental analysis result for

phen-azo- β -naphthol. The phen-azo-p-phenol and phen-azo-2,6-dimethylphenol samples (for elemental analysis) were purified by alumina chromatography using a combination solvent of EtOH and CHCl₃. EtOH and CHCl₃ can more easily be removed from the products, leaving only residual water.

¹H-NMR Spectra

(1) Starting materials

The ¹H-NMR spectra of 5-NH₂-phen, 5-NO₂-phen, and phen are shown in Figs. 3-7, 3-8, and 3-9, respectively, and peak assignments are listed in Table 3-1. For 5-NH₂-phen, assignment of the singlet at 6.15 ppm to -NH₂ was confirmed by the integration (2H) and by the disappearance of the signal upon addition of D₂O. Almost all the ¹H resonances show the effects of the electron releasing -NH₂ and electron withdrawing -NO₂ groups. The effect is especially pronounced at position 6 on the ring, where the 5-NO₂-phen and 5-NH₂-phen signals differ by > 2 ppm.

(2) Phen-azo- β -naphthol

The ¹H-NMR spectra for phen-azo- β -naphthol are shown in Figs. 3-13 a, b. Direct assignment of peaks is complicated by overlapping signals from the phen and naphthol rings. In order to more clearly make assignments, a model reaction was designed in which 2,3,4,5,6-d-aniline would be diazotized and coupled to β -naphthol (Fig. 3-4a). It was thought that the deuterated aniline moiety would be a suitable electronic analog of phenanthroline. More importantly, it would be ¹H-NMR "silent", allowing for clearer assignments of β -naphthol resonances in the complicated ¹H-NMR spectrum of phen-azo- β -naphthol. Because of the expense involved in using deuterated aniline, and in order to optimize experimental conditions, a reaction using aniline and β -naphthol was run first (Fig. 3-4b). In this reaction, aniline was diazotized by NaNO₂ in HCl at 0 °C and coupled to β -naphthol in the presence of NaOH. The product of this

reaction was phenyl-azo- β -naphthol (Sudan I).

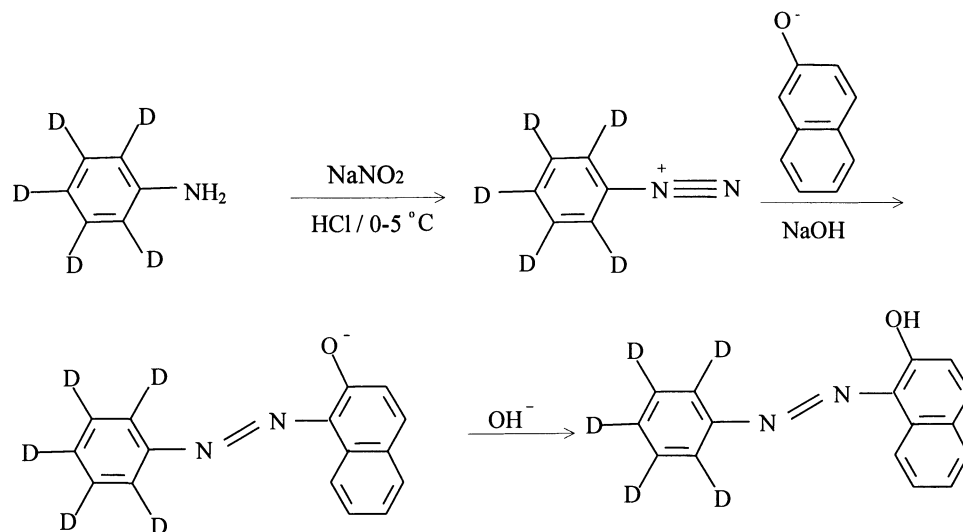


Fig. 3-4a Model reaction using 2,3,4,5,6-d-aniline and β -naphthol

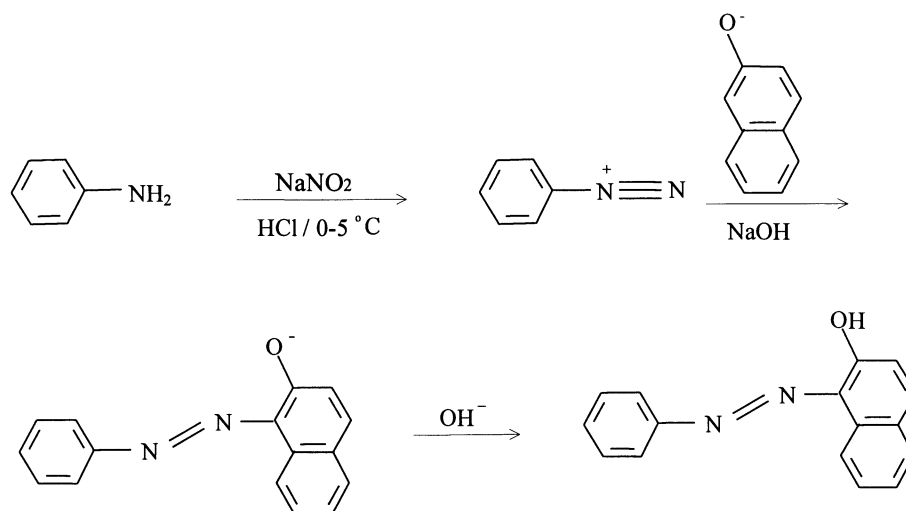


Fig. 3-4b Model reaction using aniline and β -naphthol

The $^1\text{H-NMR}$ spectrum of the phenyl-azo- β -naphthol is shown in Fig. 3-10 a, b. All peaks integrate to 12H, the total number expected for phenyl-azo- β -naphthol. The peak at 15.8 ppm is assigned to the -OH proton. This assignment is based on the $^1\text{H-NMR}$ spectrum reported for p-methoxy-phenyl- β -naphthol (in d_6 -acetone) in the literature.³³ The peak at 15.8 ppm disappeared upon the addition of D_2O to the sample,

confirming this as the -OH resonance. The hydroxyl proton is shifted dramatically downfield due to its taking part in H-bonding (vide infra).

Sudan I is a commercially available dye, and the spectrum of a sample purchased from Aldrich is shown in Fig. 3-11 a, b. The identical peak patterns of Fig. 3-10 and Fig. 3-11 confirmed that the model reaction was carried out successfully and phenyl-azo- β -naphthol was indeed produced.

2,3,4,5,6-d-Aniline was then diazotized and coupled to β -naphthol using exactly the same experimental conditions as in the previous model reaction. The $^1\text{H-NMR}$ spectrum of the 2,3,4,5,6-d-phenyl-azo- β -naphthol product is shown in Fig. 3-12 a, b. All signals in Fig. 3-12 are from the β -naphthol moiety. Peak assignments for 2,3,4,5,6-d-phenyl-azo- β -naphthol were made using Silverstein et al³⁴ and are listed in Table 3-2. For the purpose of comparison, chemical shift data for phenyl-azo- β -naphthol are also included. The significance of these data are that the $^1\text{H-NMR}$ peak pattern for β -naphthol attached to an aromatic ring through an azo linkage at position 1 was determined.

As mentioned previously, the $^1\text{H-NMR}$ spectra for phen-azo- β -naphthol are shown in Figs. 3-13 a, b. The data are summarized in Table 3-3. (For the purpose of comparison, the chemical shift data for related compounds such as phenyl-azo- β -naphthol (Fig. 3-10), 5- NO_2 -phen (Fig.3-8), and β -naphthol (Fig. 3-14) are also included.)

For phen-azo- β -naphthol, all peaks integrate to 14H, which is the total number expected. The peak at 16.7 ppm in Fig. 3-13a had an integrated intensity slightly less than one proton. As for Sudan I, this signal was assigned to the azo-OH on the basis of literature precedent.³³ The peak at 16.7 ppm disappeared upon the addition of D_2O to the sample, confirming this as the -OH resonance. Intramolecular hydrogen bonding (Fig. 3-5) explains why the peak from the hydroxylic proton is found at abnormally low field. The intramolecular hydrogen bonding decreases the electron density around the proton, and thus moves the proton absorption to lower field.

Fig. 3-5 depicts the two possible tautomers for phen-azo- β -naphthol. The azo/hydrazone tautomerization is a well-known phenomenon for phenyl-azo- β -naphthol.⁴¹ The position of the equilibrium has been found to be both solvent and

temperature dependent.^{33,41} Apparently, for phenyl-azo- β -naphthol in DMSO, the equilibrium favors the azo form since the hydroxylic proton signal at 16.7 ppm integrates to nearly one proton. The -NH resonance, expected at around 10.2 ppm (on the basis of literature reports for p-methoxy-phenyl- β -naphthol in d_6 -acetone³³) is either nonexistent or too small to be detected in DMSO. Almost all the ^1H resonances from the naphthol fragment in phen-azo- β -naphthol are shifted downfield compared with β -naphthol (Fig. 3-14). This is most likely due to the effects of the linkage of the electron withdrawing azo group. The effect is especially pronounced at position 8' on the ring, where the β -naphthol and phen-azo- β -naphthol ^1H resonances differ by ~ 1 ppm. Moreover, differences between the phenyl-azo- β -naphthol and phen-azo- β -naphthol can also be observed. In phen-azo- β -naphthol, the heterocyclic phenanthroline ring appears to decrease the electron density of the β -naphthol ring (relative to the phenyl derivative), as evidenced by small downfield shift (0.05-0.14 ppm) in β -naphthol resonances (Table 3-3).

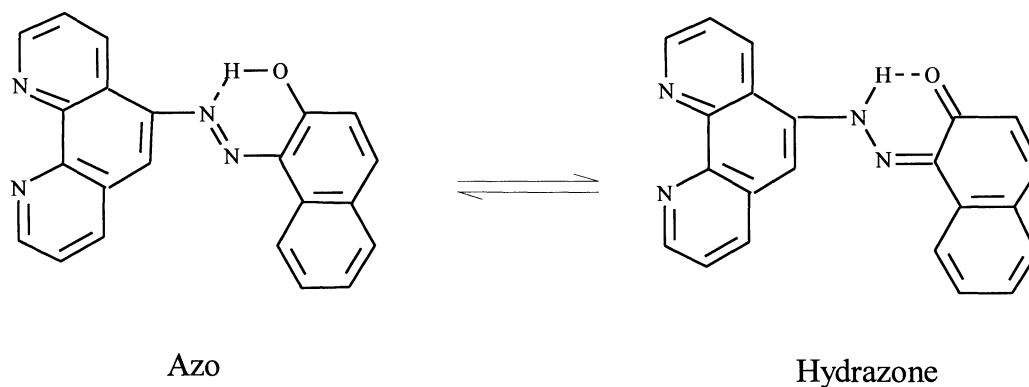


Fig. 3-5 The tautomerization and intramolecular hydrogen bond of phen-azo-2-naphthol

(3) Phen-azo-p-phenol

The ^1H -NMR spectrum for phen-azo-p-phenol is shown in Fig. 3-15, and the data are summarized in Table 3-4. (For the purpose of comparison, the chemical shift data for phenol (Fig. 3-16) and 5- NO_2 -phen (Fig. 3-8) are also included.) The ^1H -NMR signals for phen-azo-p-phenol integrate to 12H, which is the total number expected. A very broad peak at 10.4 ppm in Fig. 3-15 has an integrated intensity of about one proton.

Assignment of this signal to the azo -OH was made based on the $^1\text{H-NMR}$ spectrum of phenol (Fig. 3-16) in which the -OH proton resonance is at 9.35 ppm. The peak at 10.4 ppm disappeared upon the addition of D_2O to the sample, confirming this as the -OH. Since the phen-azo-p-phenol could not have an intramolecular hydrogen bond like phen-azo- β -naphthol, the -OH signal was not moved dramatically downfield. Assignment of other peaks was straightforward based on the assignments for phen-azo- β -naphthol (Table 3-4).

(4) Phen-azo-2,6-dimethylphenol

The $^1\text{H-NMR}$ spectra for phen-azo-2,6-dimethylphenol in $\text{d}_6\text{-DMSO}$ are shown in Fig. 3-17 a, b, and the data are summarized in Table 3-5. (For the purpose of comparison, the chemical shift data for 2,6-dimethylphenol in $\text{d}_6\text{-DMSO}$ (Fig. 3-19 a, b) and 5- NO_2 -phen (Fig. 3-8) are also included.) Assignment of peaks was made based on the assignments for phen-azo- β -naphthol (Fig. 3-13), phen-azo-p-phenol (Fig. 15), and 2,6-dimethylphenol (Fig. 3-19). Six $-\text{CH}_3$ protons can be observed at 2.33 ppm in Fig. 3-17a. The $^1\text{H-NMR}$ signals for phen-azo-2,6-dimethylphenol integrate to approximately 15H, which is one less than the total number expected. By comparison with the chemical shift of 2,6-dimethylphenol in $\text{d}_6\text{-DMSO}$, which has an -OH resonance at 8.14 ppm, we found that the missing signal in Fig. 3-17 is the -OH resonance. From experience with $^1\text{H-NMR}$ assignments for phen-azo-p-phenol, we expected that the -OH peak in the phen-azo-2,6-dimethylphenol would shift downfield by about 1 ppm compared with the -OH peak in 2,6-dimethylphenol (to around 9.1 ppm). Possibly, this -OH peak was buried by three phenanthroline signals from 9.0 - 9.5 ppm. In fact, those three peaks (as a group) do integrate to more than three protons.

An effort was made to find the -OH signal in the 2,6-dimethylphenol moiety by taking the $^1\text{H-NMR}$ spectra in CDCl_3 . The $^1\text{H-NMR}$ spectra for phen-azo-2,6-dimethylphenol and 2,6-dimethylphenol in CDCl_3 are shown in Fig. 3-18a, b, and Fig. 3-20a, b, respectively, and the data are summarized in Table 3-5. The $^1\text{H-NMR}$ signals for phen-azo-2,6-dimethylphenol in Fig. 3-18a integrate to 16H, which is the total number

expected. Six -CH_3 protons can be observed at 2.40 ppm in Fig. 3-18 a. A broad peak at 5.3 ppm in Fig. 3-18a has an integrated intensity of about one proton. Assignment of this signal to the azo -OH was made based on the $^1\text{H-NMR}$ spectrum of 2,6-dimethylphenol (Fig. 3-20) in which the -OH proton resonance is at 4.6 ppm. The peak at 5.3 ppm disappeared upon the addition of D_2O to the sample, confirming this as the -OH . A questionable peak with significant intensity (about six protons) appeared at 1.3 ppm. This is neither the water peak in the CDCl_3 (the chemical shift of dissolved water in CDCl_3 is ~ 1.5 ppm.) nor from contaminated CDCl_3 . (The blank CDCl_3 has no such signal, and the NMR tube had been cleaned and dried completely.) Additionally, no such peak appeared in the $^1\text{H-NMR}$ spectra in $d_6\text{-DMSO}$. The reasons for this strange peak are not well-understood.

(5) Re(I) complexes

The $^1\text{H-NMR}$ spectra of $\text{fac-Re}^{\text{I}}(\text{CO})_3(\text{phen})\text{Cl}$ and $\text{fac-Re}^{\text{I}}(\text{CO})_3(\text{phen-azo-p-phenol})\text{Cl}$ are shown in Fig. 3-22 and Fig. 3-23, respectively. The data are summarized in Table 3-6. (For the purpose of comparison, the chemical shift data for phen-azo-p-phenol (Fig. 3-15), phenol (Fig. 3-16), and phen (Fig. 3-9) are also included.) Assignments of proton resonances were made by analogy to the model of phen and phen-azo-p-phenol ligands.

The peak patterns for phen and $\text{fac-Re}^{\text{I}}(\text{CO})_3(\text{phen})\text{Cl}$ are very similar. All peaks from phen in $\text{fac-Re}^{\text{I}}(\text{CO})_3(\text{phen})\text{Cl}$ are shifted downfield upon metal attachment by 0.33-0.48 ppm. This is due to the positive charge from the Re(I) center. In addition, the three carbonyl groups attached to Re(I) also compete with phen for electron density from π -backbonding. Therefore, the overall electron density of the phen ring is decreased (relative to free phen) upon the attachment of the $\text{Re}^{\text{I}}(\text{CO})_3\text{Cl}$ fragment, causing the downfield shift in ^1H resonances. A similar downfield shift can be observed in the resonances of the phen moiety of $\text{fac-Re}^{\text{I}}(\text{CO})_3(\text{phen-azo-p-phenol})\text{Cl}$ (0.29-0.43 ppm) compared with the phen fragment of free phen-azo-p-phenol ligand. This result implies that attachment of the $\text{-Re}^{\text{I}}(\text{CO})_3\text{Cl}$ fragment to phen-azo-p-phenol occurs through the

1,10-phen linkage. This is confirmed by the very small downfield shift (0.04 - 0.1 ppm) for phenol moiety of coordinated phen-azo-p-phenol when compared to the free ligand. Since the Re(I) attachment is remote from the phenol ring, the effect of metal coordination is relatively small.

IR Spectra

(1) phen-dye ligands

As described previously, for phen-azo- β -naphthol, each of the phen-dye ligands can theoretically exist as either the azo or hydrazone tautomers, or a mixture of both. From $^1\text{H-NMR}$ data, both the β -naphthol and phenol derivatives seem to exist primarily in the azo form in d_6 -DMSO. A CDCl_3 solution of the dimethylphenol derivative appears to also contain a large percentage of the azo tautomer.

IR spectra can in theory, also be used to distinguish between the azo and hydrazone forms of these ligands. The azo forms would be expected to show -OH and (weak) -N=N- stretches. Alternately, the hydrazone forms would be expected to show N-H and C=O (quinone) stretches.

Unfortunately, DMSO is not an ideal IR solvent, and the ligands were not soluble enough in CHCl_3 to obtain suitable spectra (even after several hundred scans on the FT-IR). Therefore, solid state spectra (in KBr) were obtained for the three phen-dye ligands. These spectra are shown in Figs. 3-24, 3-25, and 3-26, for the β -naphthol, phenol, and dimethylphenol derivatives, respectively.

In practice, the presence of -OH and -NH absorptions in KBr pellets of these samples is hard to decipher. A significant amount of water is present in these pellets, both from the KBr and the water of crystallization. The β -naphthol derivative is further compromised by the presence of acetic acid. In addition, significant H-bonding interactions are most likely operating in these samples, both intramolecular (β -naphthol derivative) and intermolecular (phenol derivatives). Silverstein et al³⁴ have noted that these interactions can be encouraged by using condensed phase samples.

Two absorptions that might be somewhat easier to observe in the IR spectra would be the azo stretch (for azo tautomers) and the C=O (quinone) stretch (for hydrazone tautomers). Each of these two absorptions could be affected by H-bonding interactions, and the -N=N- stretch has the additional problem of being weak due to the non-polar nature of the N=N bond. Aromatic (*trans*) azo compounds typically show -N=N- absorption in the 1440- 1410 cm^{-1} range.³² It should be noted that weak absorptions at 1450 cm^{-1} , 1450 cm^{-1} , and 1455 cm^{-1} were observed for the β -naphthol, phenol, and dimethylphenol derivatives, respectively. (The dimethylphenol derivative may be more difficult to interpret due to interfering -CH₃ absorptions.) More significantly, all three ligands do not show absorptions in the 1690-1660 cm^{-1} range for quinones (C=O). Therefore, these compounds appear to exist as primarily the azo tautomers in the solid state.

(2) Re(I) complexes

The IR spectra (in KBr) for *fac*-Re^I(CO)₃(phen)Cl and *fac*-Re^I(CO)₃(phen-azo-p-phenol)Cl are shown in Fig. 3-28 and Fig. 3-29, respectively. A summary of the carbonyl stretching frequencies for these two compounds is found in Table 3-7.

Four strong bands for *fac*-Re^I(CO)₃(phen)Cl at 2018 cm^{-1} , 1933 cm^{-1} , 1904 cm^{-1} , and 1879 cm^{-1} are assigned to the three carbonyl groups based on the results reported for *fac*-Re^I(CO)₃(Me₂bpy)Cl in KBr⁴³ (Me₂bpy = 4,4'-dimethyl-2,2'-bipyridine). (Also, the literature reports three carbonyl stretching bands for *fac*-Re(CO)₃(phen)Cl in CH₂Cl₂ at 2015 cm^{-1} , 1912 cm^{-1} and 1890 cm^{-1} .⁴³) The carbonyl stretching peaks for *fac*-Re^I(CO)₃(phen)Cl are all at lower frequency than that of Re^I(CO)₅Cl. (Table 3-7) This is because upon coordination with the phen ring, the rhenium(I) accepts two pairs of electrons from the phenanthroline N atoms to form σ bonds. These σ bonds increase the electron density at the metal center, thus enhancing the Re \rightarrow CO back donation. Since the LUMO of the CO is the a π^* antibonding orbital, the Re \rightarrow CO back donation decreases the bond order and bond energy of CO, decreasing the stretching frequency.

In *fac*-Re^I(CO)₃(phen-azo-p-phenol)Cl, only three carbonyl stretching peaks can be observed at 2026 cm⁻¹, 1920 cm⁻¹ and 1896 cm⁻¹. Since phen-azo-p-phenol appears (from ¹H-NMR data) to be slightly more electron deficient than phen, it would be expected that Re(I) → CO backbonding would be less effective in *fac*-Re^I(CO)₃(phen-azo-p-phenol)Cl relative to the phen derivative. This would cause an increase in the CO stretching frequencies. This prediction appears accurate for only one observed transition (2018 cm⁻¹ → 2026 cm⁻¹ shift). There appears to be a decrease in stretching frequencies for the other regions. However, it is unclear exactly which transitions are increasing/decreasing, since the three peaks in the region for the phen derivative (1933 cm⁻¹, 1904 cm⁻¹, and 1879 cm⁻¹) combine to give two equally intense transitions at 1920 cm⁻¹ and 1896 cm⁻¹.

It should also be noted that a weak absorption at 1447 cm⁻¹ appears in the *fac*-Re^I(CO)₃(phen-azo-p-phenol)Cl spectra, with no absorption in the 1690 - 1630 cm⁻¹ range. This implies that the phen-azo-p-phenol ligand is in the azo form when coordinated to Re(I).

UV-Vis Spectra

(1) phen-dye ligands

The UV-Vis spectrum (in MeOH) of phen-azo-β-naphthol, phen-azo-p-phenol, and phen-azo-2,6-dimethylphenol are shown in Fig. 3-32, 3-35, and 3-38, respectively. (For the purpose of comparison, the UV-Vis spectra (in MeOH) of β-naphthol (Fig. 3-34), phenol (Fig. 3-37), 2,6-dimethylphenol (Fig. 3-40), and 1,10-phen (Fig. 3-31) were also included.) The λ_{max} and ε values are summarized in Table 3-8.

The absorption spectrum of 1,10-phen in MeOH (Fig. 3-31) shows two maxima (π → π*) at 230 nm and 263 nm. Since all three dye ligands contain the phen moiety, it would be expected that the UV-Vis spectrum of each dye would contain strong absorptions in these two regions. This expectation appears to be met in phen-azo-β-naphthol (224 nm, 273.5 nm), phen-azo-p-phenol (222 nm, 273.5 nm), and phen-azo-2,6-dimethylphenol (222 nm, 273.5 nm). The 224 nm maximum in phen-azo-β-naphthol

appears enhanced relative to the 273.5 nm band, probably due to the large single absorbance peak in the UV for β -naphthol (222.5 nm). The phen-azo-p-phenol and phen-azo-2,6-dimethylphenol dyes actually show an extra absorption maximum in the UV (~252 - 254 nm), probably due to the phenol and dimethylphenol moieties.

The most interesting portion of the electronic spectra of the free phen-dye ligands is the visible. For example, both phen-azo-p-phenol and phen-azo-2,6-dimethylphenol exhibit intense ($\epsilon \cong 3 \times 10^4 \text{ M}^{-1} \text{ cm}^{-1}$) absorption maximum in the 380-390 nm region, with significant tailing to > 500 nm. Moreover, phen-azo- β -naphthol shows an intense absorption at ~500 nm, with tailing past 580 nm. The introduction of the azo group is obviously responsible for these transitions. However, the azo group itself shows only weak $n \rightarrow \pi^*$ transitions. For example, Fig. 3-6 shows the structure of *trans*-azobenzene. The long wavelength maximum for this compound is 450 nm, but the absorptivity is quite low ($\epsilon = 463 \text{ M}^{-1} \text{ cm}^{-1}$). This weak transition has been assigned as $n \rightarrow \pi^*$ arising from unshared pairs of electrons on the azo nitrogens.²⁸

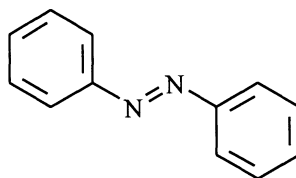


Fig. 3-6 The structure of *trans*-azobenzene

The intense long wavelength absorptions of the three phen-dye ligands most likely arise from transitions that have been shifted and/or enhanced by the interaction of the azo and hydroxyl groups with the aromatic and heterocyclic ring systems. Whether these transitions can formally be labeled as $n \rightarrow \pi^*$ or $\pi \rightarrow \pi^*$ is not clear at this time.

It should be noted that the long-wavelength absorptions of the phenol and dimethylphenol dyes appear fairly symmetrical, while that for the β -naphthol derivative appears asymmetric (high energy shoulder around 423 nm). For the analogous 1-phenyl-azo-2-naphthol, it has been suggested that the longer wavelength absorption is due to the

hydrazone form and the shorter wavelength absorption due to the azo form.⁴⁴ This equilibrium could be operating here in MeOH for phen-azo- β -naphthol.

It should be noted that the ϵ values presented in Table 3-8 for the three phen-dye ligands were obtained from Beer's Law plots of five different concentrations. Sample plots for the three dyes are shown in Fig. 3-33, 3-36, and 3-39. The ϵ values for other compounds listed in Table 3-8 were either calculated from single concentrations or retrieved from the literature.

(2) Re(I) complexes

The UV-Vis spectra (in MeOH) of *fac*-Re^I(CO)₃(phen)Cl and *fac*-Re^I(CO)₃(phen-azo-p-phenol)Cl are shown in Fig. 3-41 and Fig. 3-42. The $\lambda_{\max}(\epsilon)$ values for these and related compounds are listed in Table 3-8.

The spectra of *fac*-Re^I(CO)₃(phen)Cl in MeOH (Fig. 3-41) can be compared with that of 1,10-phenanthroline monohydrate in the same solvent (Fig. 3-31). It can be seen that the peaks at 273 nm and 217 nm for *fac*-Re^I(CO)₃(phen)Cl are most likely $\pi \rightarrow \pi^*$ transitions arising from the phenanthroline portion of the molecule. These peaks are slightly shifted compared to 1,10-phen ($\lambda_{\max} = 264$ nm and 229 nm). This is typical for polypyridine ligands chelated to positively charged transition metal center.^{38,39} The peak at 370 nm ($\epsilon = 4.17 \times 10^3$) for *fac*-Re^I(CO)₃(phen)Cl is assigned to the low energy metal to ligand charge transfer band (MLCT) arising from promotion of an electron from the HOMO ($d\pi$) t_{2g} Re(I) orbital to the LUMO π^* orbital of the 1,10-phen. (This is close to that reported in the literature for a CH₂Cl₂ solution of the complex (377 nm).³⁷)

The spectrum of *fac*-Re^I(CO)₃(phen-azo-p-phenol)Cl in MeOH (Fig. 3-42) can be compared with that of phen-azo-p-phenol (Fig. 3-35) in the same solvent. It can be seen that the high energy absorption at 222 nm in the free ligand appears to be blue-shifted significantly (almost off the x-scale, actually). This is a similar but more severe shift than that seen previously between free 1,10-phen (229 nm) and of *fac*-Re^I(CO)₃(phen)Cl (217 nm). The peak at 273.5 nm in free phen-azo-p-phenol appears to be red-shifted slightly in

the metal complexes (280 nm), while the 252 nm absorption in the free ligand is slightly blue-shifted (to 248 nm).

The most important feature in the UV-Vis spectra of *fac*-Re^I(CO)₃(phen-azo-p-phenol)Cl is the strong absorption at 390 nm ($\epsilon = 3.35 \times 10^4$). This peak, in fact, is a mixture of MLCT and ligand-centered (LC) bands. The MLCT absorption maximum for *fac*-Re^I(CO)₃(phen-azo-p-phenol)Cl would be expected to be slightly red-shifted compared to that for phen derivative. For example, Wrighton et. al reported a shift from 377 nm to 397 nm for replacement of phen by 5-NO₂-phen in *fac*-Re^I(CO)₃(LL)Cl complexes in CH₂Cl₂ solution.³⁷ Since the azo group in the phen-azo-p-phenol would be expected to exert an electron withdrawing influence (similar to -NO₂ in 5-NO₂-phen), the MLCT band for *fac*-Re^I(CO)₃(phen-azo-p-phenol)Cl might be expected to red-shift about 10-20 nm. Interestingly, the λ_{\max} for *fac*-Re^I(CO)₃(phen-azo-p-phenol)Cl is red-shifted by 10 nm compared to the phen derivative. It is also remarkable that the ϵ value for this λ_{\max} is quite close to the sum of the ϵ values for the *fac*-Re^I(CO)₃(phen)Cl MLCT band and the λ_{\max} for free phen-azo-p-phenol. This implies that both the MLCT for *fac*-Re^I(CO)₃(phen-azo-p-phenol)Cl and the LC transition for coordinated phen-azo-p-phenol are red-shifted ~ 10 nm relative to the *fac*-Re^I(CO)₃(phen)Cl and free phen-azo-p-phenol, respectively. If the λ_{\max} (at 380 nm) of free phen-azo-p-phenol originated from a $\pi \rightarrow \pi^*$ transition, it could be that lowering of the π^* energy level (relative to the π level) due to coordination of Re(I) could be responsible for the red-shift in the LC transition for the coordinated ligand.

Preliminary emission measurements were obtained for both the *fac*-Re^I(CO)₃(phen)Cl (Fig. 3-43) and *fac*-Re^I(CO)₃(phen-azo-p-phenol)Cl (Fig. 3-44) in MeOH solution. When excited near its λ_{\max} (MLCT band), *fac*-Re^I(CO)₃(phen)Cl did emit at ~ 560 nm, consistent with literature reports.³⁷ However, when *fac*-Re^I(CO)₃(phen-azo-p-phenol)Cl was irradiated at its λ_{\max} (390 nm), no emission was observed (Fig. 3-44). This is most likely due to the fact that the LC transition for coordinated phen-azo-p-phenol dominates at this wavelength, and excited state decay

proceeds via nonradiative pathways. These results are, however, only preliminary – further spectroscopic work is planned for both free and coordinated phen-azo-dye ligands.

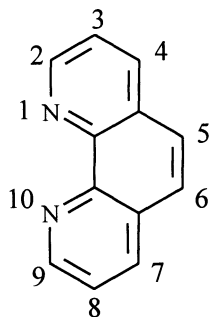
Summary

The use of 5-NH₂-1,10-phenanthroline and variety of coupling components produces three azo dyes absorbing over a wide range of visible wavelengths. The phen-azo-p-phenol ligand attached to a -Re^I(CO)₃Cl fragment through the phenanthroline linkage. This is supported by both FT-IR and ¹H-NMR spectral data. Transition metal complexes of phen-dye ligands will, in theory, be complexes that retain the stability and redox properties of traditional polypyridyl complexes while possessing enhanced abilities to absorb visible light due to the presence of the dye moiety. Such complexes may be useful in areas such as solar energy conversion and photosynthesis. The design and synthesis of these kind of molecules that strongly absorb sunlight over a broad spectrum of wavelengths will increase the probability of successfully harnessing the sun's energy.

Future research work will involve the synthesis of a series of phen-azo-amine ligands: phen-azo-aniline and phen-azo-*o*-naphtholamine. This may provide an even broader range of absorption in the visible region. In addition, detailed solvent and temperature dependence studies will further clarify the azo ⇌ hydrazone equilibria conditions. Re^I-dye complexes will be further investigated with regards to their excited state properties in order to determine whether or not the presence of the dye ligands will enhance production of useful states by visible light absorption.

Table 3-1¹H-NMR for 5-NO₂-phen, phen, and 5-NH₂-phen ^a

	Chemical shift (ppm) ^b								
	2	3	4	5	6	7	8	9	11
5-NO ₂ -phen	9.29	7.97	8.89	—	9.04 (S) ^c	8.78	7.94	9.24	—
1,10-phen	9.12	7.79	8.51	8.01 (S) ^c		8.51	7.79	9.12	—
5-NH ₂ -phen	8.67	7.52	8.04	—	6.86 (S) ^c	8.66	7.73	9.05	6.15 (S) ^c

^a DMSO was used as solvent.^b All chemical shift values, except where indicated, represent centers of multiplets.^c S = singlet.

phen

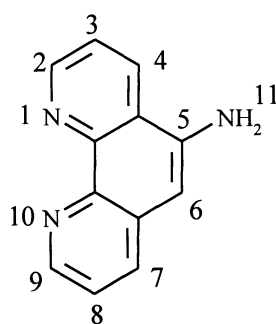
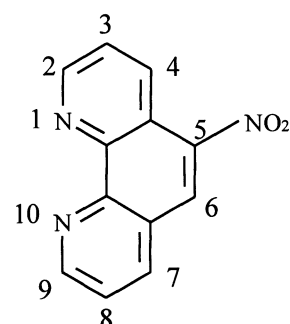
5-NH₂-phen5-NO₂-phen

Table 3-2

¹H-NMR for 2,3,4,5,6-d phenyl-azo-β-naphthol and
phenyl-azo-β-naphthol ^a

a. Aniline moiety:

	Chemical shift (ppm) ^b				
	2	3	4	5	6
Phenyl-azo-β-naphthol	7.89	7.56	7.39	7.56	7.89
2,3,4,5,6-d-phenyl-azo-β-naphthol	—	—	—	—	—

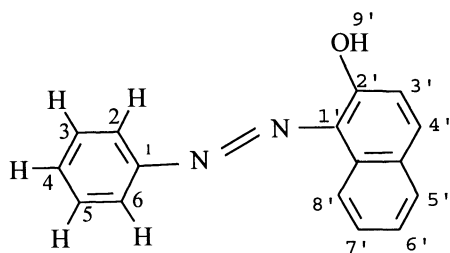
b. β-naphthol moiety.

	Chemical shift (ppm) ^b						
	3'	4'	5'	6'	7'	8'	9'
Phenyl-azo-β-naphthol	6.95	7.80	7.98	7.48	7.63	8.57	15.8 (S) ^c
2,3,4,5,6-d-phenyl-azo-β-naphthol	6.94	7.80	7.97	7.48	7.64	8.58	15.8 (S) ^c

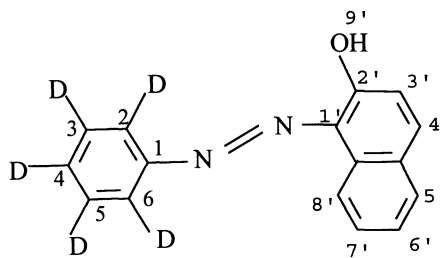
^a DMSO was used as solvent.

^b All chemical shift values, except where indicated, represent centers of multiplets.

^c S = singlet.



phenyl-azo-2-naphthol



2,3,4,5,6-d-phenyl-azo-2-naphthol

Table 3-3

¹H-NMR for phen-azo-β-naphthol and related compounds ^a

a. Phen moiety:

	Chemical shift (ppm) ^b							
	2	3	4	5	6	7	8	9
phen-azo-β-naphthol	9.26	8.02	8.75	—	8.67 (S) ^c	8.75	7.83	9.10
5-NO ₂ -phen	9.29	7.97	8.89	—	9.04 (S) ^c	8.78	7.94	9.24

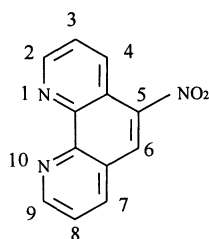
b. β-naphthol moiety:

	Chemical shift (ppm) ^b							
	1'	3'	4'	5'	6'	7'	8'	9'
Phen-azo-β-naphthol	—	7.02	7.85	8.07	7.55	7.71	8.71	16.7 (S) ^c
Phenyl-azo-β-naphthol	—	6.95	7.80	7.98	7.48	7.63	8.57	15.8 (S) ^c
β-naphthol	7.12 (S) ^c	7.08	7.68	7.75	7.24	7.37	7.76	9.74 (S) ^c

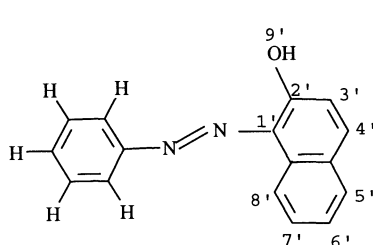
^a DMSO was used as solvent.

^b All chemical shift values, except where indicated, represent centers of multiplets.

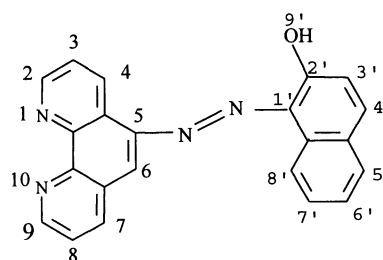
^c S = singlet.



5-NO₂-phen



phenyl-azo-2-naphthol



phen-azo-2-naphthol

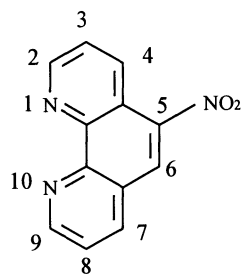
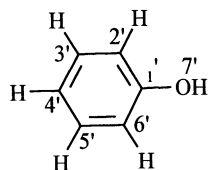
Table 3-4¹H-NMR for phen-azo-p-phenol and related compounds

a. Phen moiety:

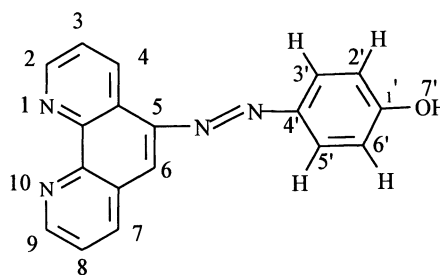
	Chemical shift (ppm) ^c							
	2	3	4	5	6	7	8	9
phen-azo-p-phenol ^a	9.32	7.93	9.14	—	8.16 (S) ^d	8.70	7.82	9.23
phen-azo-β-naphthol ^a	9.24	8.02	8.75	—	8.67 (S) ^d	8.75	7.83	9.07
5-NO ₂ -phen ^a	9.29	7.97	8.89	—	9.04 (S) ^d	8.78	7.94	9.24

b. phenol moiety:

	Chemical shift (ppm)					
	2'	3'	4'	5'	6'	7'
Phen-azo-p-phenol ^a	7.02	8.05	—	7.02	8.05	10.6 (S) ^d
phenol ^a	6.76	7.16	6.76	7.16	6.76	9.35 (S) ^d
phenol ^b	6.83	7.24	6.93	7.24	6.83	4.54 (S) ^d

^a DMSO was used as solvent.^b CDCl₃ was used as solvent.^c All chemical shift values, except where indicated, represent centers of multiplets.^d S = singlet.5-NO₂-phen

phenol



phen-azo-p-phenol

Table 3-5

¹H-NMR for phen-azo-2,6-dimethylphenol and related compounds

a. Phen moiety:

	Chemical shift (ppm) ^c							
	2	3	4	5	6	7	8	9
phen-azo-2,6-dimethylphenol ^a	9.34	7.81	9.13	—	8.12 (S) ^d	8.69	7.93	9.22
phen-azo-2,6-dimethylphenol ^b	9.32	7.68	9.22	—	8.01 (S) ^d	8.39	7.73	9.32
phen-azo-p-phenol ^a	9.32	7.93	9.14	—	8.16 (S) ^d	8.70	7.82	9.23
5-NO ₂ -phen ^a	9.29	7.97	8.89	—	9.04 (S) ^d	8.78	7.94	9.24

b. 2,6-dimethylphenol moiety:

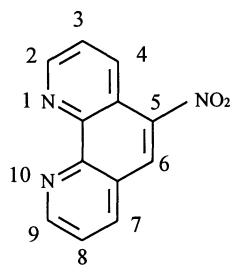
	Chemical shift (ppm) ^c					
	3'	4'	5'	7'	8'	9'
Phen-azo-2,6-dimethylphenol ^a	7.80	—	7.80	—	2.33 (S) ^d	2.33 (S) ^d
Phen-azo-2,6-dimethylphenol ^b	7.81	—	7.81	5.25	2.40 (S) ^d	2.40 (S) ^d
2,6-dimethylphenol ^a	6.88	6.62	6.88	8.14	2.15 (S) ^d	2.15 (S) ^d
2,6-dimethylphenol ^b	6.97	6.75	6.97	4.6	2.25	2.25

^a DMSO was used as solvent.

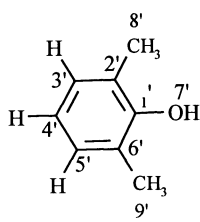
^b CDCl₃ was used as solvent.

^c All chemical shift values, except where indicated, represent centers of multiplets.

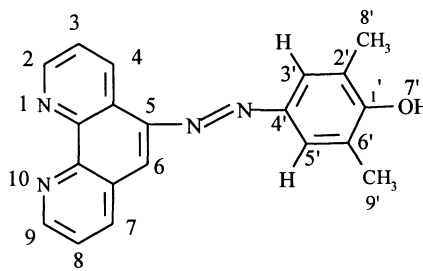
^d S = singlet.



5-NO₂-phen



2,6-dimethylphenol



phen-azo-2,6-dimethylphenol

Table 3-6

$^1\text{H-NMR}$ assignment for $fac\text{-Re}^I(\text{CO})_3(\text{phen})\text{Cl}$, $fac\text{-Re}^I(\text{CO})_3(\text{phen-azo-p-phenol})\text{Cl}$
and related compounds ^a

a. Phen moiety:

	Chemical shift (ppm) ^b							
	2	3	4	5	6	7	8	9
$fac\text{-Re}^I(\text{CO})_3(\text{phen})\text{Cl}$	9.45	8.12	8.99	8.34 (S) ^c		8.99	8.12	9.45
1,10-phen	9.12	7.79	8.51	8.01 (S) ^c		8.51	7.79	9.12
$fac\text{-Re}^I(\text{CO})_3(\text{phen-azo-p-phenol})\text{Cl}$	9.66	8.22	9.44	—	8.45 (S) ^c	9.13	8.12	9.55
phen-azo-p-phenol	9.32	7.93	9.14	—	8.16 (S) ^c	8.70	7.82	9.23

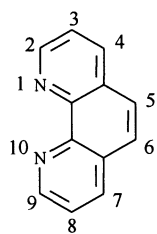
b. phenol moiety:

	Chemical shift (ppm) ^b					
	2'	3'	4'	5'	6'	7'
$fac\text{-Re}^I(\text{CO})_3(\text{phen-azo-p-phenol})\text{Cl}$	7.06	8.09	—	7.06	8.09	10.7
Phen-azo-p-phenol	7.02	8.05	—	7.02	8.05	10.6
phenol	6.76	7.16	6.76	7.16	6.76	9.35

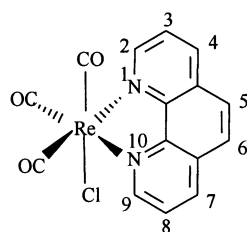
^a DMSO was used as solvent.

^b All chemical shift values, except where indicated, represent centers of multiplets.

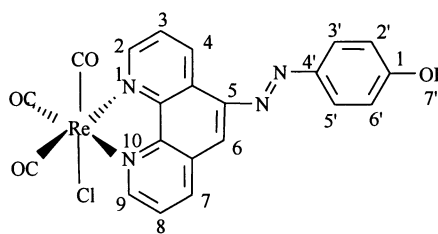
^c S = singlet.



phen



$fac\text{-Re}(\text{CO})_3(\text{phen})\text{Cl}$



$fac\text{-Re}(\text{CO})_3(\text{phen-azo-p-phenol})\text{Cl}$

Table 3-7Carbonyl Stretching Frequencies ^a

Complex	$\nu_{\text{C=O}}$ (cm^{-1})			
$\text{Re}^{\text{I}}(\text{CO})_5\text{Cl}^{\text{b}}$	2151	2044	2013	1979
<i>fac</i> - $\text{Re}^{\text{I}}(\text{CO})_3((\text{CH}_3)_2\text{bpy})\text{Cl}^{\text{b}}$	2018	1932	1919	1878
<i>fac</i> - $\text{Re}^{\text{I}}(\text{CO})_3(\text{phen})\text{Cl}$ (literature) ^c	2015	1912	1890	
<i>fac</i> - $\text{Re}^{\text{I}}(\text{CO})_3(\text{phen})\text{Cl}$ (this work)	2018	1933	1904	1879
<i>fac</i> - $\text{Re}^{\text{I}}(\text{CO})_3(\text{phen-azo-p-phenol})\text{Cl}$	2026	1920	1896	

^a In KBr unless otherwise noted.

^b Reference 43. Taken in KBr.

^c Reference 37. Taken in CH_2Cl_2 .

Table 3-8

UV-Vis data for phen-azo dyes and related compounds.

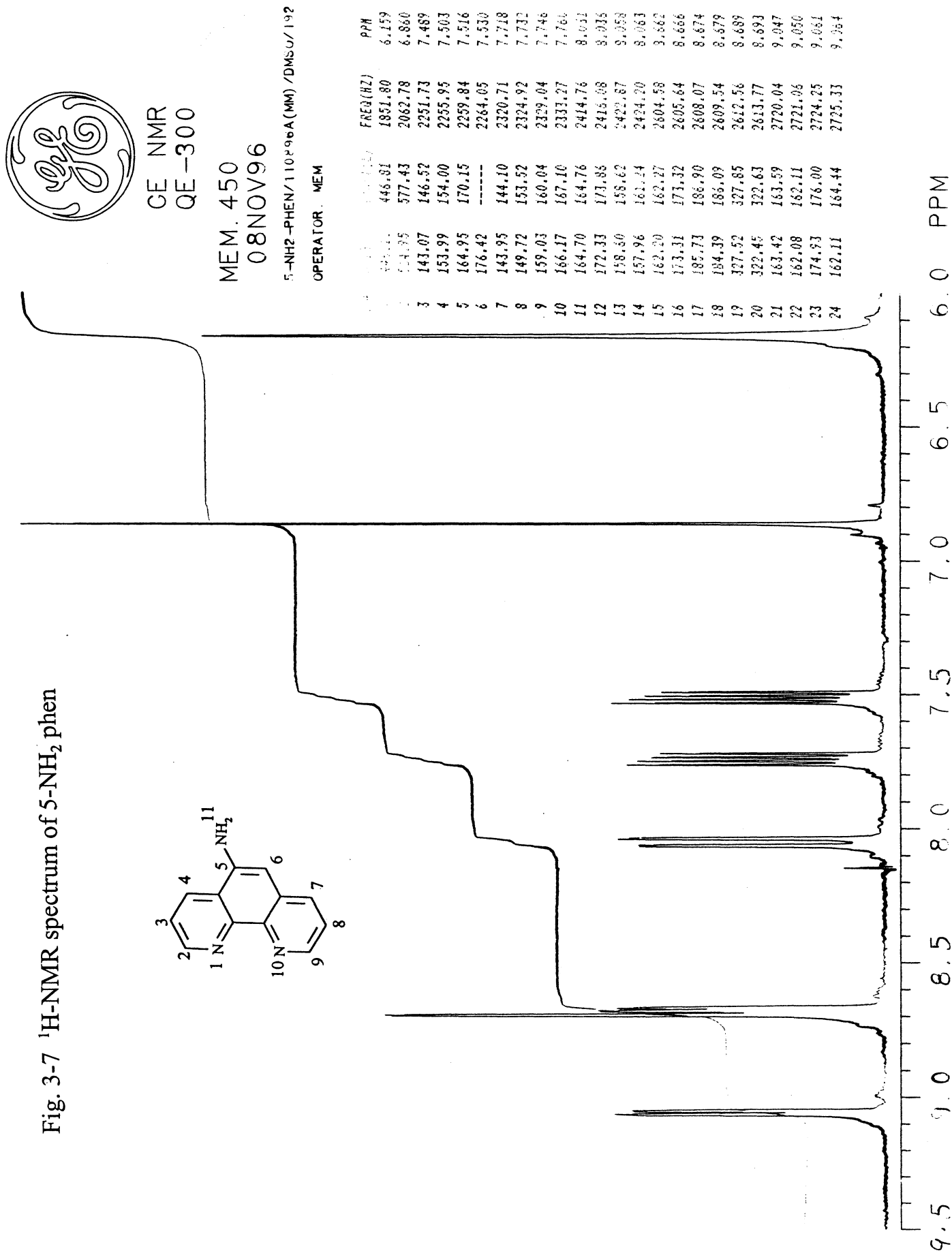
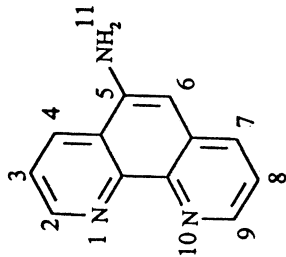
Compounds	solvent	λ_{\max} (nm) (ϵ in $M^{-1} cm^{-1}$)
phen-azo-2-naphthol	MeOH	498.0 (2.03×10^4) 422.5 (sh) 324.5 (sh) 273.5 (2.43×10^4) 224.0 (6.17×10^4)
2-naphthol	MeOH	330.5 (2.08×10^3) 318.5 (1.95×10^3) 285.5 (3.45×10^3) 274.5 (4.79×10^3) 264.5 (4.24×10^3) 253.0 (sh) (2.91×10^3) 225.5 (7.29×10^4)
phen-azo-p-phenol	MeOH	380.0 (2.77×10^4) 273.5 (2.23×10^4) 252.0 (2.36×10^4) 222.0 (3.34×10^4)
phenol	MeOH	280.0 (sh) 273.0 (1.68×10^3) 217.5 (5.49×10^3)

Table 3-8 (contd)

phen-azo-2,6-dimethylphenol	MeOH	389.5 (2.28×10^4) 273.5 (sh) 254.0 (2.06×10^4) 222.0 (3.10×10^4)
2,6-dimethylphenol	MeOH	280.0 (sh) 273.0 (1.40×10^3) 215.0 (sh)
phen	MeOH	263.5 (2.74×10^4) 229.5 (4.26×10^4)
phen ^a	CH ₃ CN	275(sh), 263, 230, 226, 197
<i>fac</i> -Re ^I (CO) ₃ (phen)Cl	MeOH	370.0 (4.17×10^3) (broad) 291.5 (sh) 273.5 (2.62×10^4) 258.0 (sh) 217.0 (sh)
<i>fac</i> -Re ^I (CO) ₃ (phen-azo-p-phenol)Cl	MeOH	390.0 (3.35×10^4) 280.0 (2.34×10^4) 248.0 (3.15×10^4)

^a reference 36.

Fig. 3-7 ¹H-NMR spectrum of 5-NH₂ phen



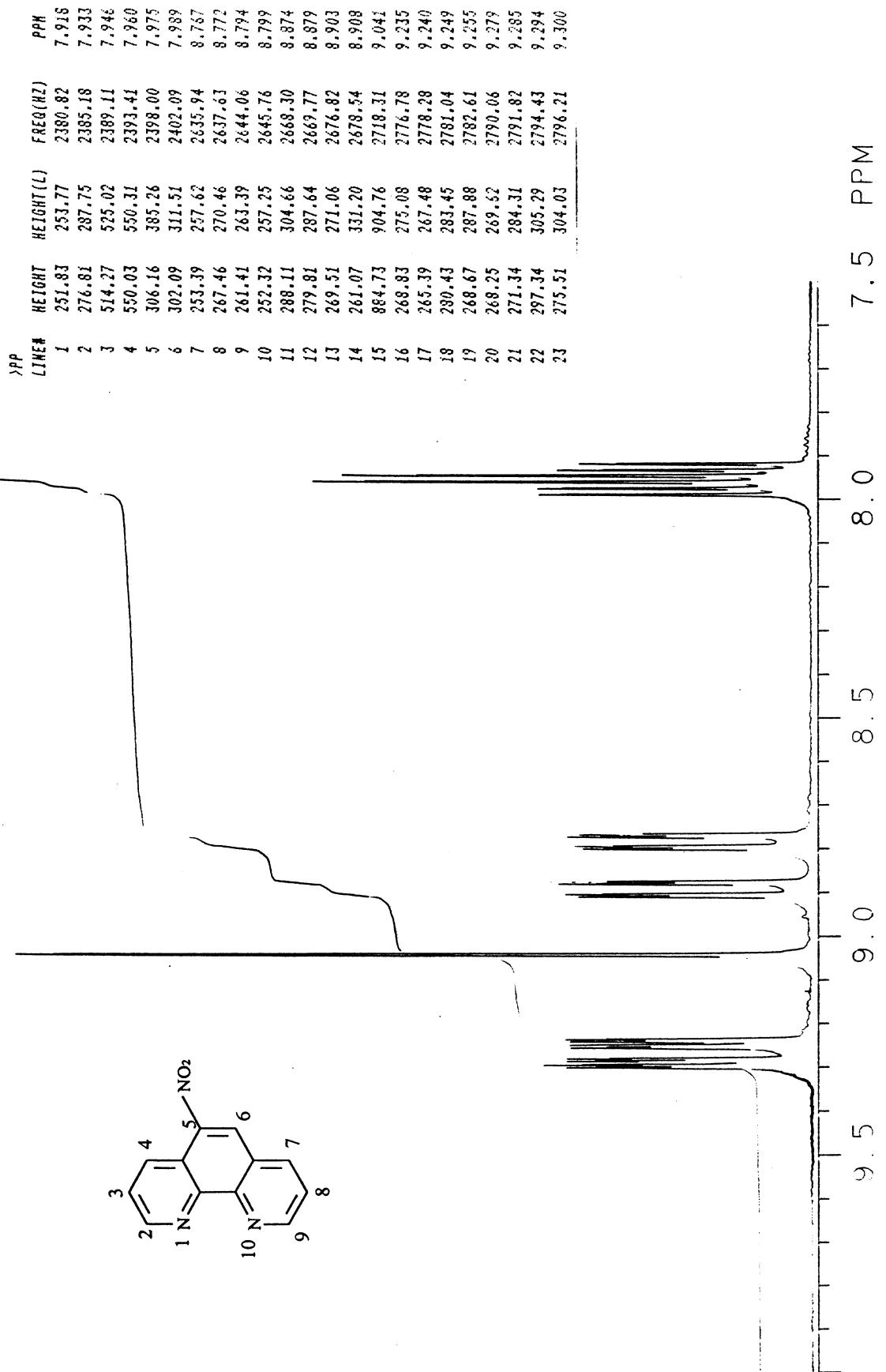
GE NMR
QE-300

MEM. 450
08NOV96

5-NH₂-PHEN/110²96A(NM)/DMSO/192
OPERATOR: MEM

LINE	PPM	FREQ(HZ)	PPM
1	9.10	446.81	1881.80
2	8.80	577.43	2062.78
3	8.43	146.52	2251.73
4	8.39	154.00	2255.95
5	8.35	170.15	2259.84
6	8.32	-----	2264.05
7	8.28	144.10	2320.71
8	8.25	153.52	2324.92
9	8.22	160.04	2329.04
10	8.18	167.10	2333.27
11	8.15	184.76	2414.76
12	8.12	173.86	2418.08
13	8.08	188.62	2422.87
14	8.05	161.34	2424.20
15	8.02	162.27	2604.58
16	7.98	173.32	2605.64
17	7.95	186.90	2608.07
18	7.92	186.09	2609.54
19	7.88	327.85	2612.56
20	7.85	322.63	2613.77
21	7.82	163.59	2720.04
22	7.78	162.08	2721.95
23	7.75	174.93	2724.25
24	7.72	164.44	2725.33

Fig. 3-8 ¹H-NMR spectrum of 5-NO₂ phen





MEMO NMR
NO. 100

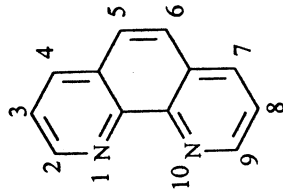
MEM. 704

22 JUN 66

PHEN IN DMF-D₂

TEMPERATURE 300

Fig. 3-9 ¹H-NMR spectrum of phen



LINE#	HEIGHT	HEIGHT(L)	FREQ(HZ)	PPM
1	344.94	359.80	2336.26	7.770
2	359.92	362.19	2340.59	7.784
3	388.41	406.87	2344.34	7.797
4	384.39	385.39	2348.62	7.811
5	1355.79	1414.19	2408.42	8.010
6	491.95	497.63	2554.18	8.495
7	394.27	427.48	2555.73	8.500
8	469.70	473.63	2562.25	8.522
9	365.63	367.01	2563.78	8.527
10	461.35	461.84	2739.72	9.112
11	371.45	371.87	2741.17	9.117
12	464.62	474.68	2744.02	9.126
13	356.42	371.97	2745.45	9.131

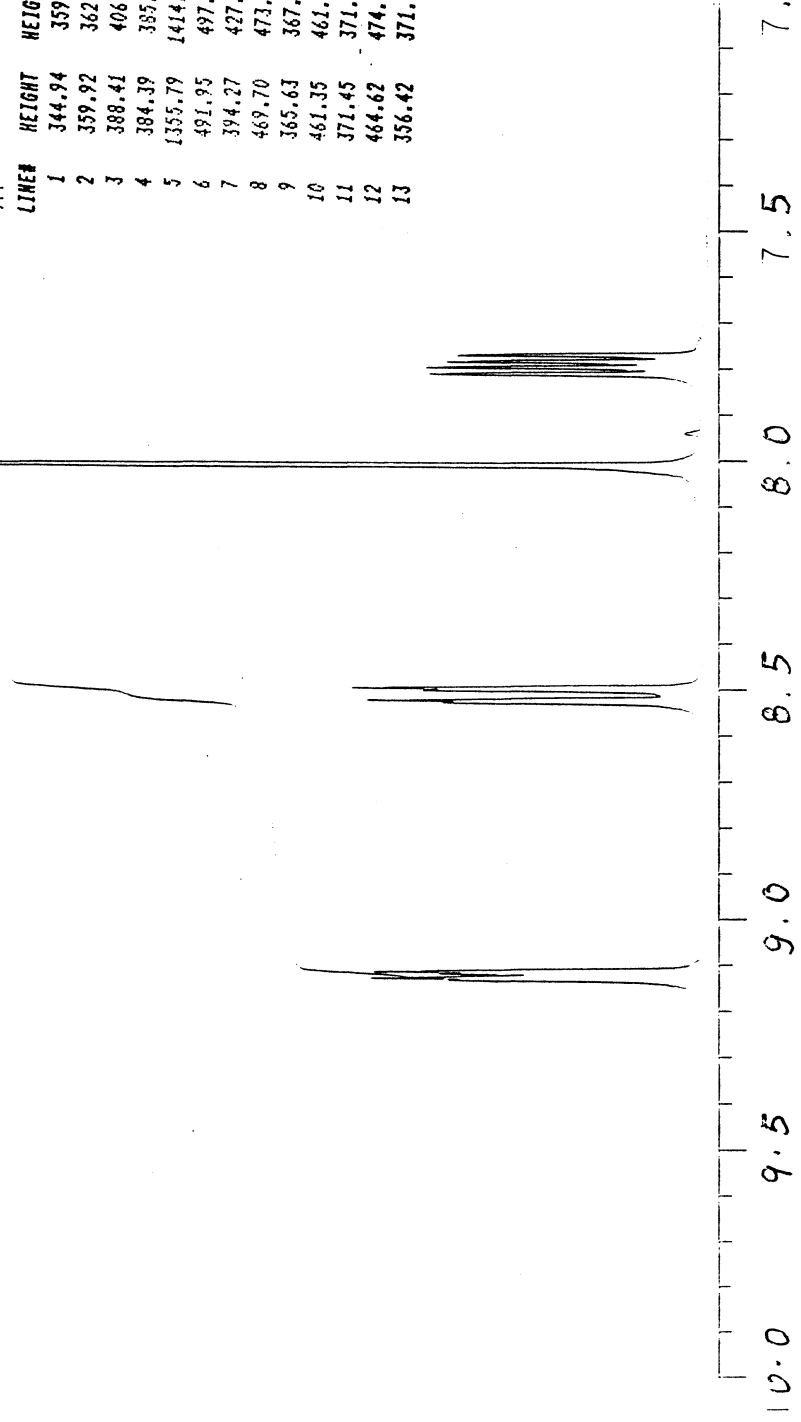


Fig. 3-10 a ¹H-NMR spectrum of phenyl-azo-β-naphthol (16.0 - 6.5 ppm) (product of model reaction)

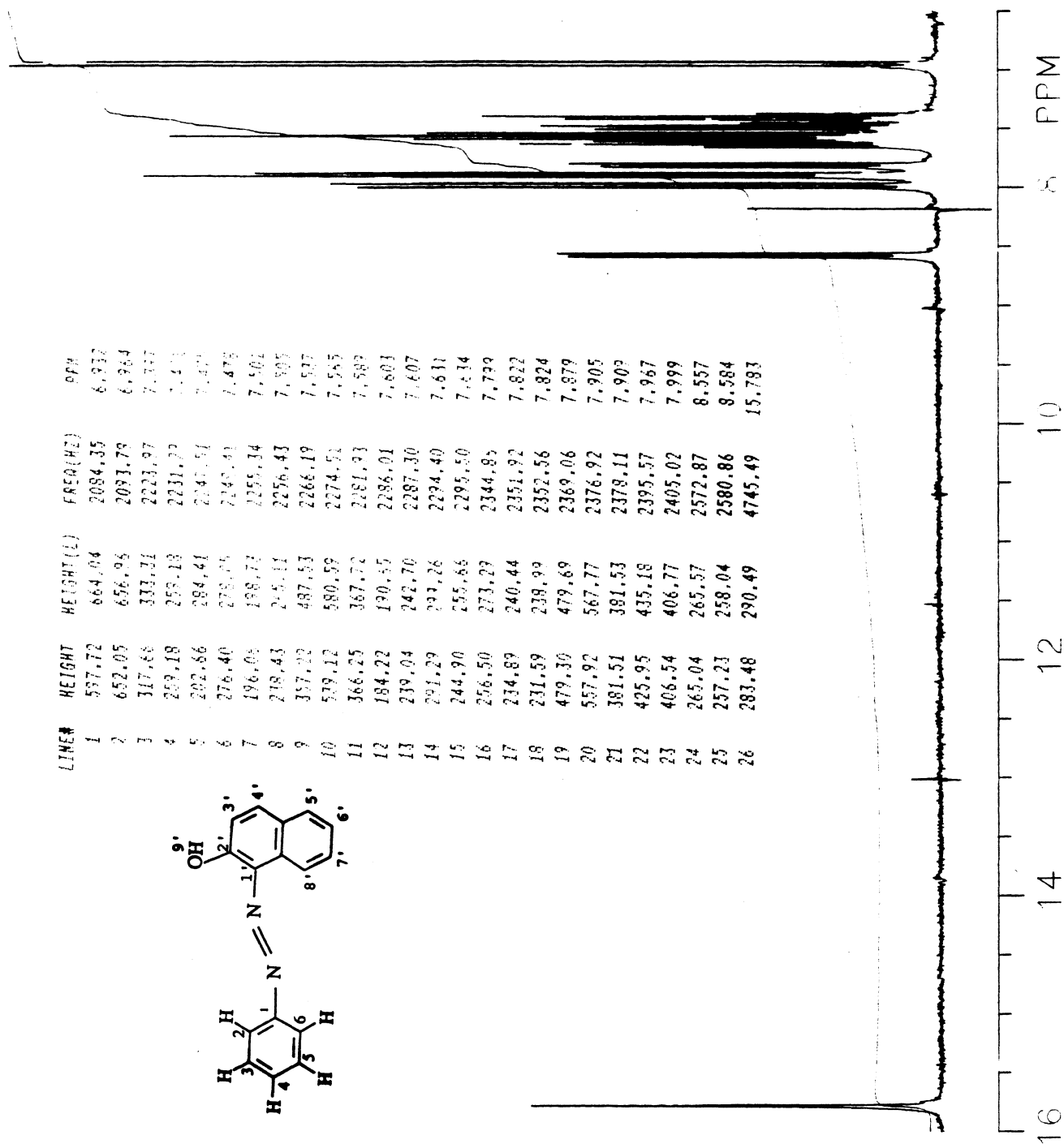


Fig. 3-10 b ¹H-NMR spectrum of phenyl-azo-β-naphthol (9.0 - 6.5 ppm) (product of model reaction)

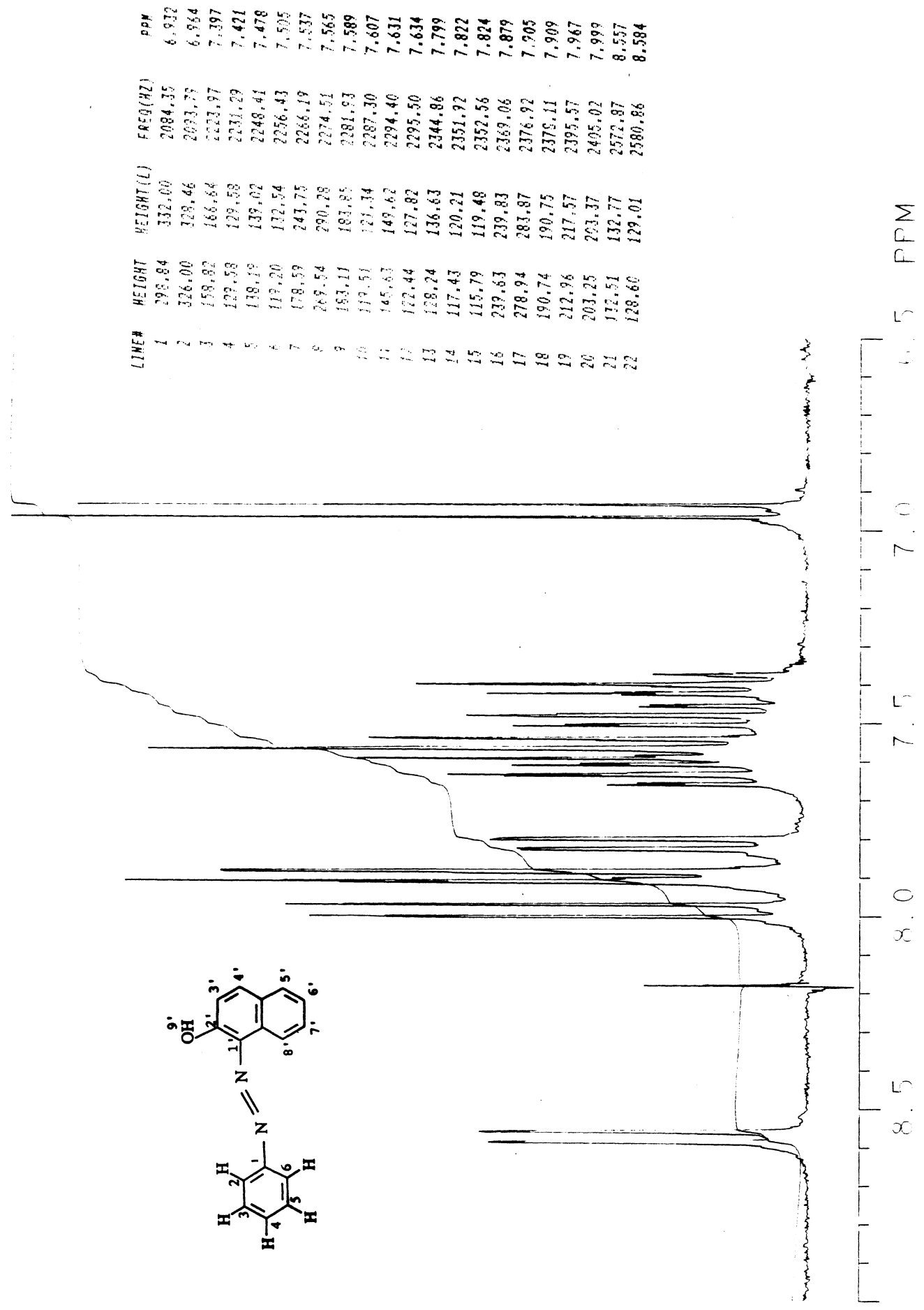


Fig. 3-11 a ¹H-NMR spectrum of phenyl-azo-β-naphthol (16.0 - 6.5 ppm) (97%, from Aldrich)

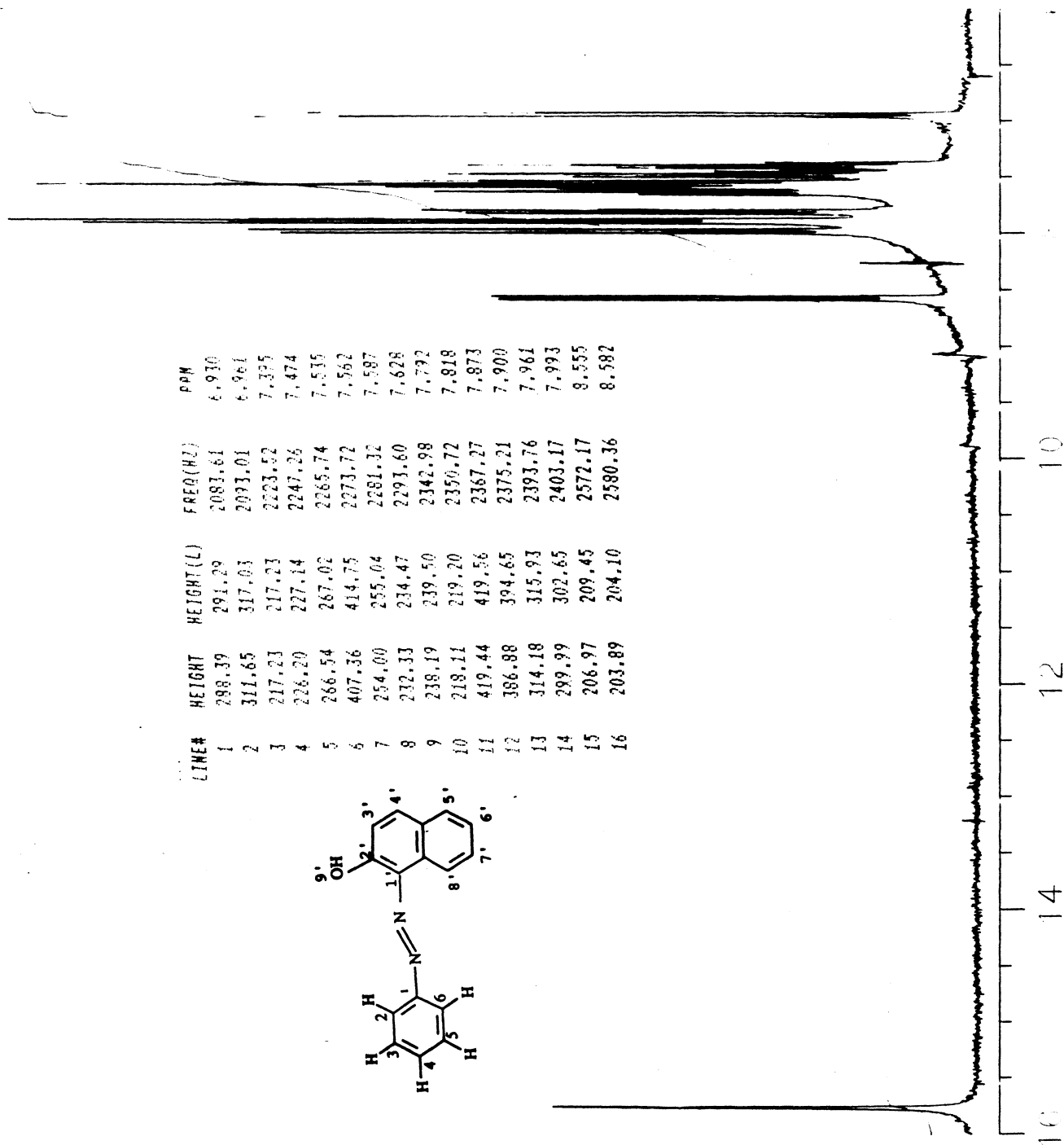


Fig. 3-11 b ¹H-NMR spectrum of phenyl-azo-β-naphthol (97%, from Aldrich)

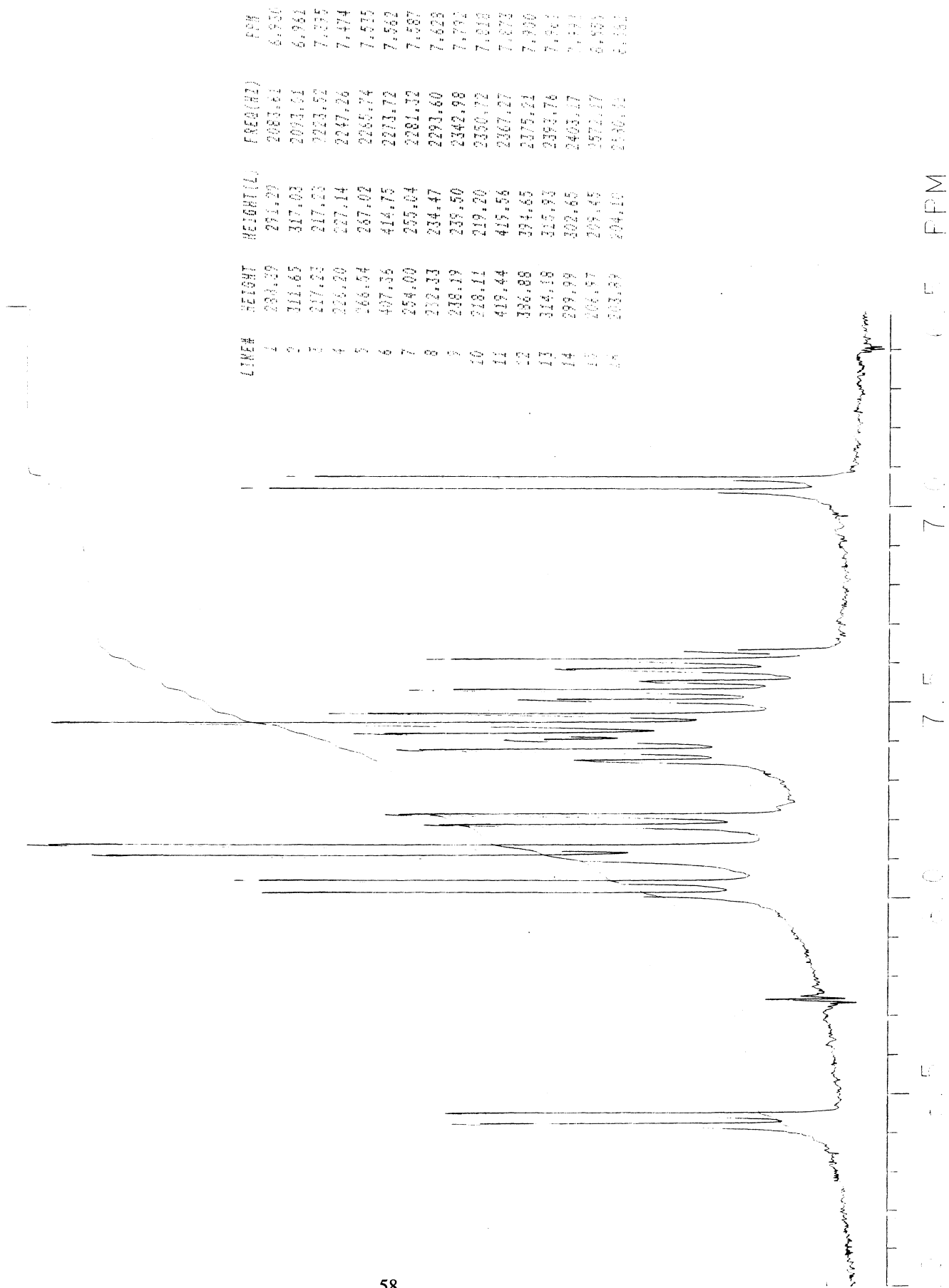
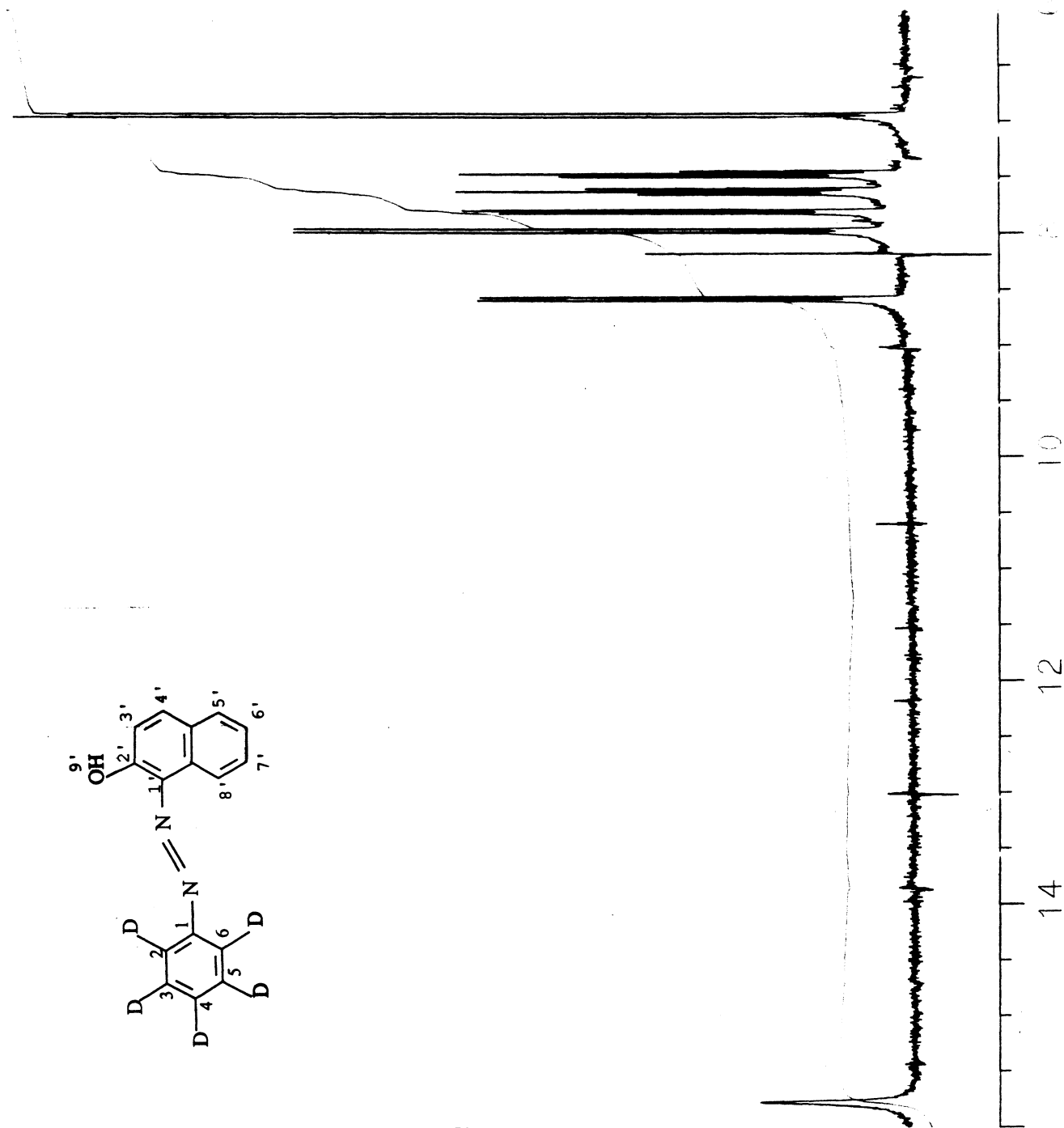
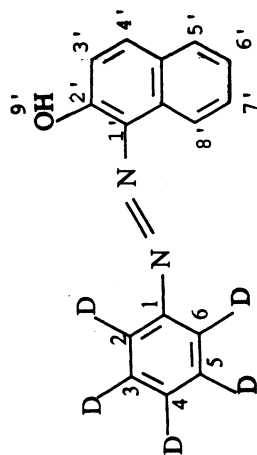


Fig. 3-12 a ¹H-NMR spectrum of 2,3,4,5,6-d-phenyl-azo-β-naphthol (16.0 - 6.5 ppm)



LINE#	HEIGHT	HEIGHT(L)	FREQ(HZ)	PPM
1	620.07	644.98	2082.60	6.926
2	660.60	741.34	2092.01	6.958
3	138.81	147.72	2337.70	7.442
4	164.57	164.89	2338.70	7.446
5	327.67	327.79	2245.84	7.469
6	253.93	274.34	2252.57	7.492
7	251.49	252.25	2253.57	7.495
8	168.11	232.82	2284.03	7.596
9	234.03	235.96	2285.35	7.601
10	329.99	332.58	2292.46	7.624
11	287.51	298.00	2293.50	7.628
12	172.26	195.46	2299.40	7.647
13	195.21	200.89	2300.67	7.652
14	325.35	326.28	2342.74	7.792
15	297.76	305.73	2350.61	7.818
16	452.81	494.84	2392.35	7.957
17	453.05	481.23	2401.75	7.988
18	189.84	192.06	2459.13	8.179
19	311.80	312.32	2575.82	8.567
20	314.00	314.03	2583.96	8.594
21	106.33	106.44	4743.96	15.778
22	103.52	103.73	4745.27	15.783

Fig. 3-12 b $^1\text{H-NMR}$ spectrum of 2,3,4,5,6-d-phenyl-azo- β -naphthol (9.0 - 6.5 ppm)

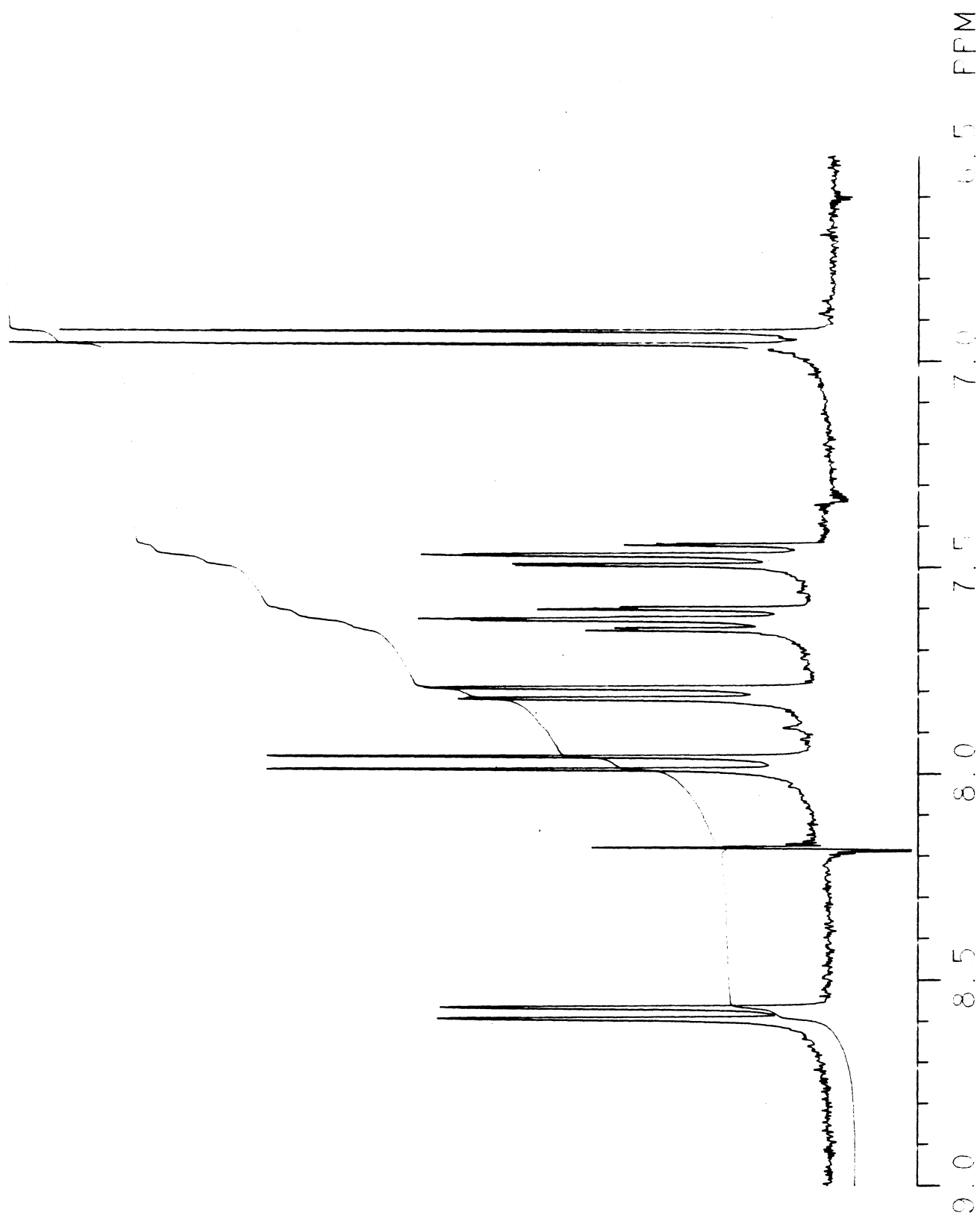


Fig. 3-13 a ¹H-NMR spectrum of phen-azo-β-naphthol (17.3 - 6.5 ppm)

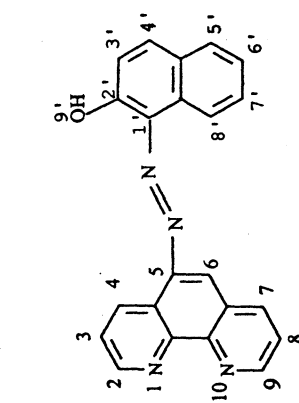


GE NMR
QE -200

MEM. 595
17 APR 96

PHEN-AZO-β-NAPH/0417/1A 1MM
FRAN/45.45.10 1HL.ET.ME

OPERATOR: MM



LINE#	HEIGHT	HEIGHT(L)	FREQ(HZ)	PPM
1	303.54	310.00	2107.05	7.008
2	323.56	323.84	2116.52	7.039
3	96.45	103.00	2263.10	7.527
4	224.90	227.23	2270.72	7.552
5	174.11	176.47	2278.07	7.576
6	145.29	146.32	2312.44	7.691
7	203.90	214.46	2319.74	7.715
8	220.75	222.49	2320.44	7.717
9	143.34	143.38	2327.69	7.742
10	167.52	169.71	2349.02	7.812
11	182.17	188.76	2353.33	7.827
12	287.17	298.00	2357.67	7.841
13	296.94	299.65	2358.81	7.845
14	269.35	269.55	2360.66	7.851
15	244.68	245.18	2366.84	7.872
16	159.70	167.42	2408.86	8.011
17	172.40	173.43	2413.08	8.026
18	186.56	187.13	2417.26	8.039
19	198.53	203.04	2421.56	8.054
20	337.24	337.24	2424.49	8.064
21	307.20	311.85	2433.99	8.095
22	90.35	-----	2454.74	8.164
23	407.81	411.03	2459.05	8.178
24	553.11	564.19	2605.57	8.666
25	209.03	209.46	2619.60	8.712
26	369.49	392.18	2627.61	8.739
27	431.25	432.83	2635.52	8.765
28	256.41	259.20	2643.51	8.792
29	190.72	196.19	2733.21	9.090
30	199.02	199.12	2734.12	9.093
31	234.18	234.40	2737.97	9.106
32	214.89	215.95	2782.59	9.255
33	225.15	225.78	2786.75	9.268

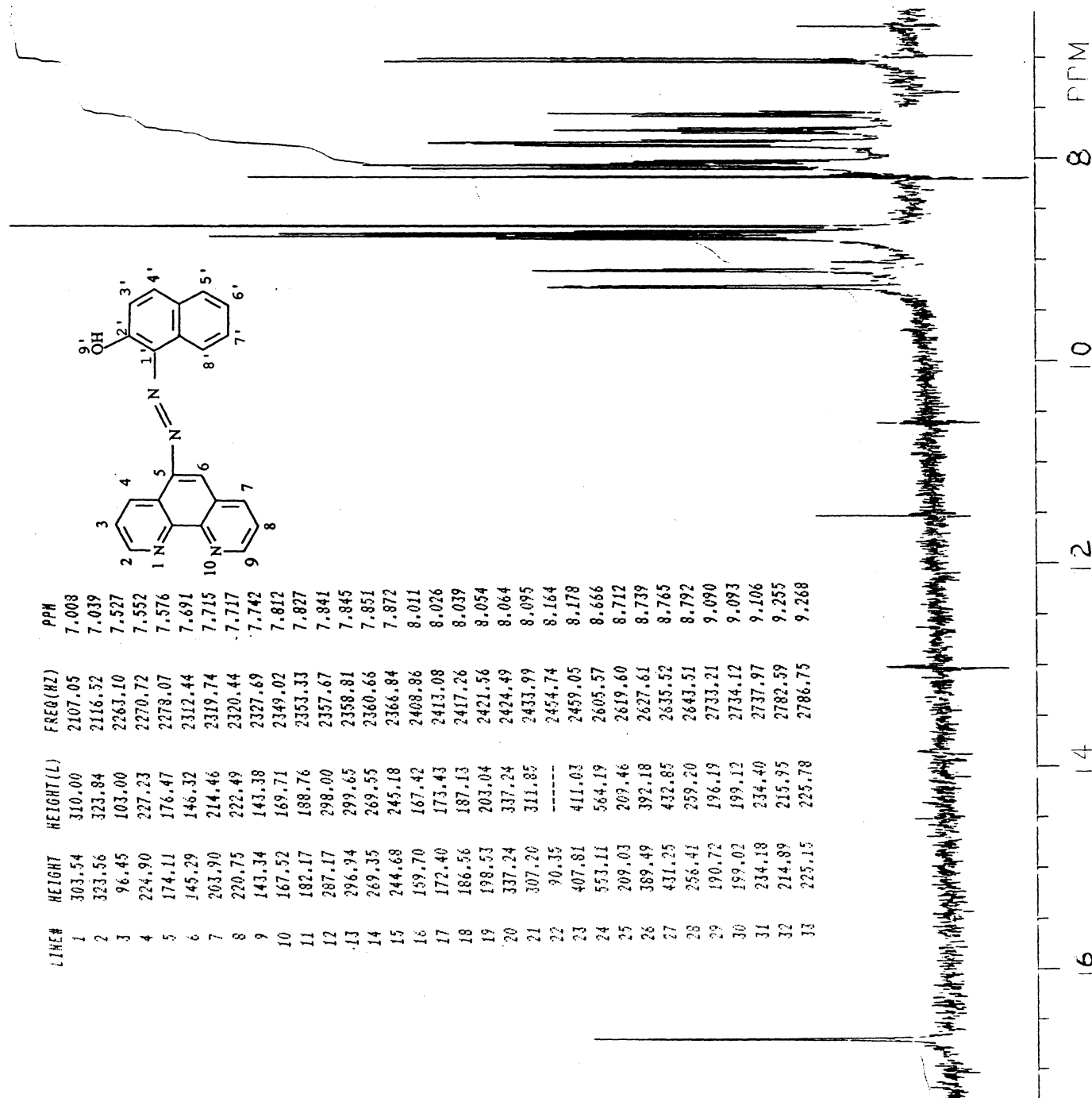


Fig. 3-13 b ¹H-NMR spectrum of phen-azo-β-naphthol (10.0 - 6.5 ppm)

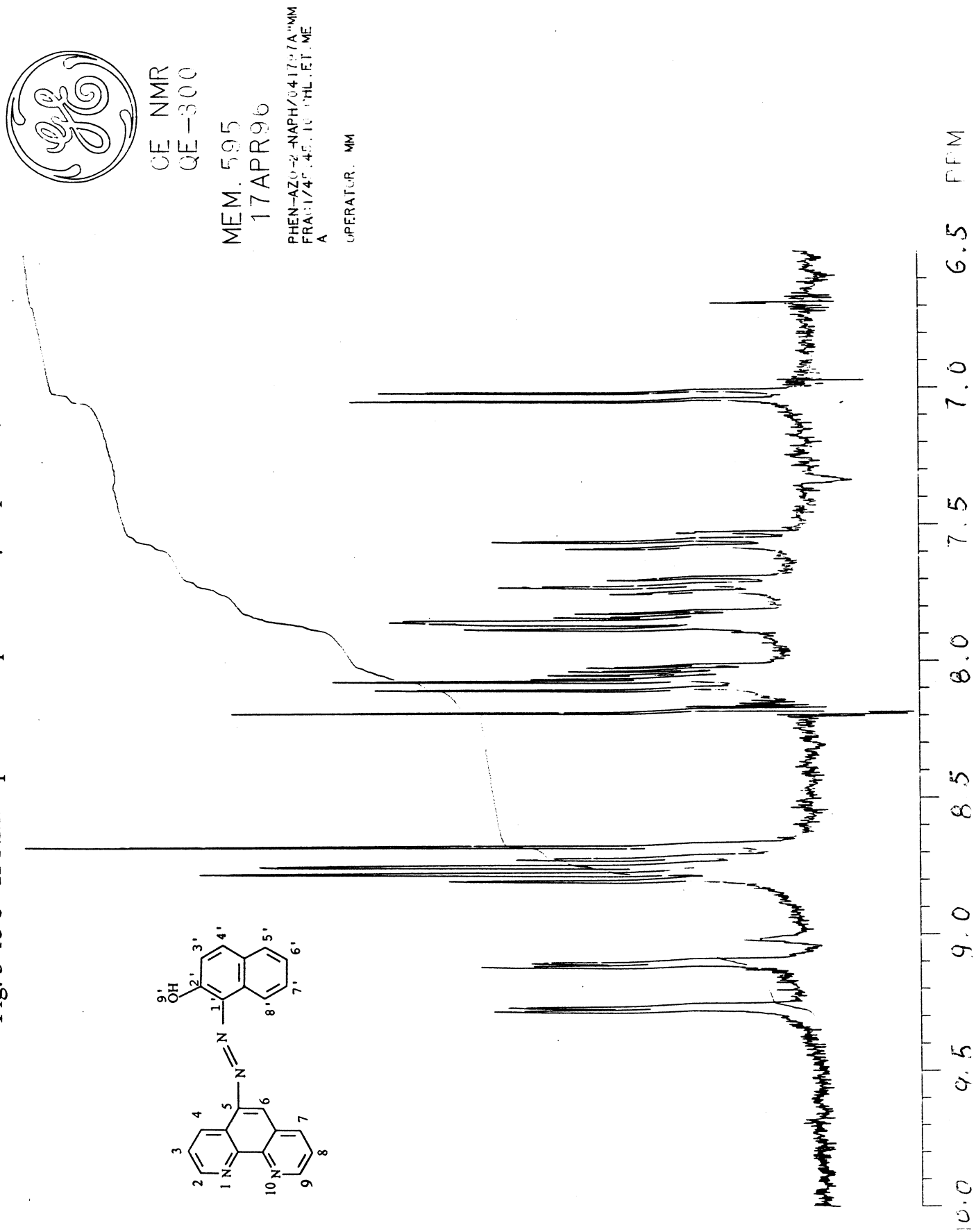
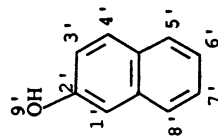


Fig. 3-14 ¹H-NMR spectrum of β-naphthol



2-NAPHTHOL
IN D₆-DMSO

LINE#	HEIGHT	HEIGHT (L)	FREQ(HZ)	PPM
1	251.96	254.79	2121.38	7.062
2	336.25	340.60	2125.03	7.068
3	336.13	337.56	2125.59	7.069
4	240.91	243.56	2132.14	7.091
5	438.42	441.02	2133.90	7.097
6	455.15	464.12	2134.39	7.099
7	710.56	717.44	2138.01	7.111
8	218.60	220.07	2172.69	7.226
9	395.46	402.49	2179.59	7.249
10	394.14	412.38	2180.69	7.253
11	338.08	348.20	2187.61	7.276
12	273.87	276.82	2211.08	7.354
13	347.23	357.73	2218.14	7.377
14	414.16	418.61	2219.19	7.381
15	259.83	260.13	2226.09	7.404
16	464.27	464.37	2302.52	7.658
17	400.83	402.66	2310.75	7.685
18	544.41	547.19	2325.58	7.735
19	479.50	481.20	2329.51	7.748
20	538.74	544.18	2334.33	7.764
21	447.24	448.43	2337.58	7.774
22	420.91	422.15	2928.20	9.739

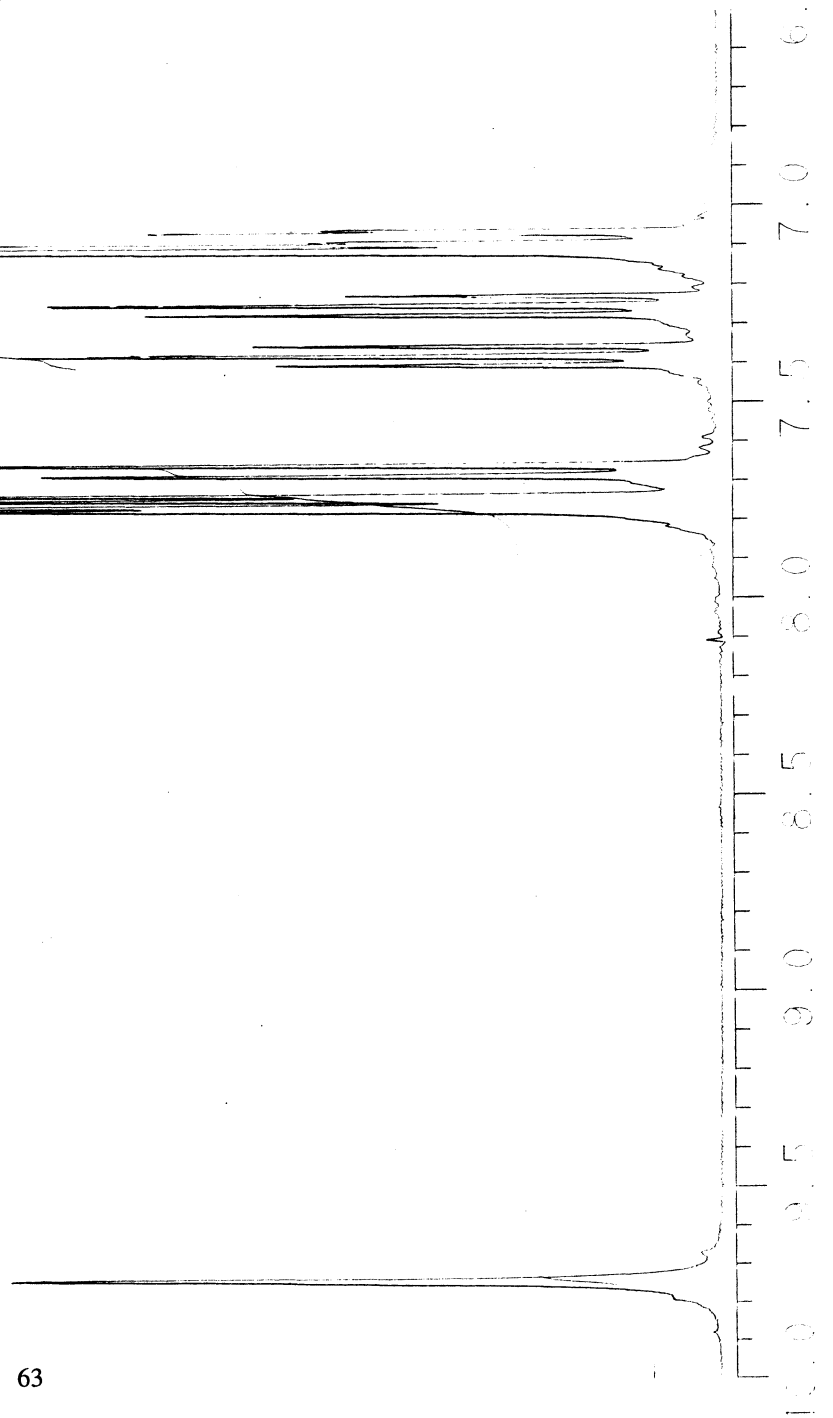


Fig. 3-15 ¹H-NMR spectrum of phen-azo-p-phenol

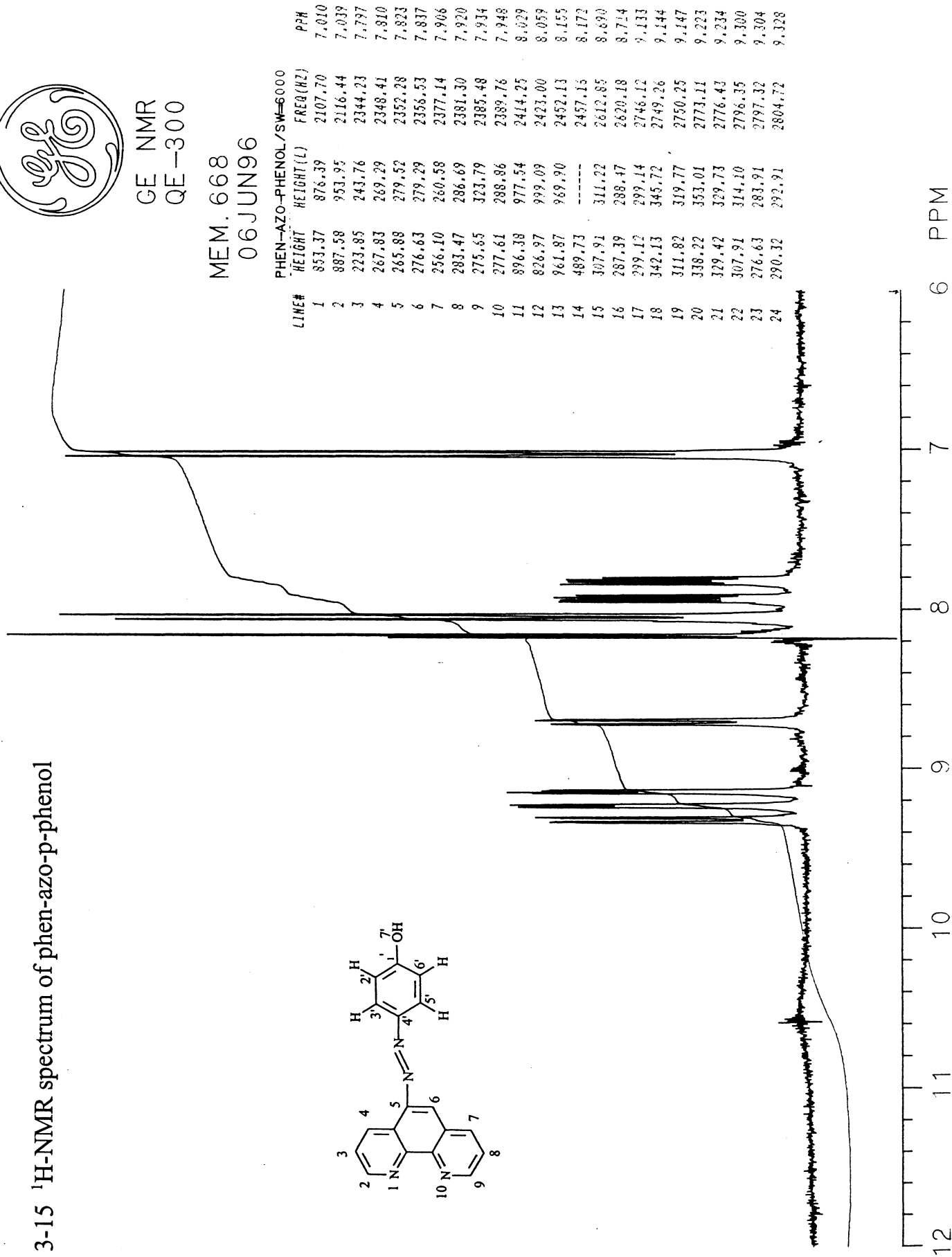
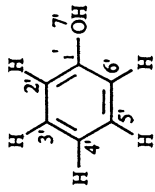


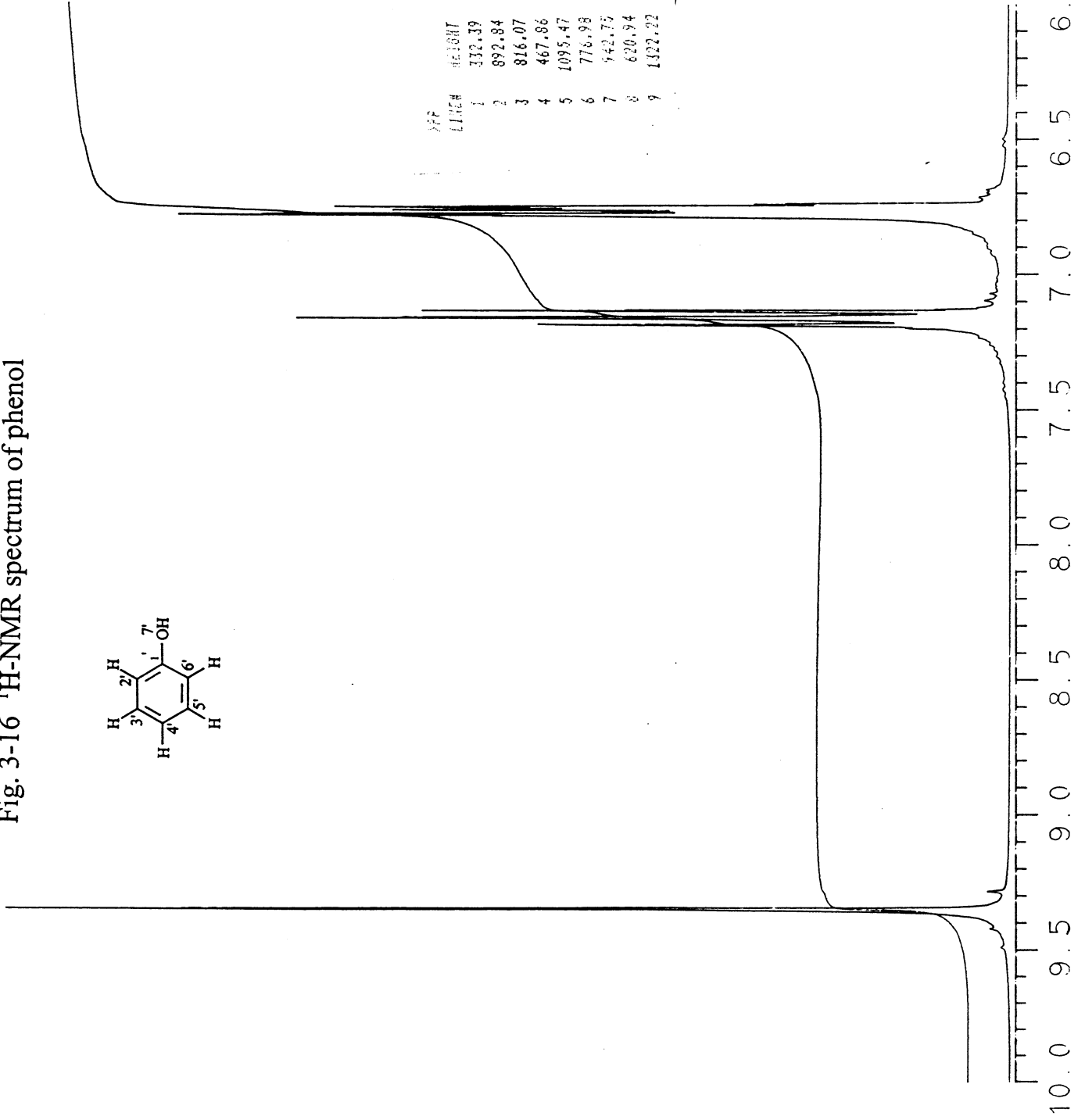
Fig. 3-16 ¹H-NMR spectrum of phenol



GE NMR
QE-300

MEM. 675
09JUN96

PHENOL IN DMSO
OPERATOR: MM



PPM	LINE#	HEIGHT	HEIGHT(L)	FREQ(HZ)	PPM
6.742	1	332.39	335.03	2027.04	6.742
6.771	2	892.84	893.08	2036.25	6.771
6.781	3	816.07	880.60	2033.31	6.781
6.771	4	467.86	468.07	2035.77	6.771
6.781	5	1095.47	1095.56	2033.04	6.781
7.136	6	776.98	777.13	2145.58	7.136
7.163	7	942.75	1002.26	2153.69	7.163
7.188	8	620.94	692.99	2161.35	7.188
9.350	9	1322.22	1396.99	2811.25	9.350

Fig. 3-17 a ¹H-NMR spectrum of phen-azo-2,6-dimethylphenol (in DMSO) (10.0 - 0.5 ppm)



GE NMR
QE-300

MEM. 592
17 APR 96

PHEN-AZO-DIMETHYLPHENOL
0.41797MM/50.50 CHCL3.ETOH
AL

OPERATOR: MM

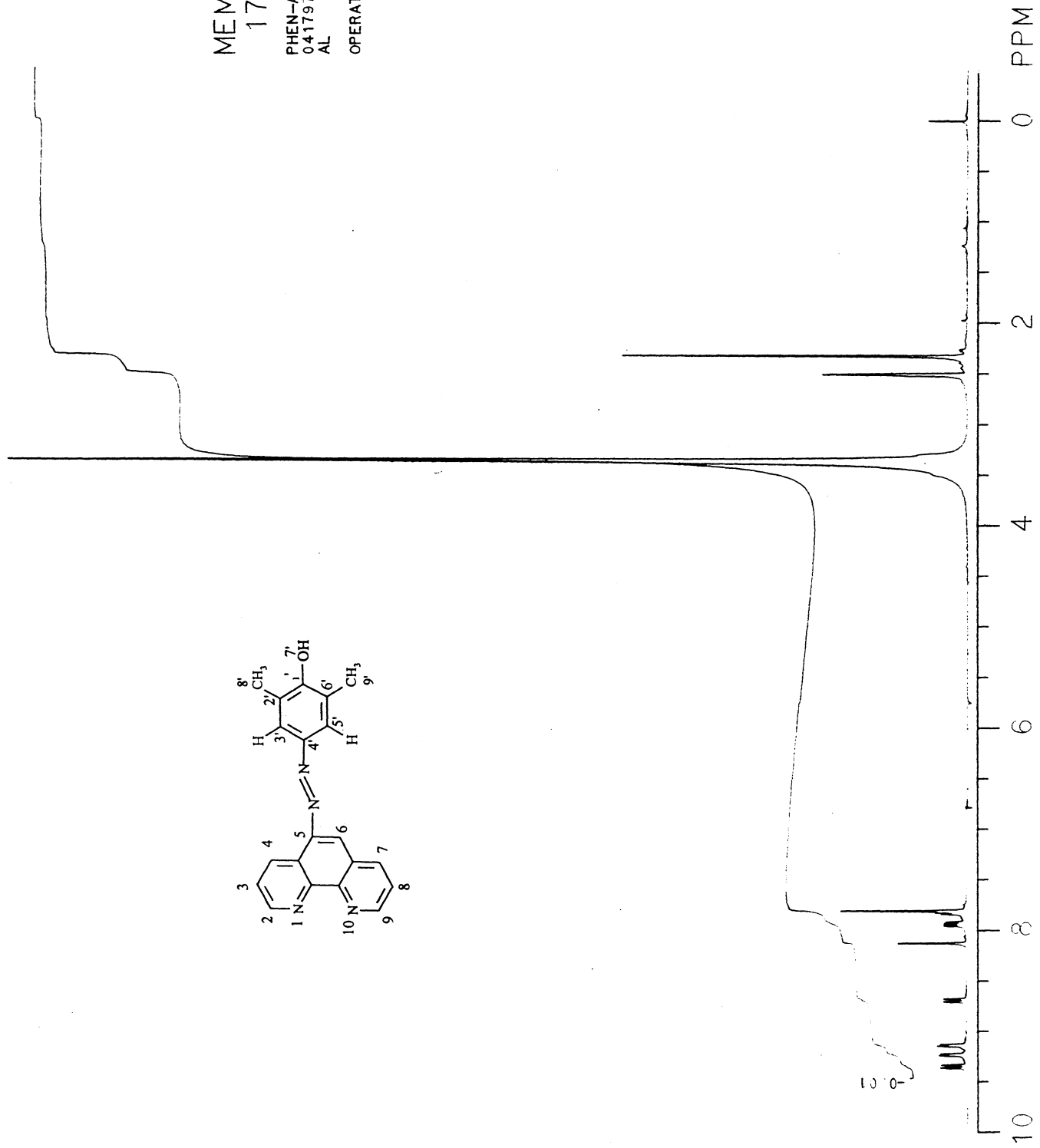
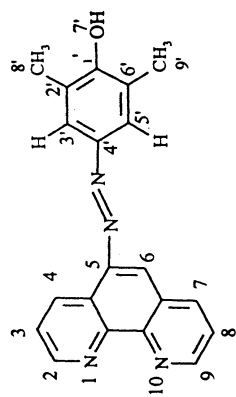


Fig. 3-17 b ¹H-NMR spectrum of phen-azo-2,6-dimethylphenol (in DMSO) (10.0 - 7.0 ppm)

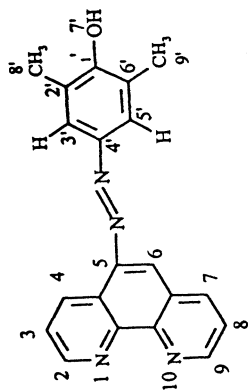


GE NMR
QE-300

MEM. 592
17 APR 96

PHEN-AZO-DIMETHYLPHENOL
0.41797MM/50:50 CHCL3.ETOH
AL

OPERATOR: MM



LINE#	HEIGHT	HEIGHT(L)	FREQ(HZ)	PPM
1	1400.72	1411.97	2346.10	7.803
2	355.91	356.00	2350.74	7.818
3	287.06	290.46	2355.32	7.833
4	236.34	236.41	2378.12	7.909
5	255.02	259.51	2382.40	7.924
6	255.93	256.13	2386.44	7.937
7	254.89	256.34	2390.70	7.951
8	769.08	769.75	2441.34	8.120
9	261.61	262.95	2606.74	8.670
10	243.78	247.91	2607.79	8.673
11	262.65	267.65	2614.88	8.697
12	226.88	233.35	2615.98	8.700
13	300.00	302.88	2743.07	9.133
14	288.46	289.29	2744.27	9.137
15	336.14	338.29	2747.21	9.137
16	277.36	287.68	2748.51	9.142
17	259.21	300.47	2771.38	9.217
18	284.38	295.29	2772.72	9.222
19	309.03	311.33	2775.54	9.231
20	275.40	279.31	2776.57	9.235
21	283.46	284.90	2804.18	9.328
22	244.27	246.46	2805.20	9.332
23	294.02	294.35	2812.49	9.358

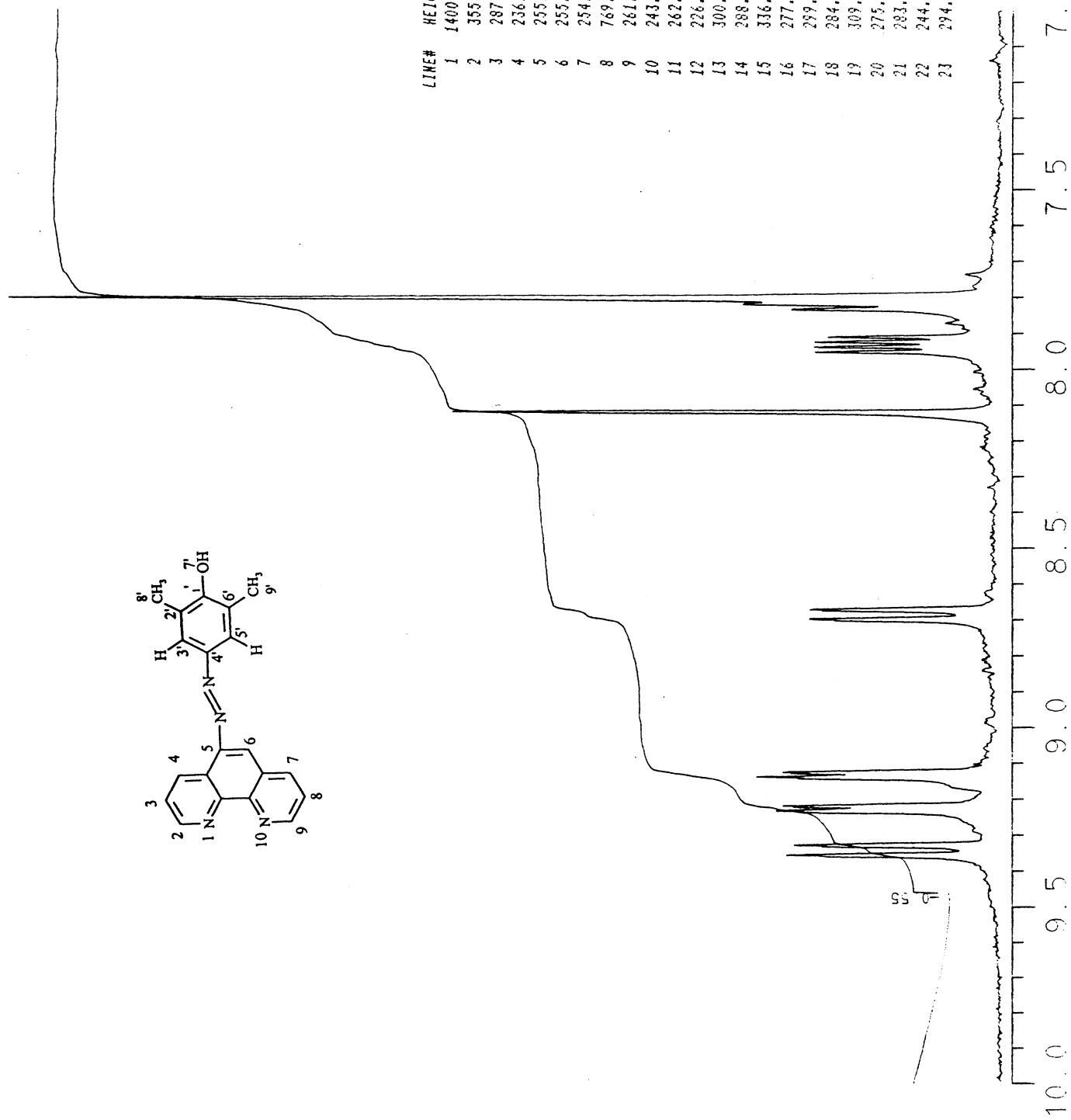


Fig. 3-18 a ¹H-NMR spectrum of phen-azo-2,6-dimethylphenol (in CDCl₃) (10.0 - 2.0 ppm)

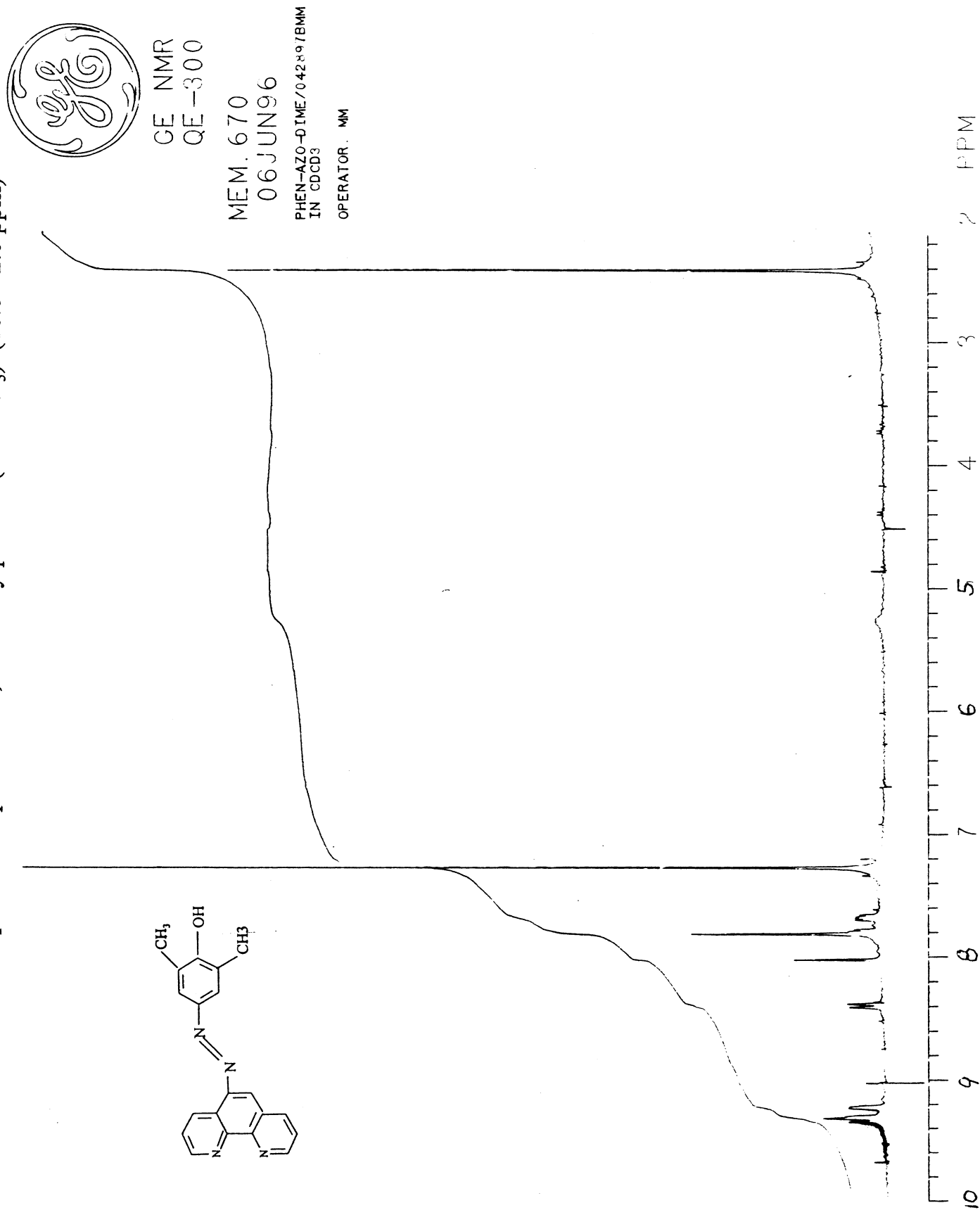


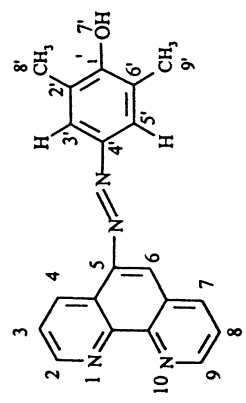
Fig. 3-18 b ¹H-NMR spectrum of phen-azo-2,6-dimethylphenol (in CDCl₃) (9.5 - 5.0 ppm)



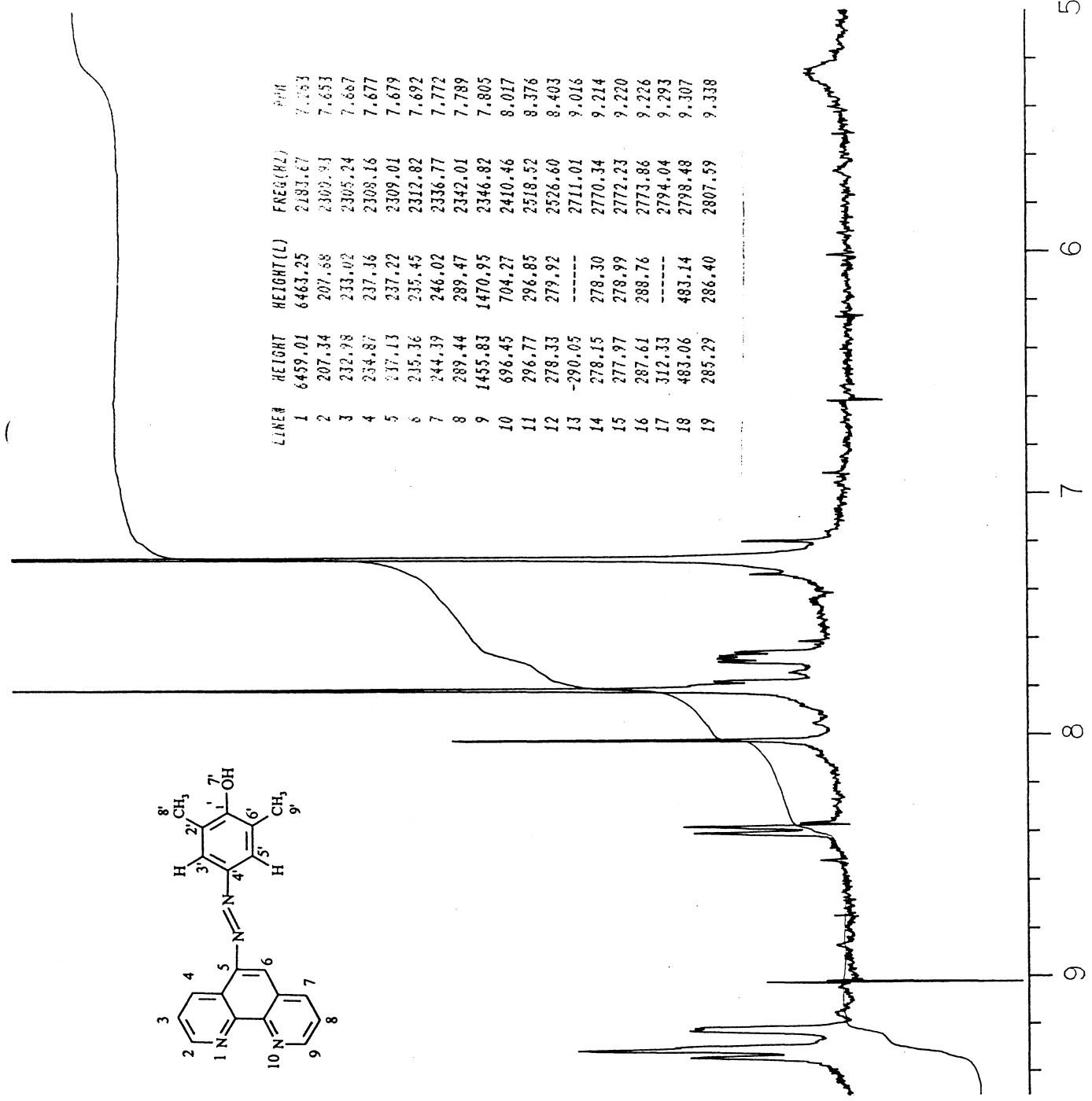
GE NMR
QE-300

MEM. 670
06JUN96

PHEN-AZO-DIME/042897BMM
IN CDCl₃
OPERATOR: MM



LINE#	HEIGHT	HEIGHT(L)	FREQ(Hz)	PPM
1	6459.01	6463.25	2181.67	7.153
2	207.34	207.68	2309.91	7.653
3	232.98	233.02	2305.24	7.667
4	234.87	237.16	2309.16	7.677
5	237.13	237.22	2309.01	7.679
6	235.36	235.45	2312.82	7.692
7	244.39	246.02	2336.77	7.772
8	289.44	289.47	2342.01	7.789
9	1455.83	1470.95	2346.82	7.805
10	696.45	704.27	2410.46	8.017
11	296.77	296.85	2518.52	8.376
12	278.33	279.92	2526.60	8.403
13	-290.05	-----	2711.01	9.016
14	278.15	278.30	2770.34	9.214
15	277.97	278.99	2772.23	9.220
16	287.61	288.76	2773.86	9.226
17	312.33	-----	2794.04	9.293
18	483.06	483.14	2798.48	9.307
19	285.29	286.40	2807.59	9.338



9 8 7 6 5 PPM

Fig. 3-19 a ¹H-NMR spectrum of 2,6-dimethylphenol (in DMSO) (9 - -0.5 ppm)

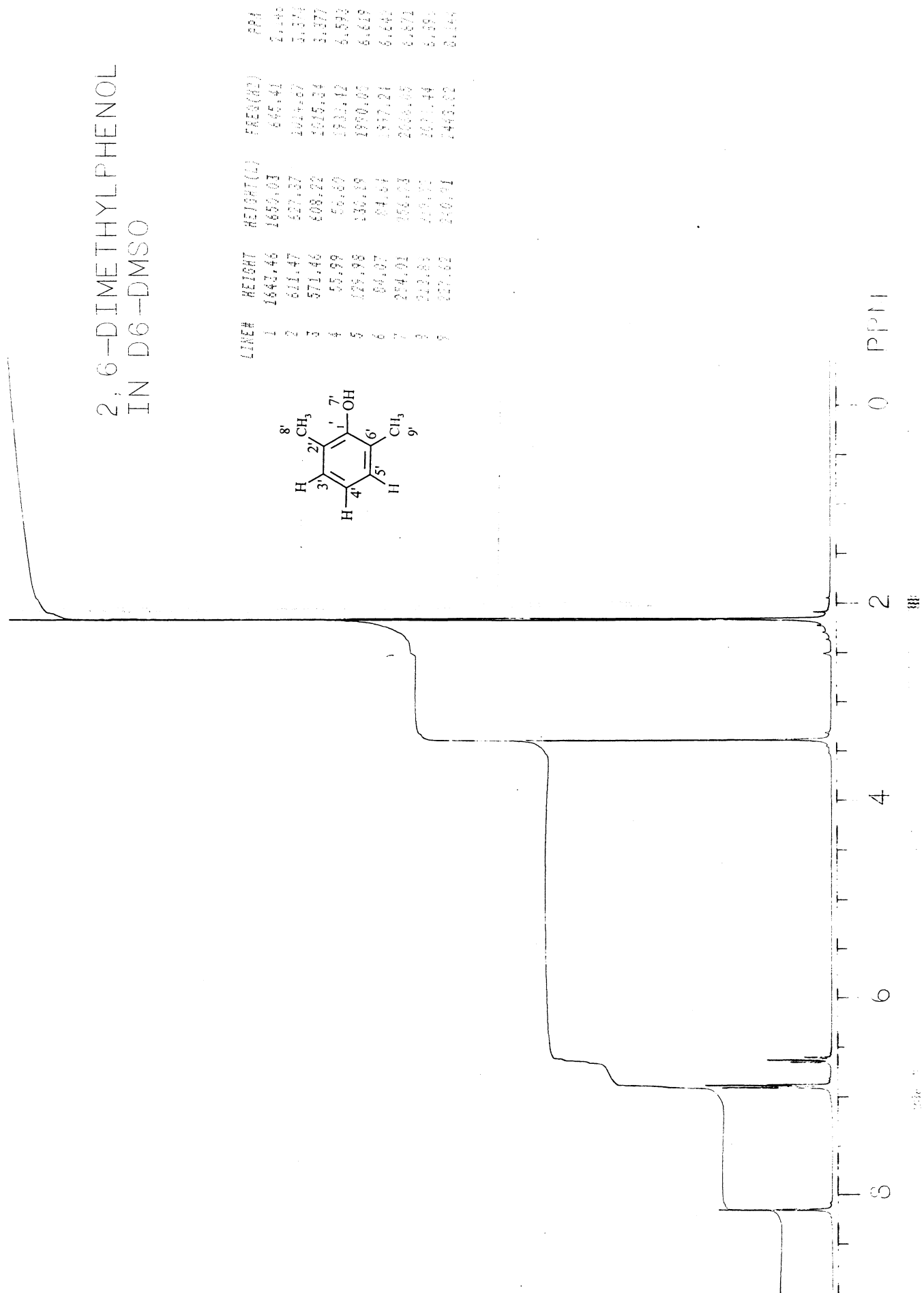


Fig. 3-19 b ¹H-NMR spectrum of 2,6-dimethylphenol (in DMSO) (8.5 - 6.0 ppm)

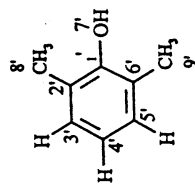


GE NMR
QE-300

MEM. 676
09JUN96

DIMETHYLPHENOL IN DMSO

OPERATOR: MM



LINES	HEIGHT	HEIGHT(L)	FREQ(HZ)	PPM
1	111.98	113.20	1982.42	6.593
2	259.96	260.39	1990.05	6.619
3	168.15	169.29	1997.24	6.642
4	508.03	513.86	2086.05	6.871
5	437.76	439.04	2073.44	6.896
6	455.25	481.83	2448.82	8.144

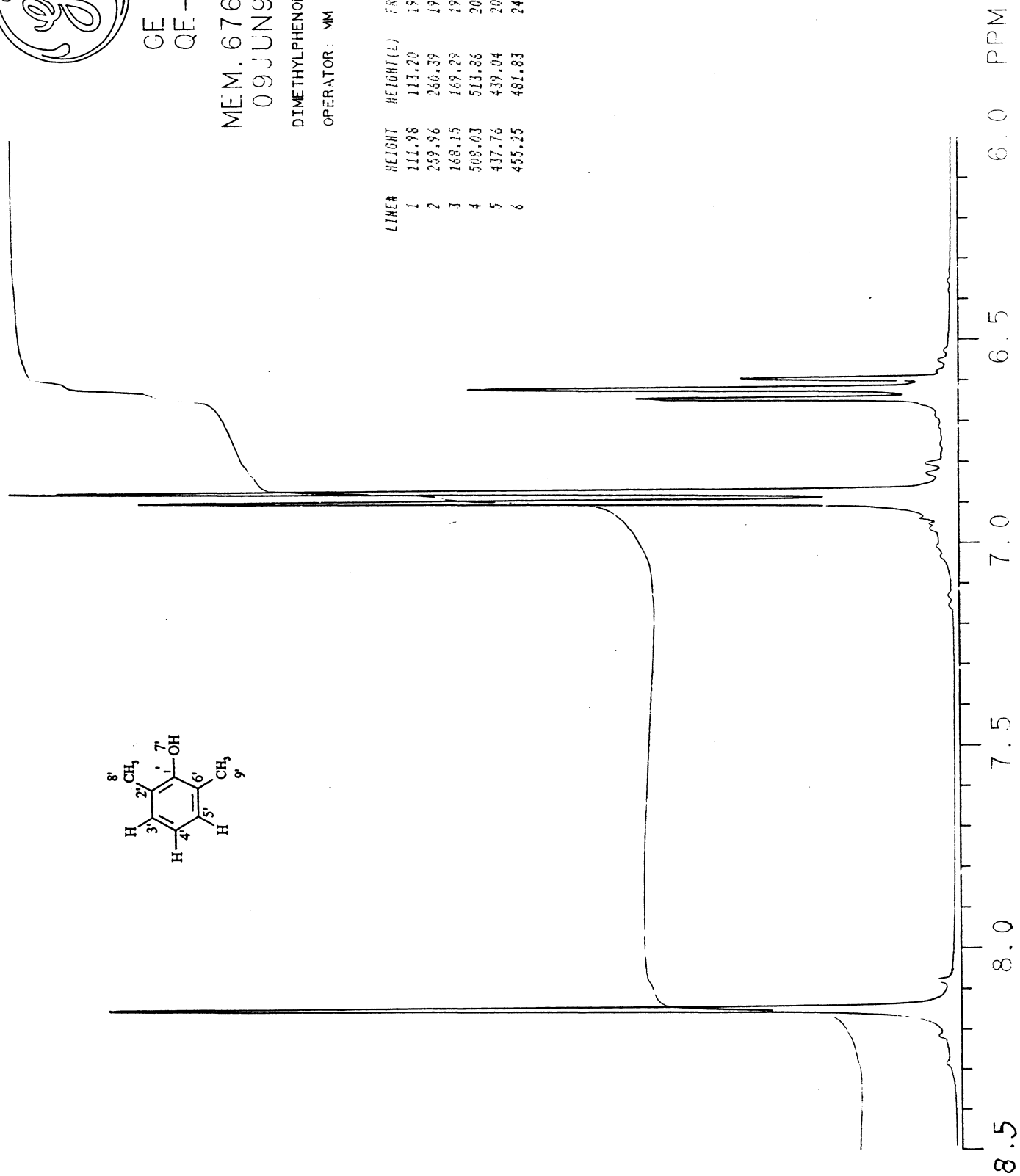


Fig. 3-20 a ¹H-NMR spectrum of 2,6-dimethylphenol (in CDCl₃) (9 - -0.5 ppm)

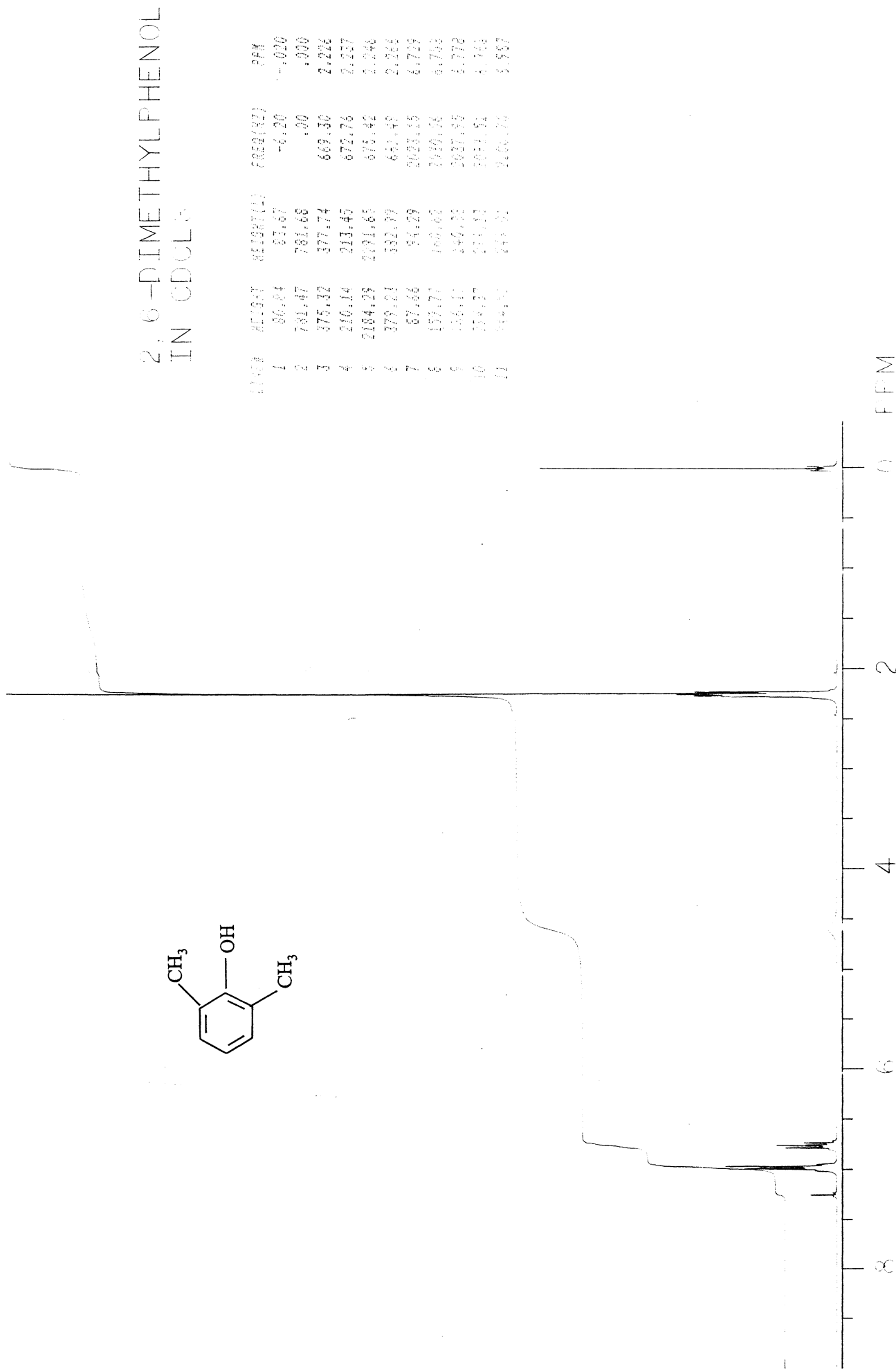


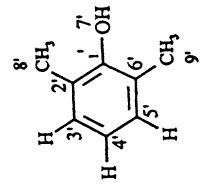
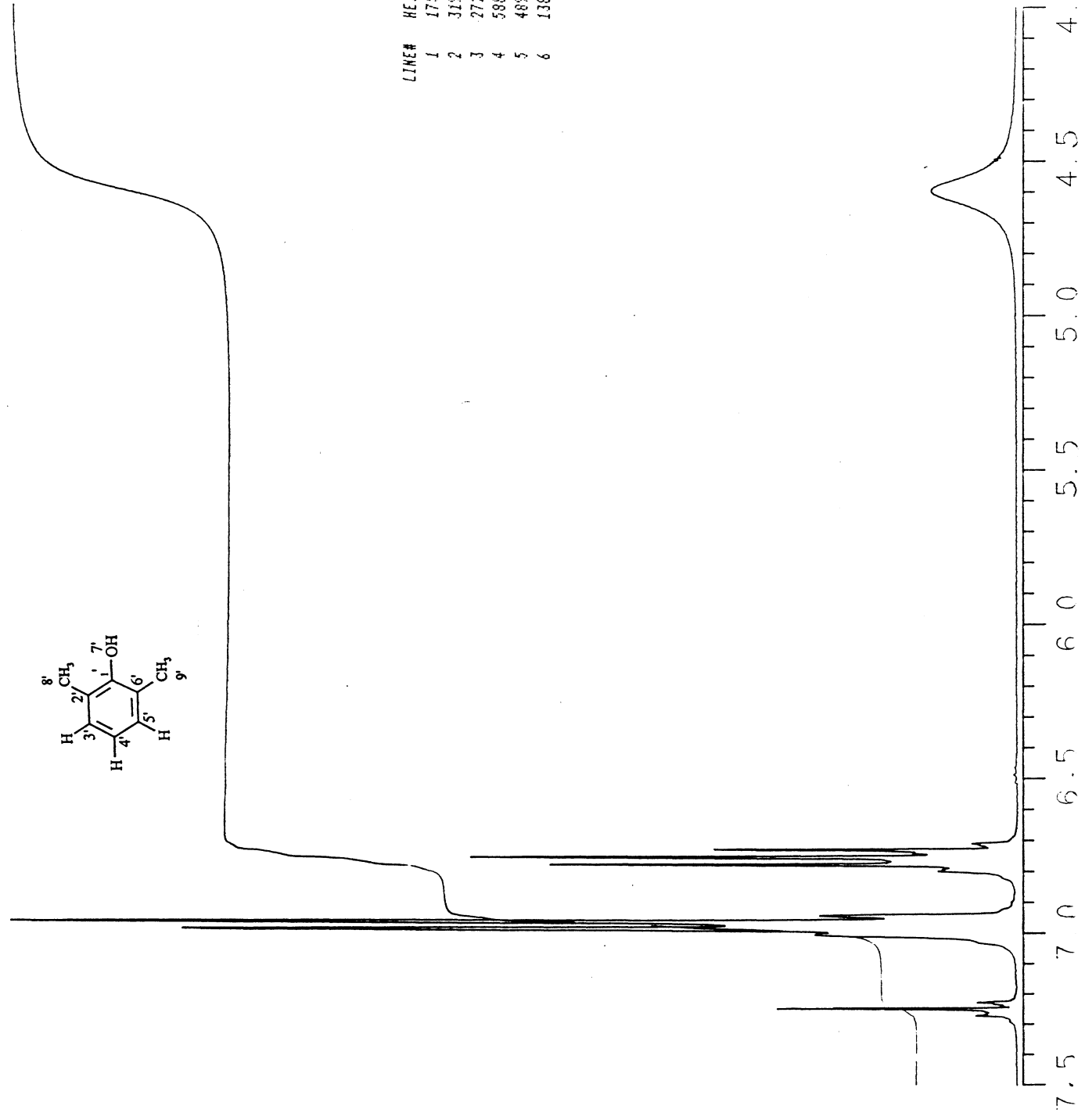
Fig. 3-20 b ¹H-NMR spectrum of 2,6-dimethylphenol (in CDCl₃) (7.5 - 4.0 ppm)



GE NMR
QE-300

MEM. 677
09JUN96

DIMETHYLPHENOL IN CDCL₃
OPERATOR: MM



LINE#	HEIGHT	HEIGHT(L)	FREQ(HZ)	PPM
1	175.32	188.58	2023.15	6.729
2	319.55	321.26	2030.56	6.753
3	272.22	281.76	2037.95	6.778
4	588.76	598.28	2043.51	6.803
5	489.02	498.04	2100.70	6.987
6	138.55	250.88	2178.85	7.216

Fig. 3-21 ¹H-NMR spectrum of phen-azo-phen

LINE#	HEIGHT	HEIGHT (L)	FREQ (HZ)	PPM
1	213.73	214.39	2429.97	8.052
2	269.48	269.92	2434.89	8.065
3	293.64	293.98	2429.51	8.080
4	212.69	213.45	2432.38	8.090
5	223.81	224.92	2470.24	8.216
6	285.74	286.16	2471.41	8.226
7	216.40	216.41	2476.68	8.237
8	294.95	295.04	2478.81	8.244
9	218.20	218.84	2481.64	8.254
10	193.08	194.28	2498.82	8.311
11	247.04	247.31	2504.27	8.329
12	298.58	299.35	2506.90	8.338
13	246.47	246.50	2510.12	8.348
14	314.30	314.94	2512.39	8.356 ^{TI}
15	202.25	204.40	2532.34	8.422
16	253.40	254.87	2537.48	8.439
17	307.92	309.23	2540.86	8.451
18	243.77	243.82	2543.51	8.459
19	313.35	316.48	2545.94	8.467
20	570.38	571.58	2582.47	8.587
21	244.22	245.74	2681.96	8.920
22	354.13	354.20	2687.29	8.938
23	257.58	258.86	2729.34	9.077
24	177.67	178.66	2731.47	9.091
25	323.26	323.96	2737.93	9.106
26	283.26	284.03	2769.93	9.212
27	462.56	463.78	2774.31	9.257
28	182.60	183.87	2782.38	9.254
29	174.30	174.31	2783.26	9.257
30	364.04	364.76	2789.62	9.278
31	476.49	476.49	2793.21	9.290
32	783.10	786.40	2797.87	9.305
33	206.74	207.93	2812.88	9.355
34	189.24	189.90	2814.74	9.361
35	182.86	184.02	2815.84	9.365
36	173.05	173.39	2816.58	9.368
37	302.32	302.75	2832.09	9.419
38	396.10	396.39	2837.06	9.436
39	229.61	230.25	2962.62	9.853
40	183.62	183.80	2954.84	9.861
41	306.56	306.72	2971.13	9.882
42	253.20	253.98	3007.66	10.091
43	322.78	325.13	3016.19	10.091

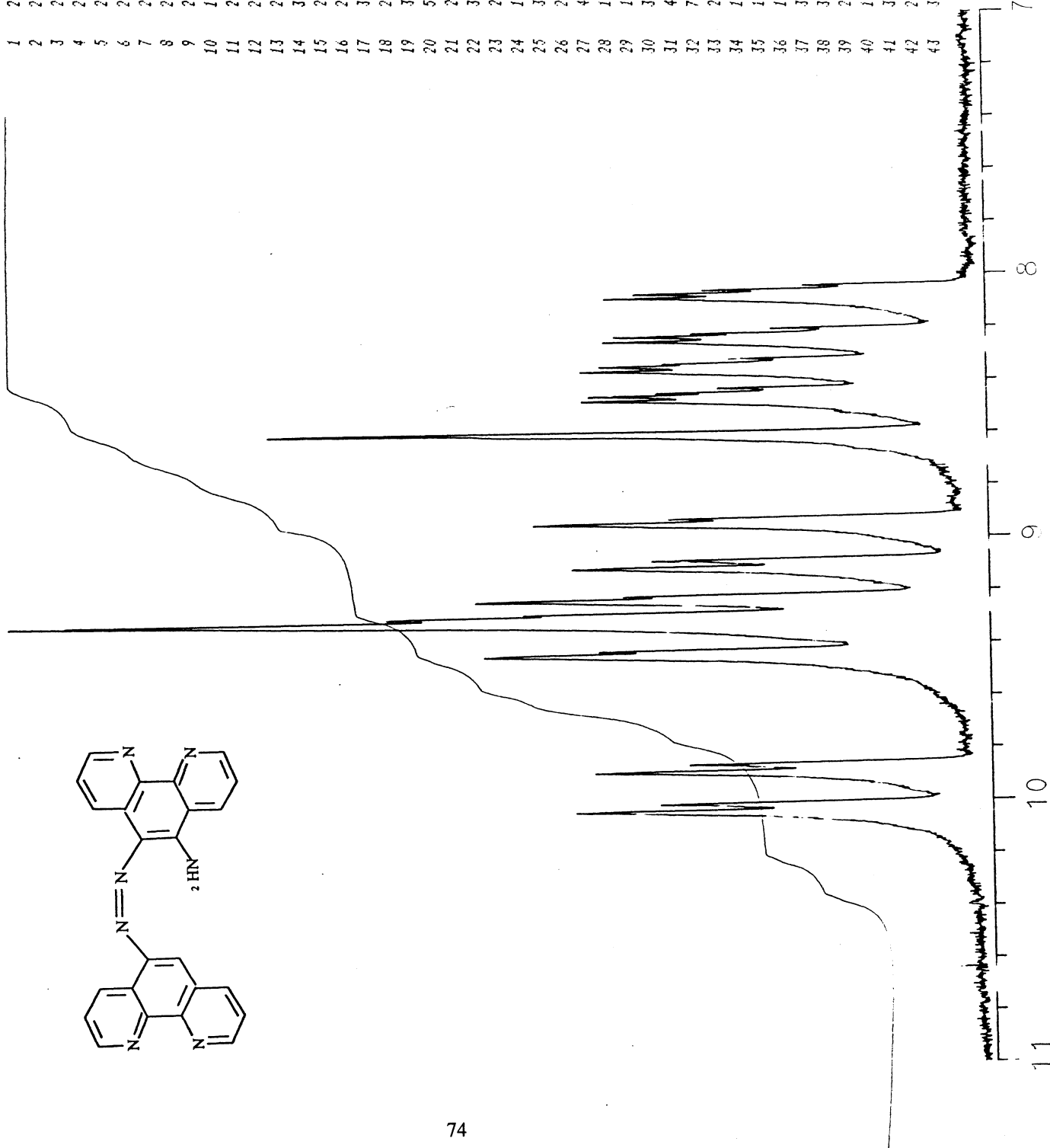


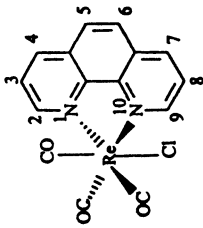
Fig. 3-22 ¹H-NMR spectrum of *fac*-Re^I(CO)₃(phen)Cl



GE NMR
QE-300

MEM. 699
17 JUN 96

RE(CO)₃CL (PHEN)
061707AMM/RECRYSTALIZED
OPERATOR. MM



LINE#	HEIGHT	HEIGHT(L)	FREQ(HZ)	PPM
1	478.87	478.94	2435.29	8.099
2	560.92	561.60	2440.40	8.116
3	596.47	595.33	2443.51	8.127
4	573.62	575.44	2448.60	8.144
5	1784.85	1786.51	2508.50	8.343
6	795.98	796.34	2698.96	8.976
7	675.94	682.15	2707.25	9.004
8	686.69	691.99	2838.44	9.440
9	700.61	703.31	2842.83	9.455
10	719.41	719.76	2843.39	9.457

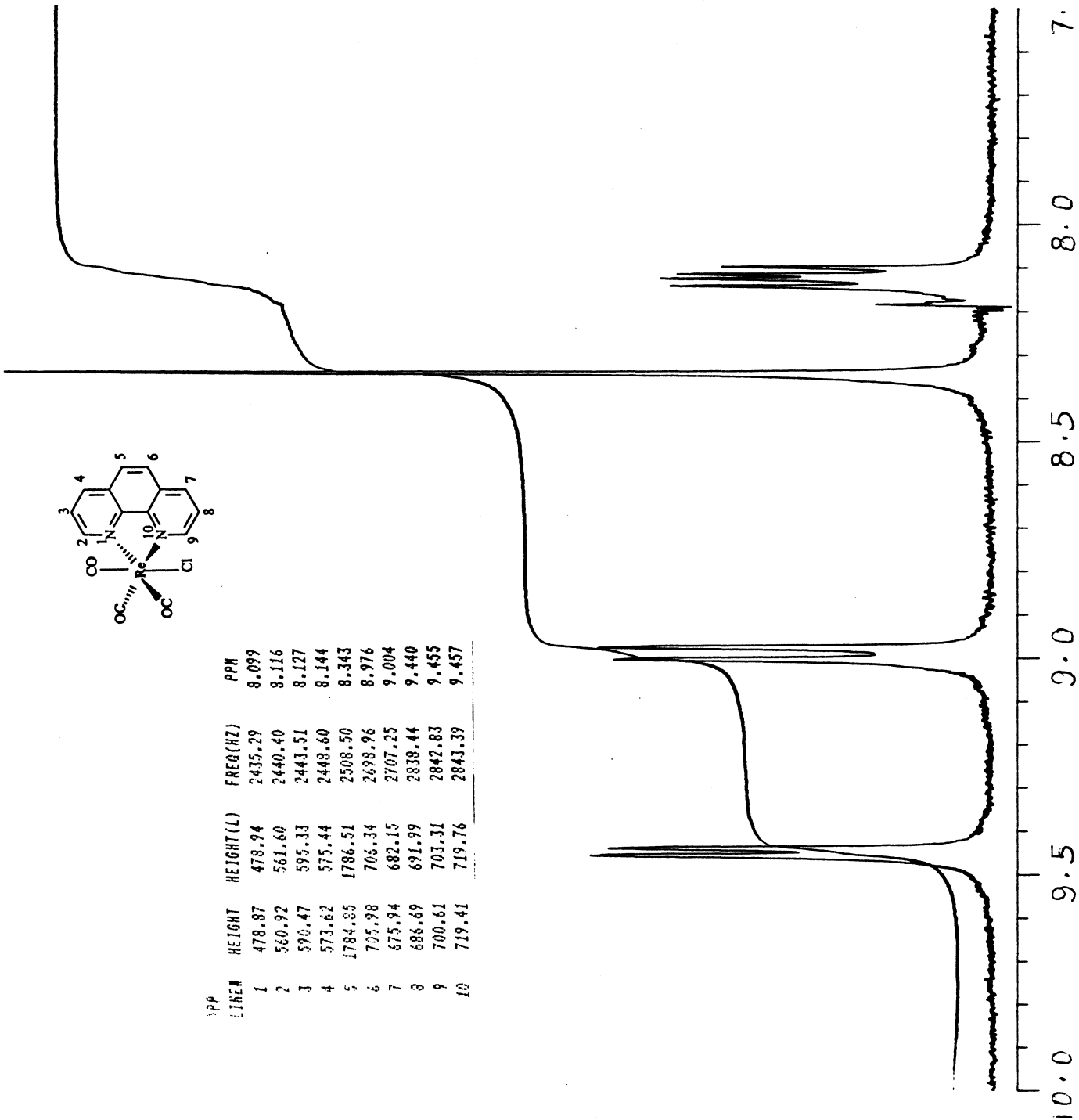


Fig. 3-23 ¹H-NMR spectrum of *fac*-Re^I(CO)₃(phen-azo-p-phenol)Cl

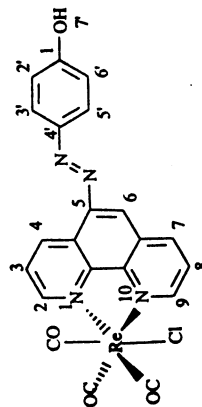


GE NMR
QE-300

MEM. 694
17 JUN 96

061297AMM/RE(CO)₃CL
(PHEN-AZO-PHENOL)

OPERATOR: MEM



LINE#	HEIGHT	HEIGHT (L)	FREQ(HZ)	PPM
1	453.54	457.24	2116.88	7.040
2	517.76	517.80	2125.58	7.069
3	529.36	530.71	2431.39	8.086
4	433.15	433.22	2432.83	8.091
5	645.83	646.84	2440.03	8.115
6	350.14	-----	2447.28	8.139
7	188.98	189.08	2464.89	8.198
8	206.07	206.23	2470.04	8.215
9	216.94	218.07	2473.26	8.226
10	202.66	202.92	2478.47	8.243
11	574.16	575.65	2541.71	8.453
12	217.18	217.20	2741.82	9.119
13	222.56	222.60	2749.93	9.146
14	236.35	237.14	2837.89	9.438
15	261.50	262.38	2842.81	9.455
16	247.34	249.14	2869.92	9.545
17	267.12	267.75	2874.80	9.561
18	239.77	242.39	2898.95	9.642
19	241.36	241.64	2907.53	9.670

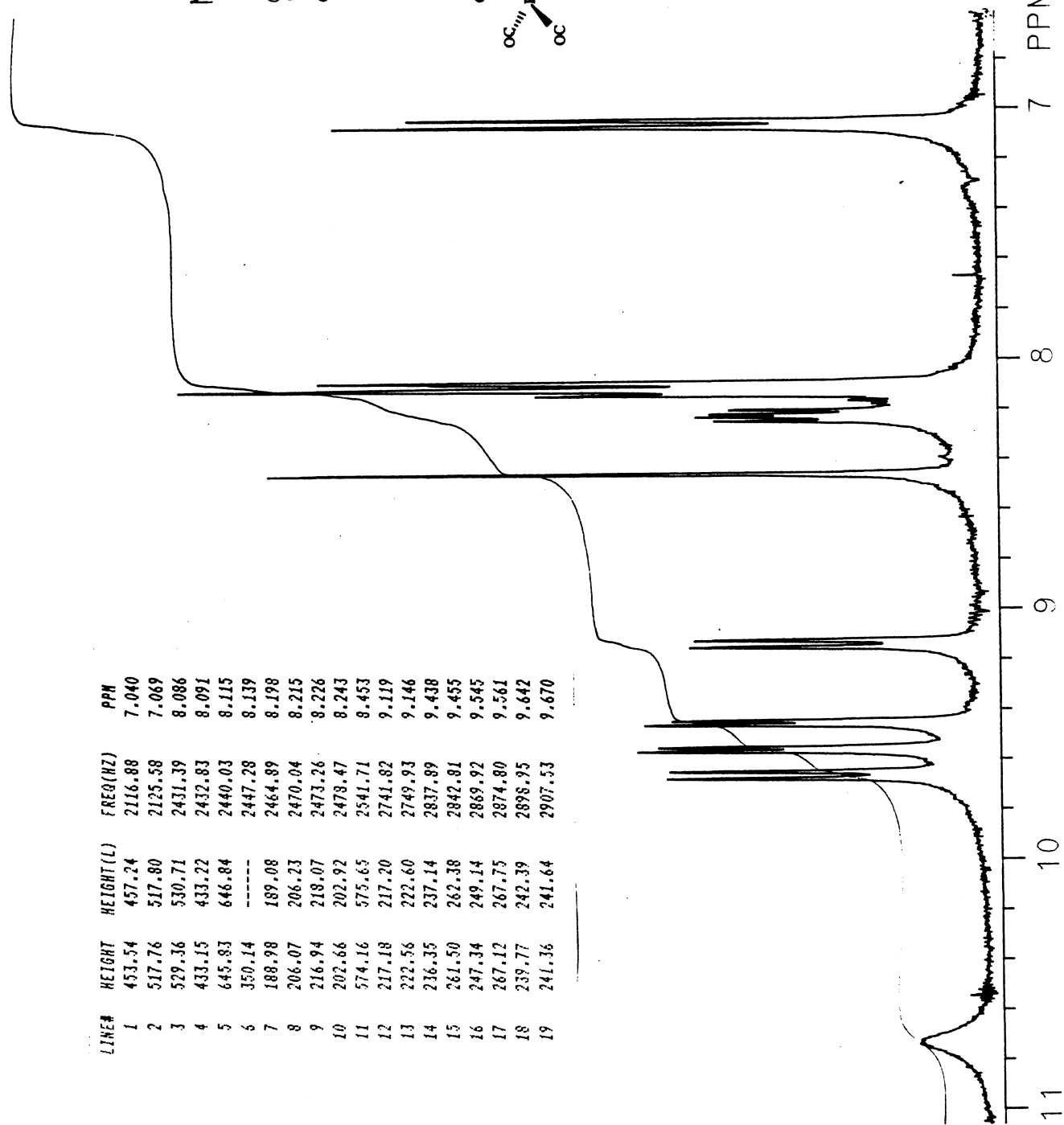


Fig. 3-24 IR spectrum of phen-azo- β -naphthol

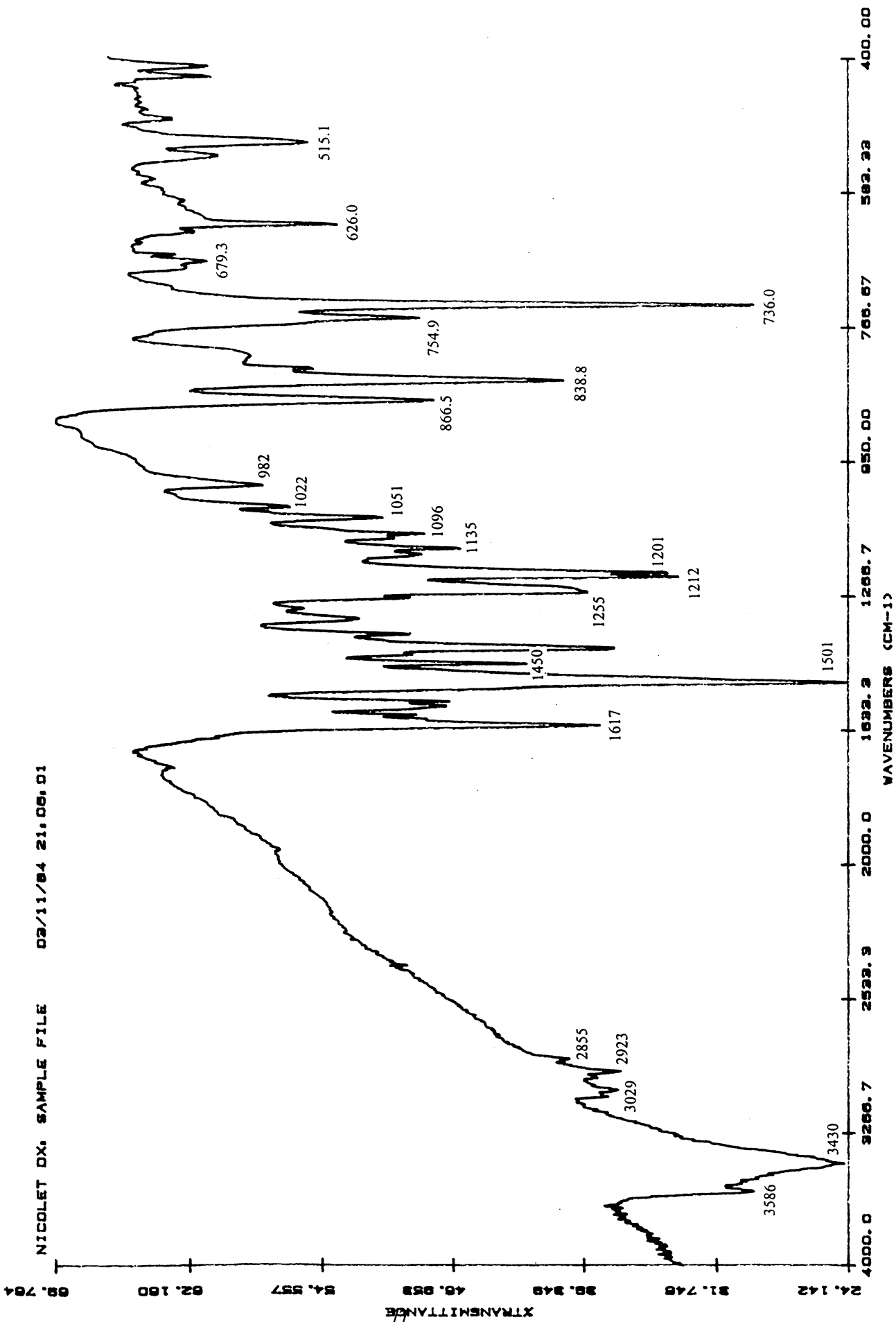


Fig. 3-25 IR spectrum of phen-azo-p-phenol

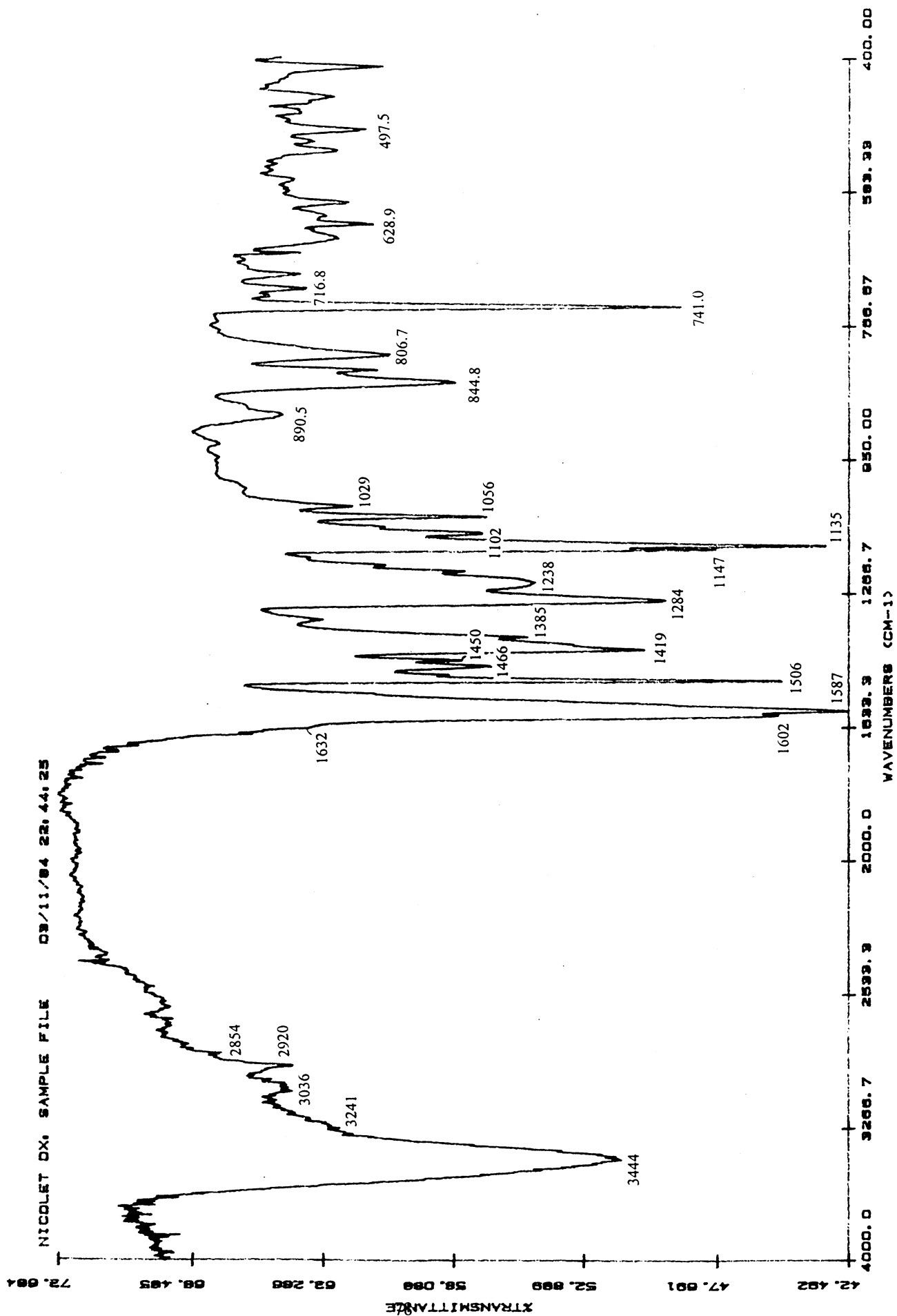


Fig. 3-26 IR spectrum of phen-azo-2,6-dimethylphenol

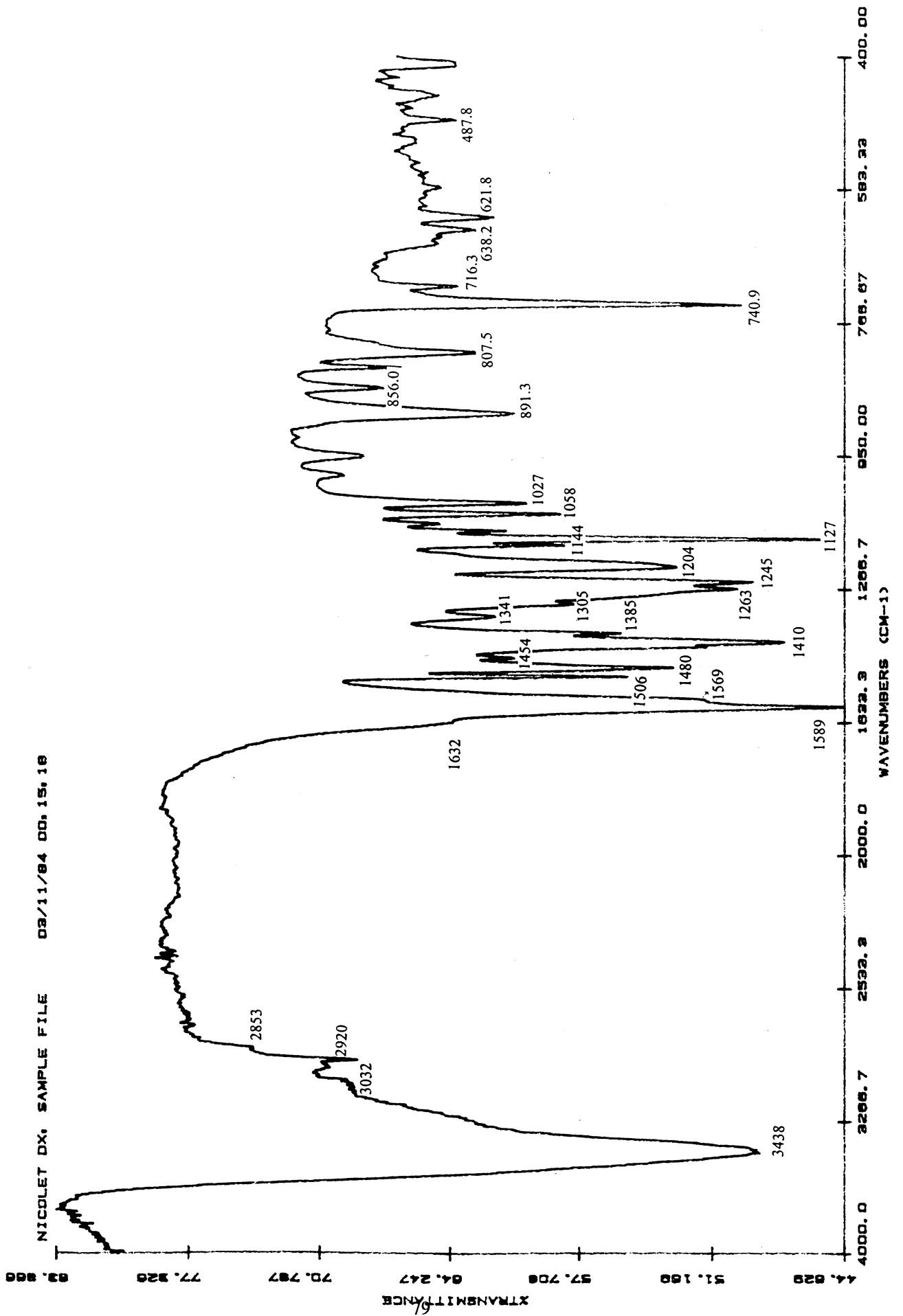


Fig. 3-27 IR spectrum of phen-azo-phen

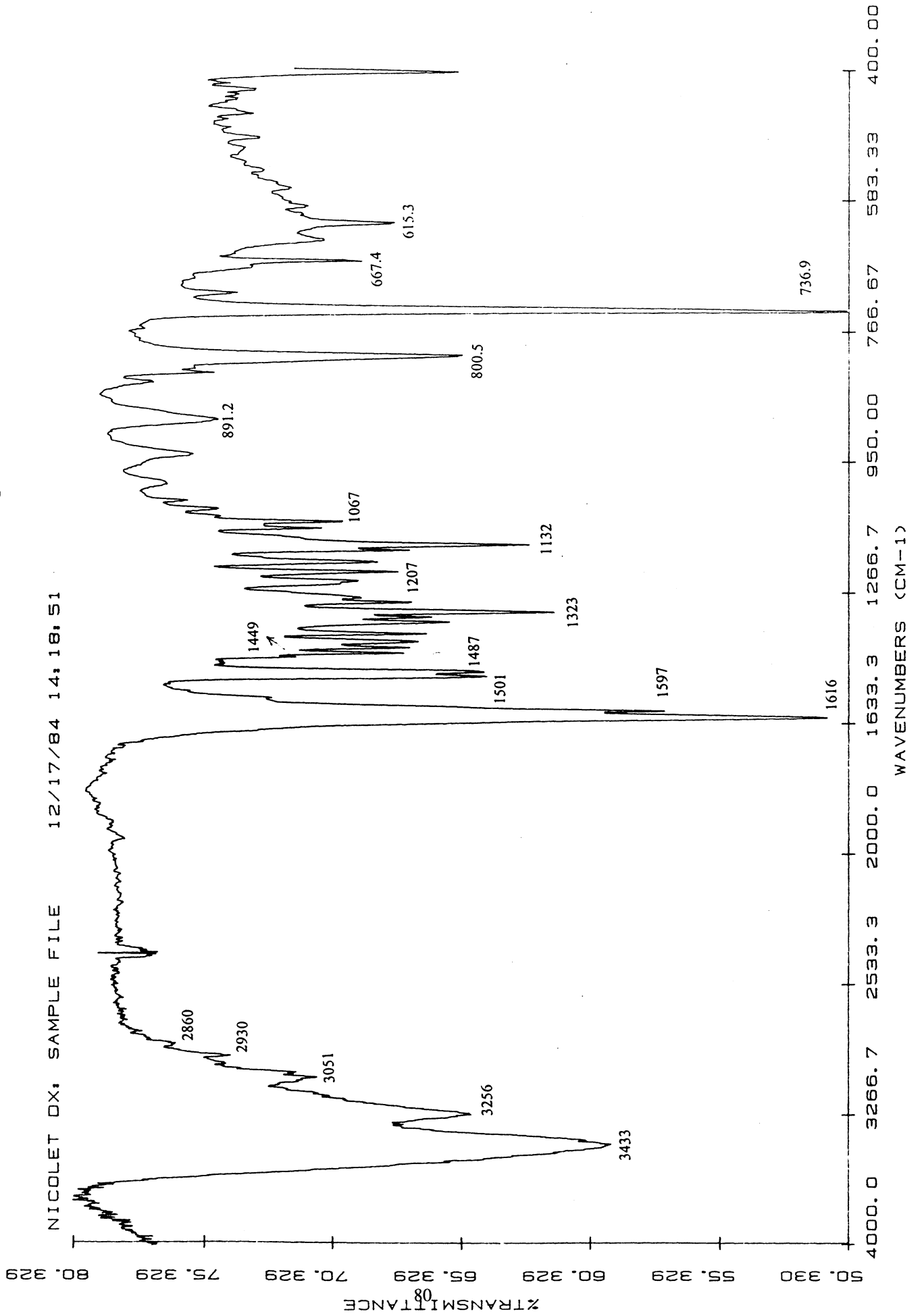


Fig. 3-28 IR spectrum of *fac*-Re^I(CO)₃(phen)Cl

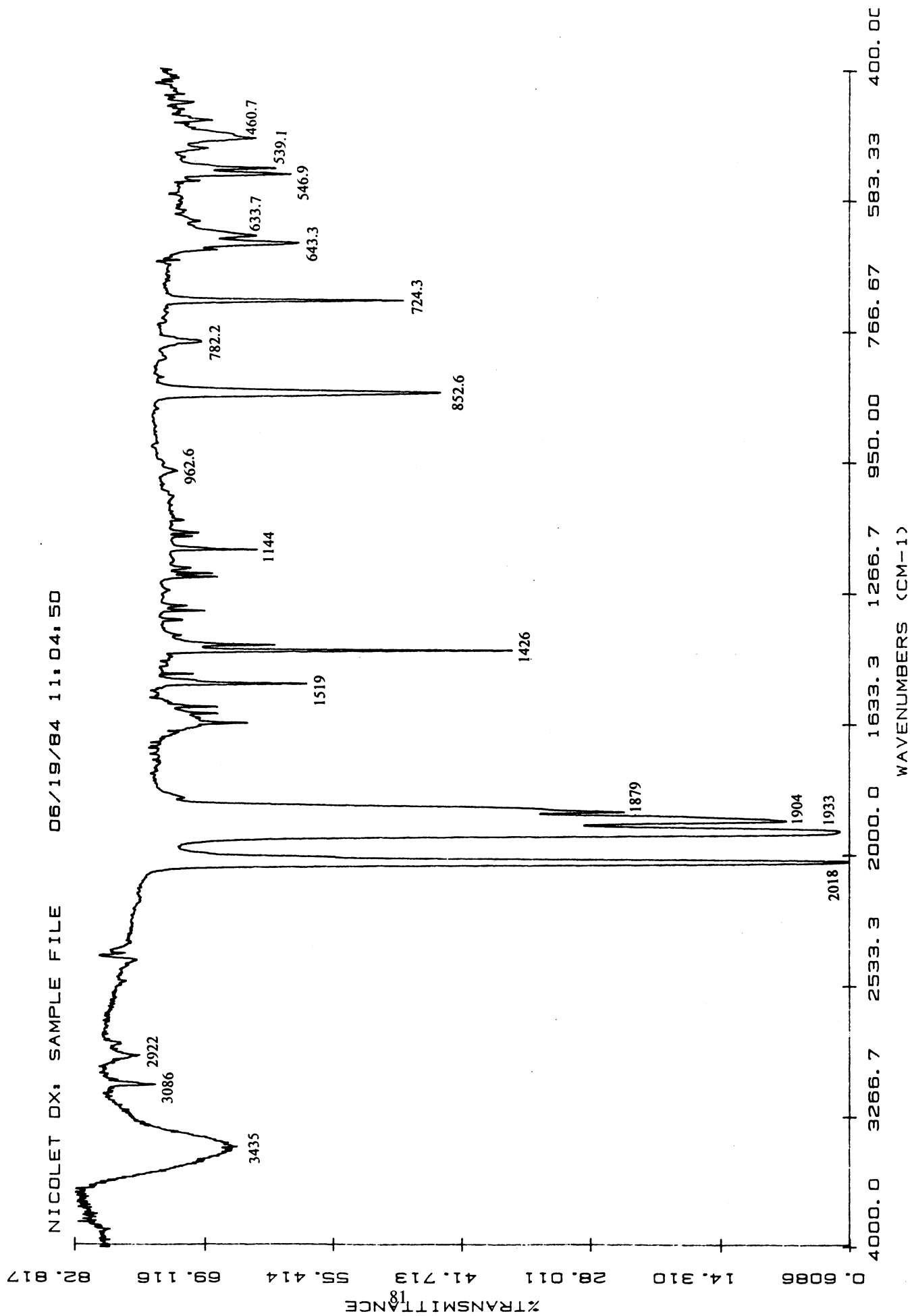


Fig. 3-29 IR spectrum of *fac*- $\text{Re}^{\text{I}}(\text{CO})_3(\text{phen-azo-p-phenol})\text{Cl}$

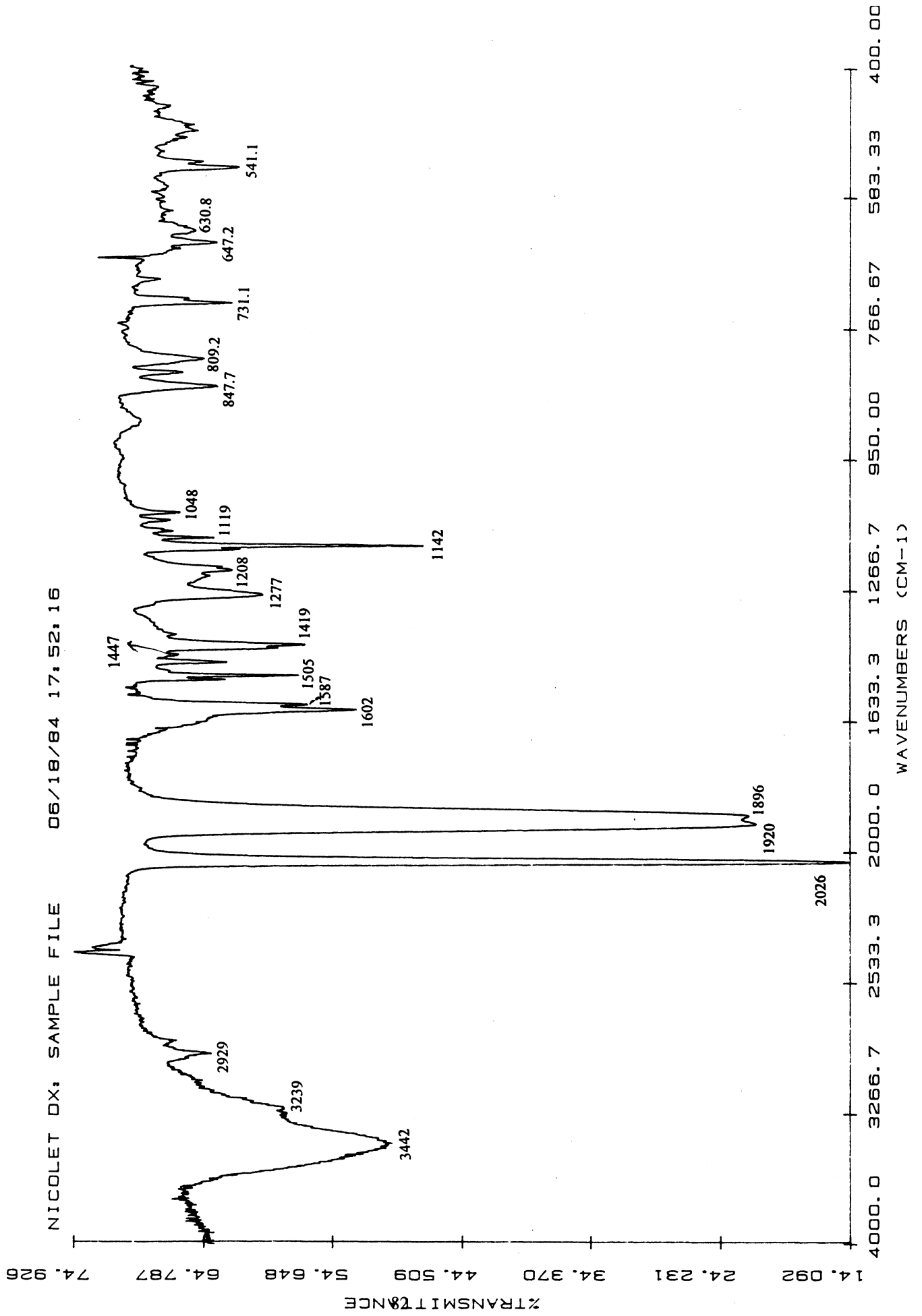


Fig. 3-30 UV-Vis spectrum of 5-NH₂ phen

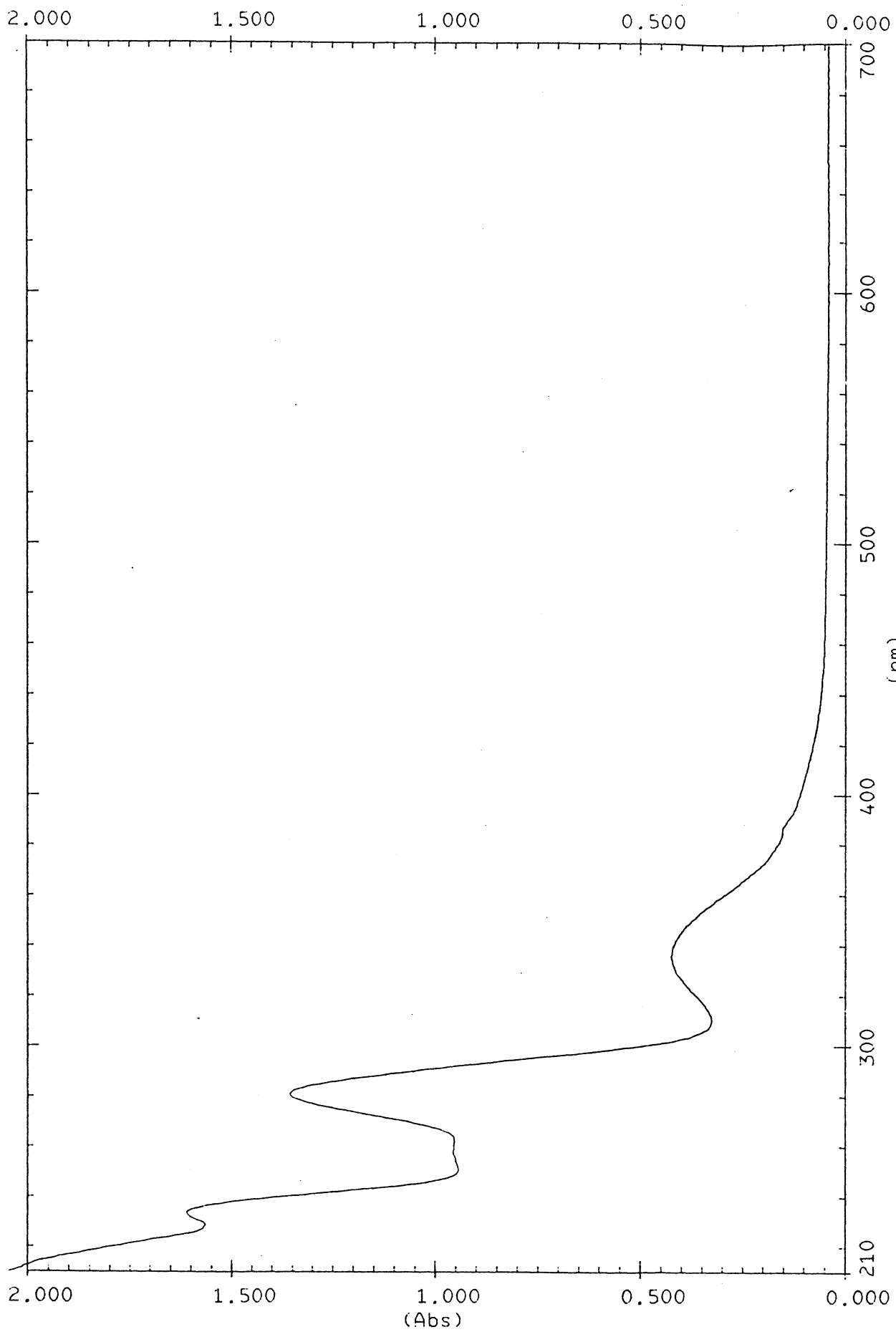


Fig. 3-31 UV-Vis spectrum of phen

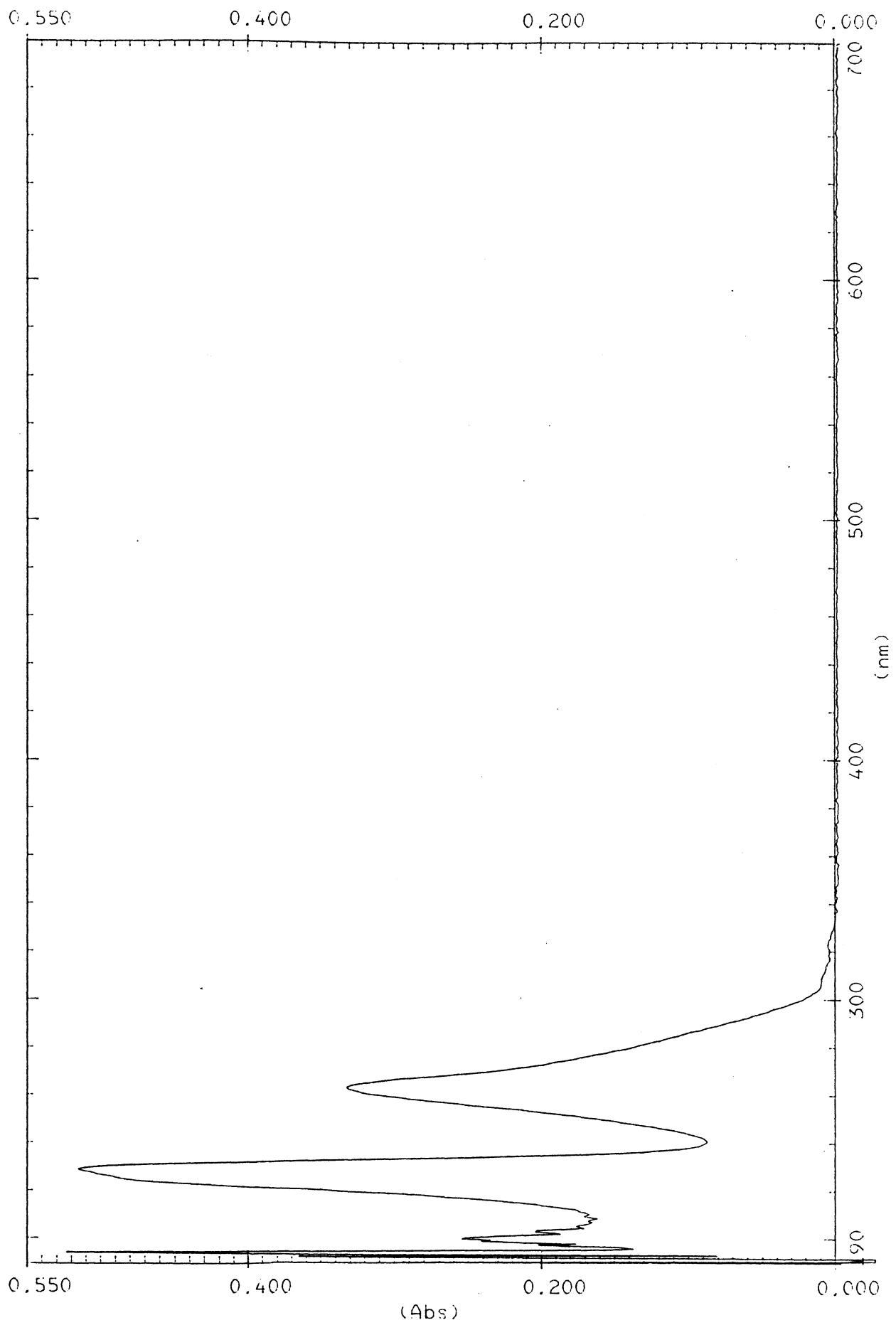


Fig. 3-32 UV-Vis spectrum of phen-azo- β -naphthol

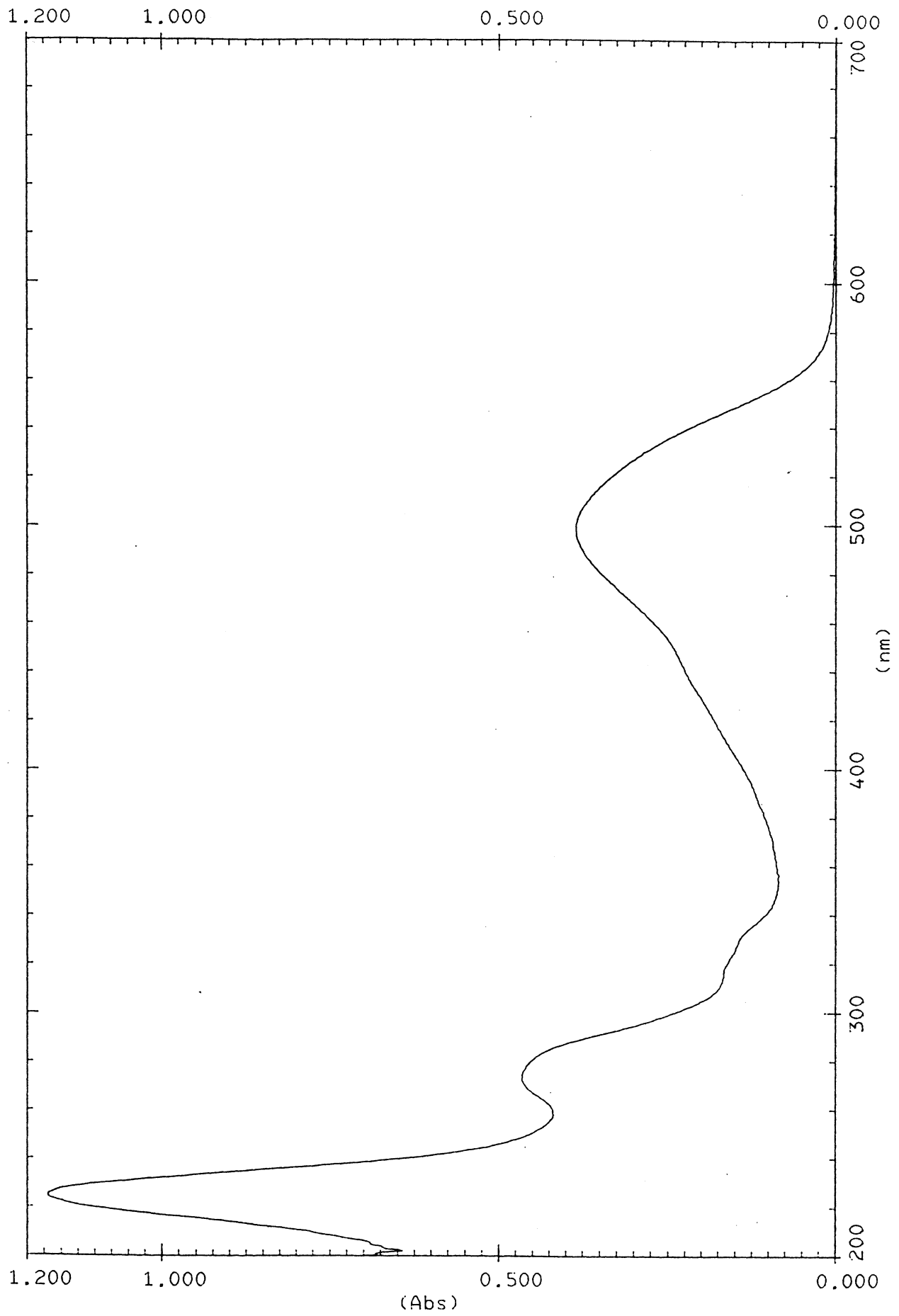


Fig. 3-33 Beer-Lambert plot of phen-azo- β -naphthol
498 nm peak

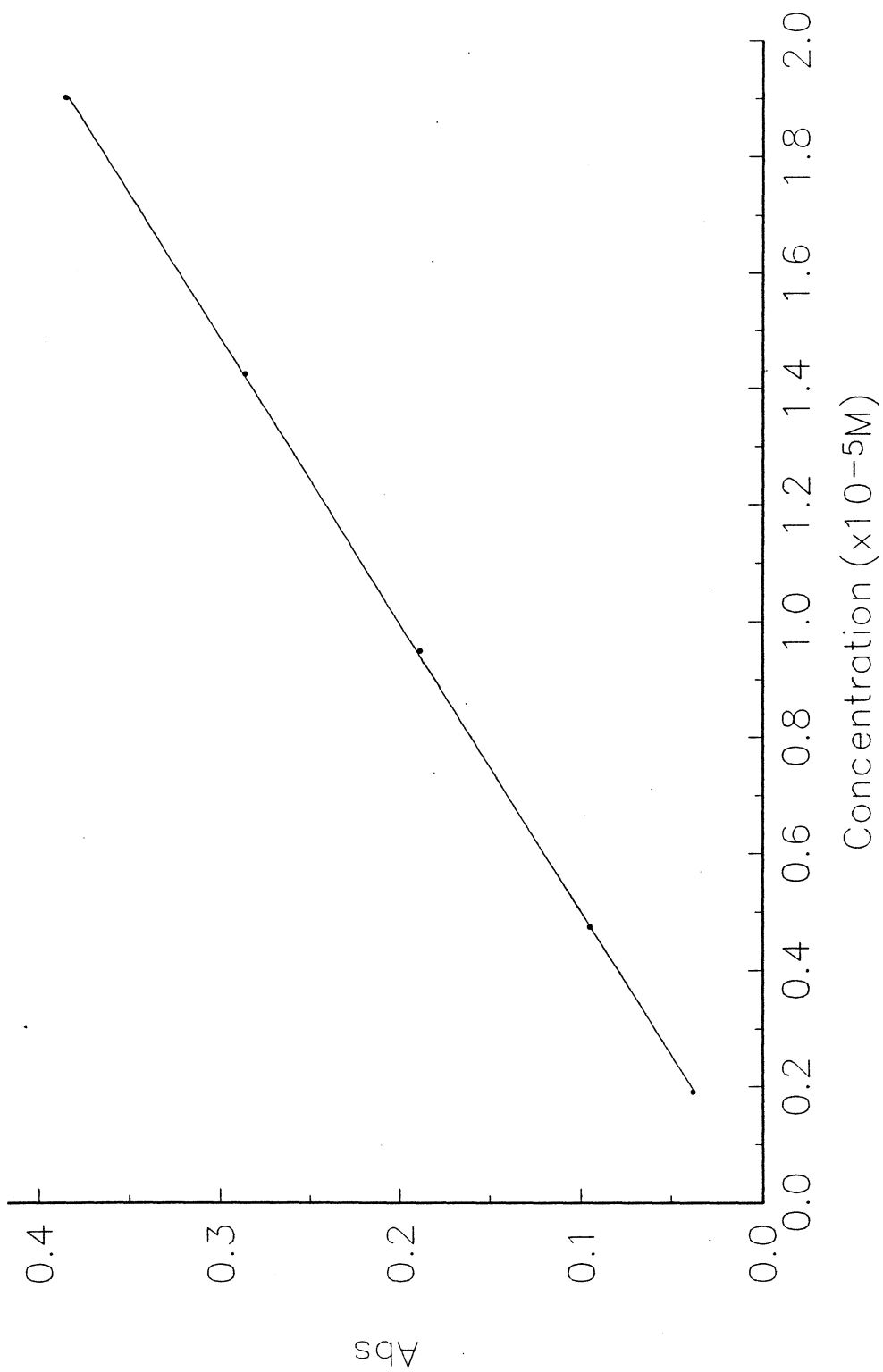


Fig. 3-34 UV-Vis spectrum of β -naphthol

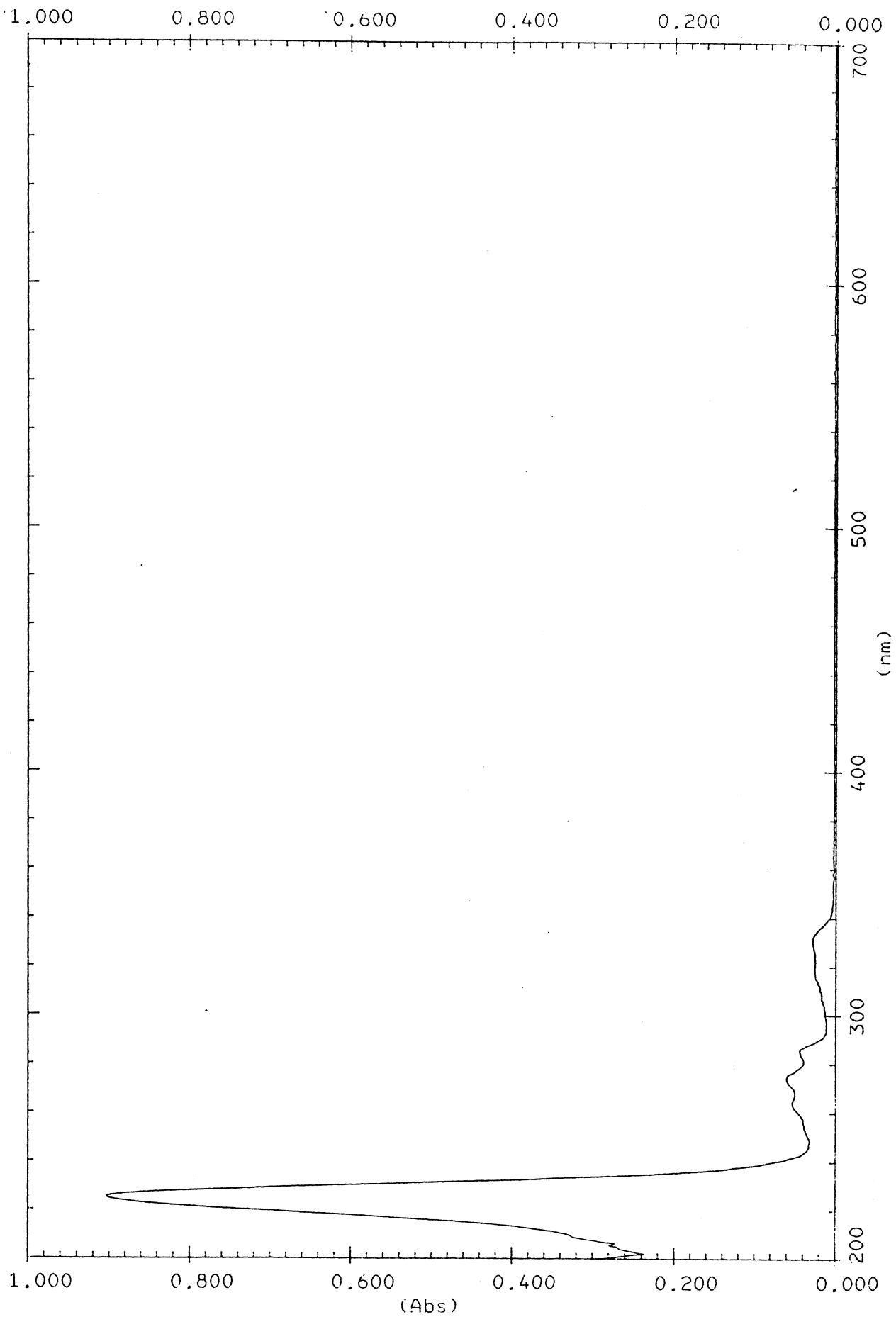


Fig. 3-35 UV-Vis spectrum of phen-azo-p-phenol

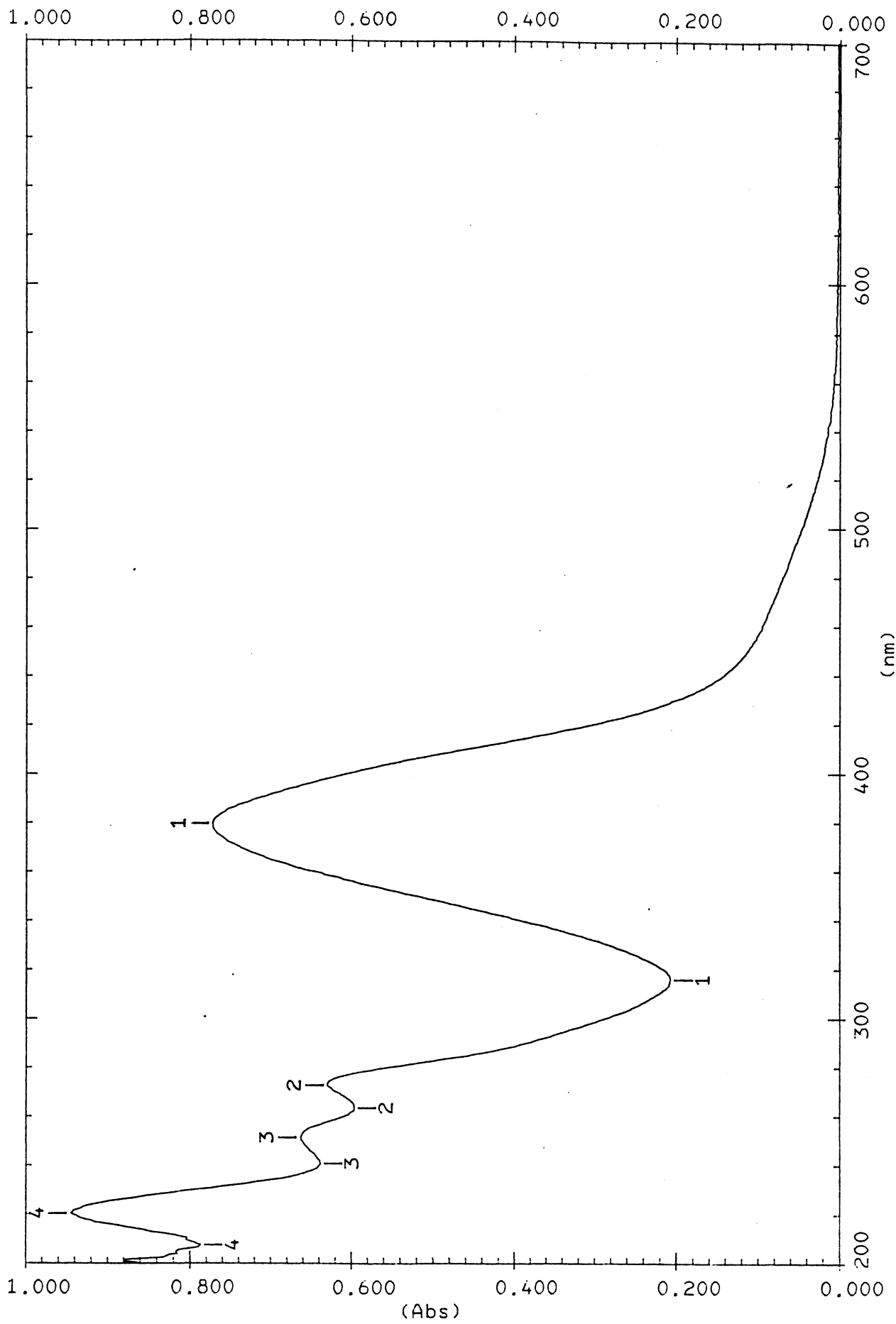


Fig. 3-36 Beer-Lambert plot of phen-azo-p-phenol
380 nm peak

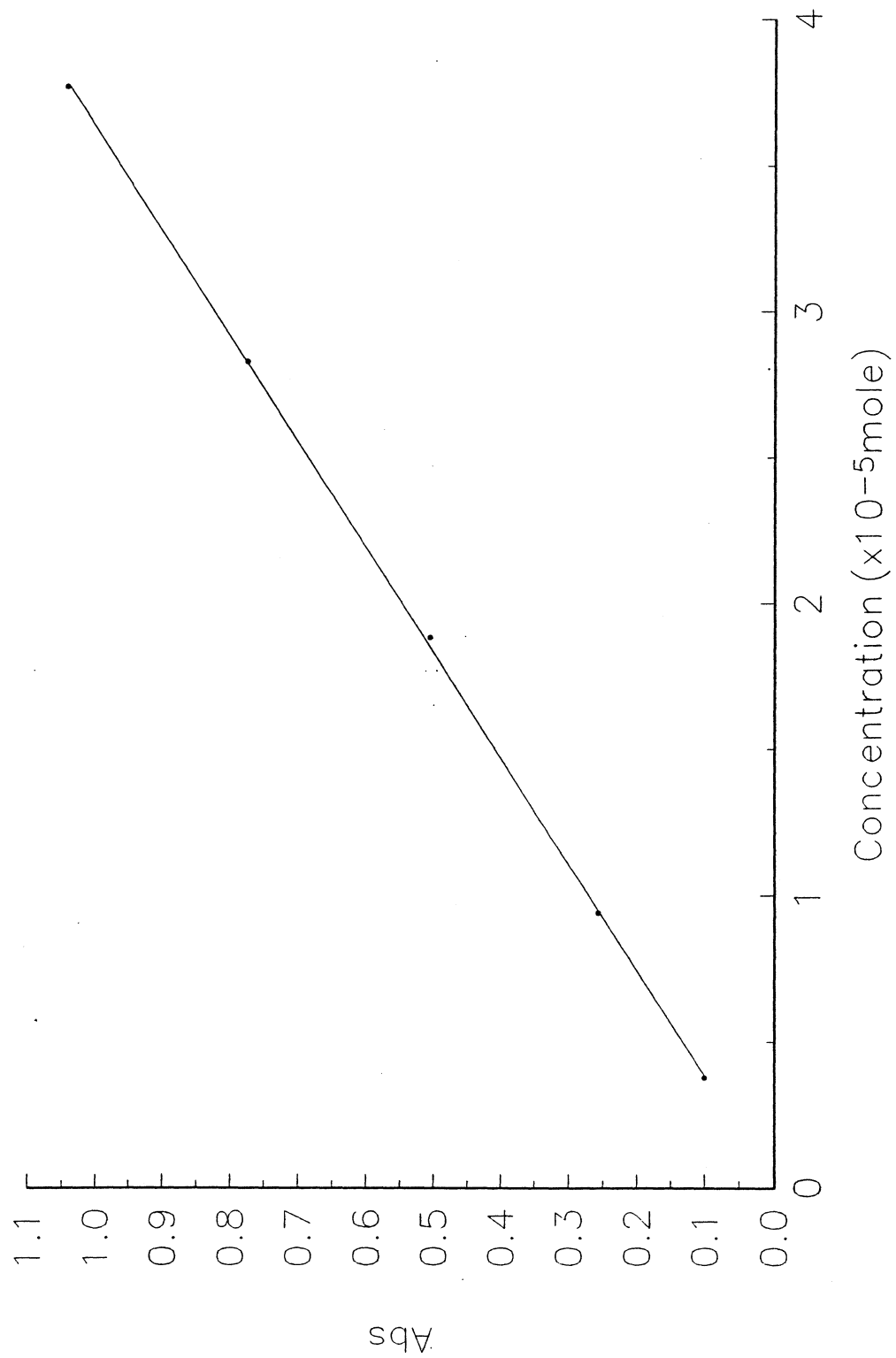


Fig. 3-37 UV-Vis spectrum of phenol

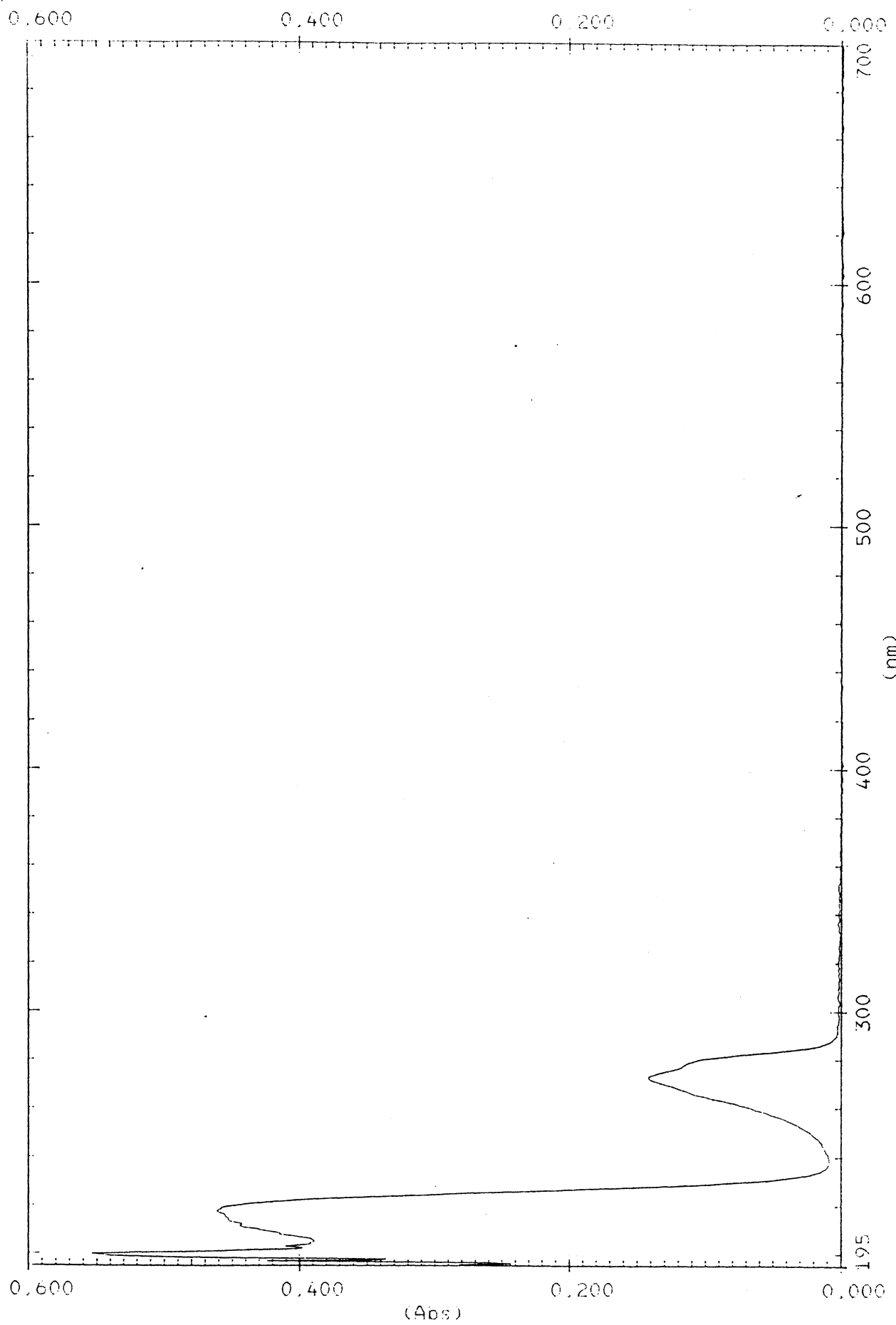


Fig. 3-38 UV-Vis spectrum of phen-azo-2,6-dimethylphenol

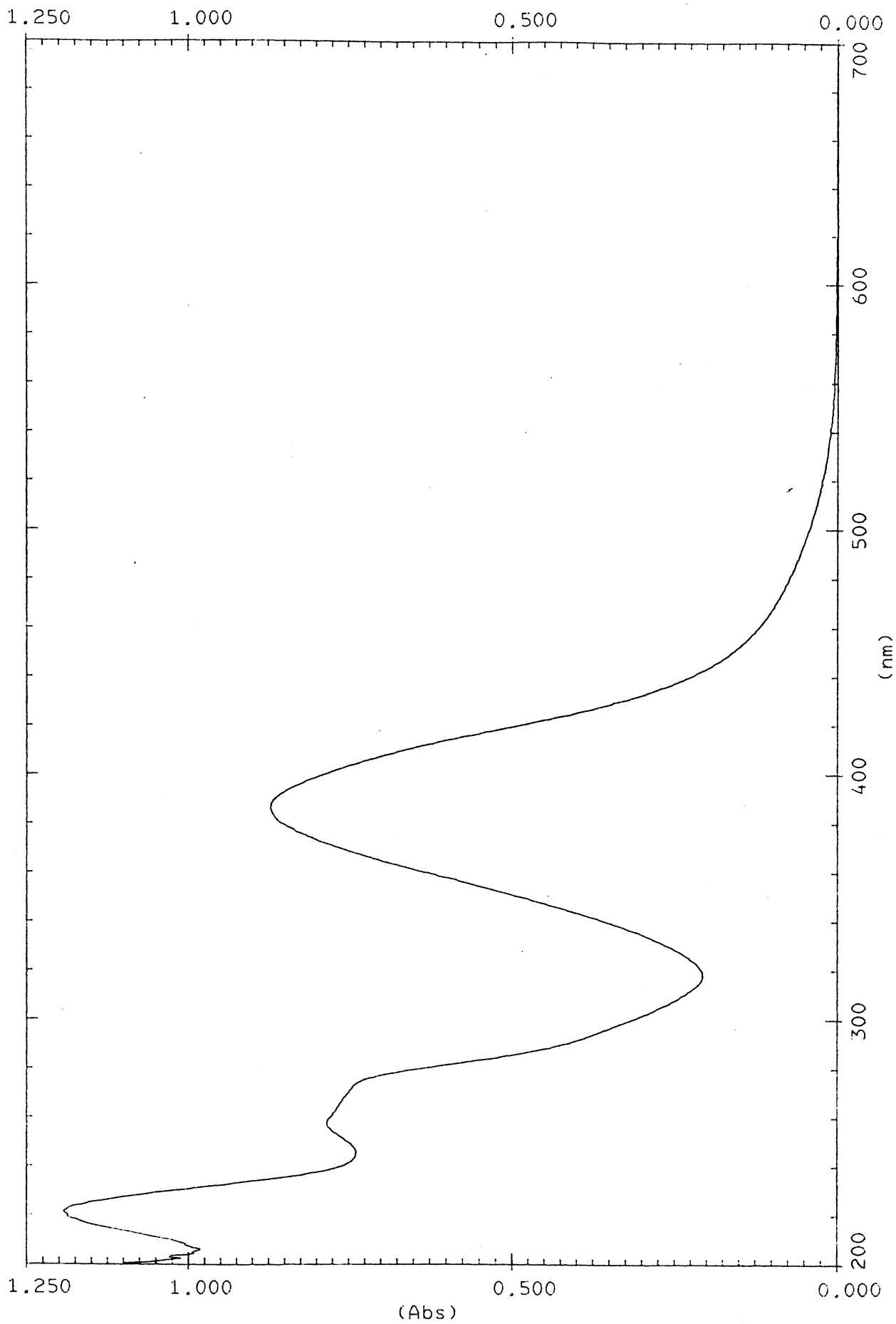


Fig. 3-39 Beer-Lambert plot of phen-azo-2,6-dimethylphenol
383 nm peak

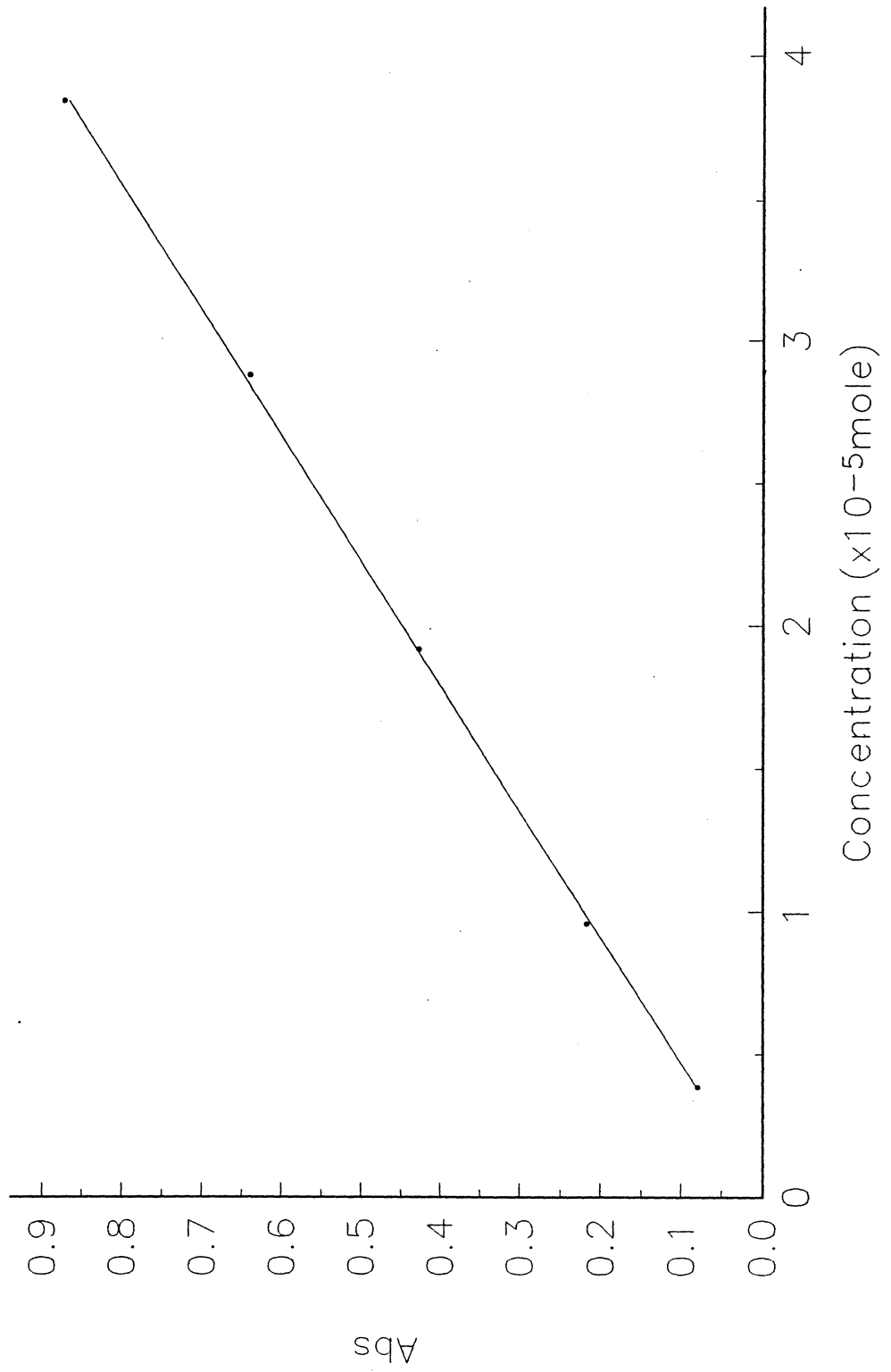


Fig. 3-40 UV-Vis spectrum of 2,6-dimethylphenol

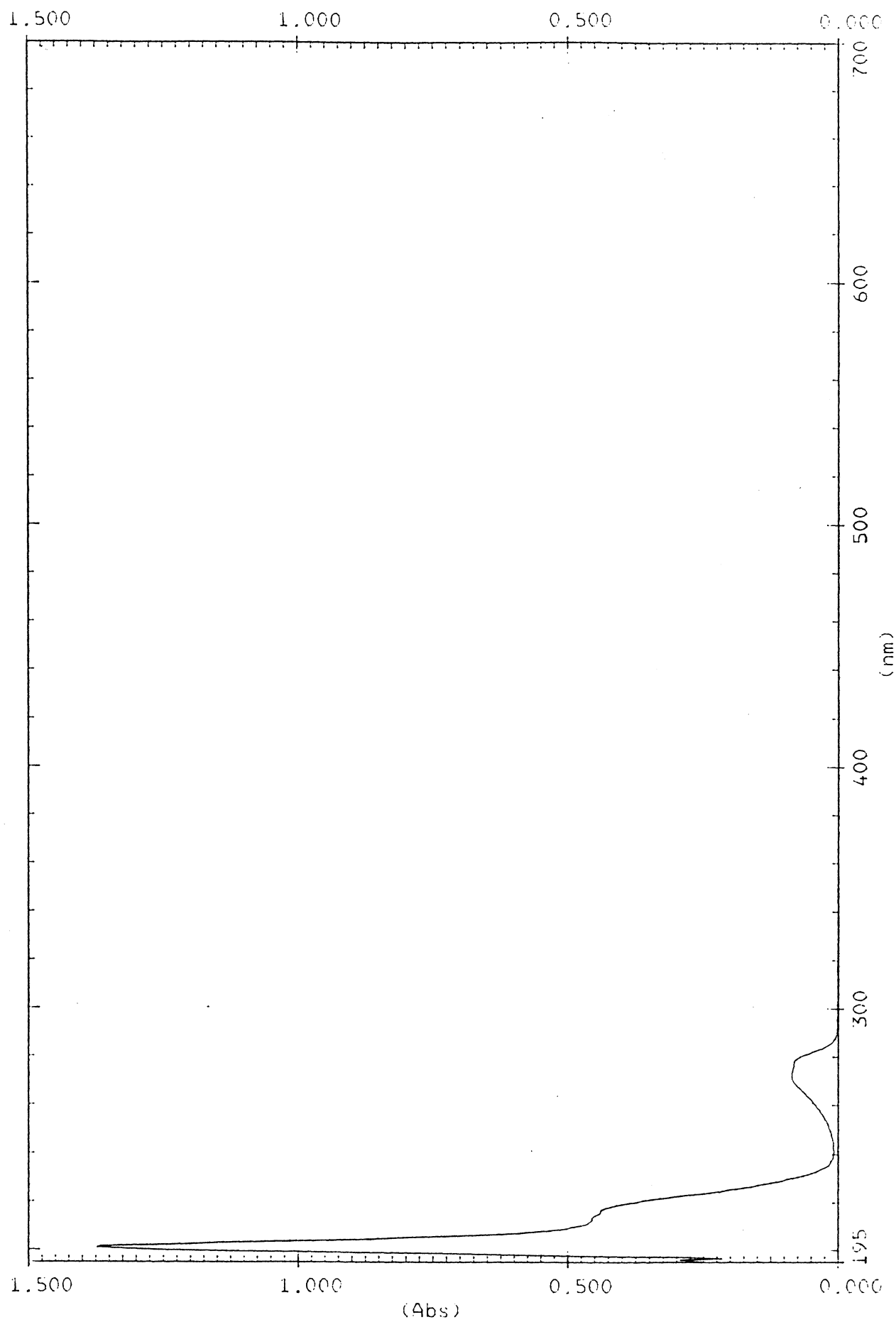


Fig. 3-41 UV-Vis spectrum of *fac*-Re^I(CO)₃(phen)Cl

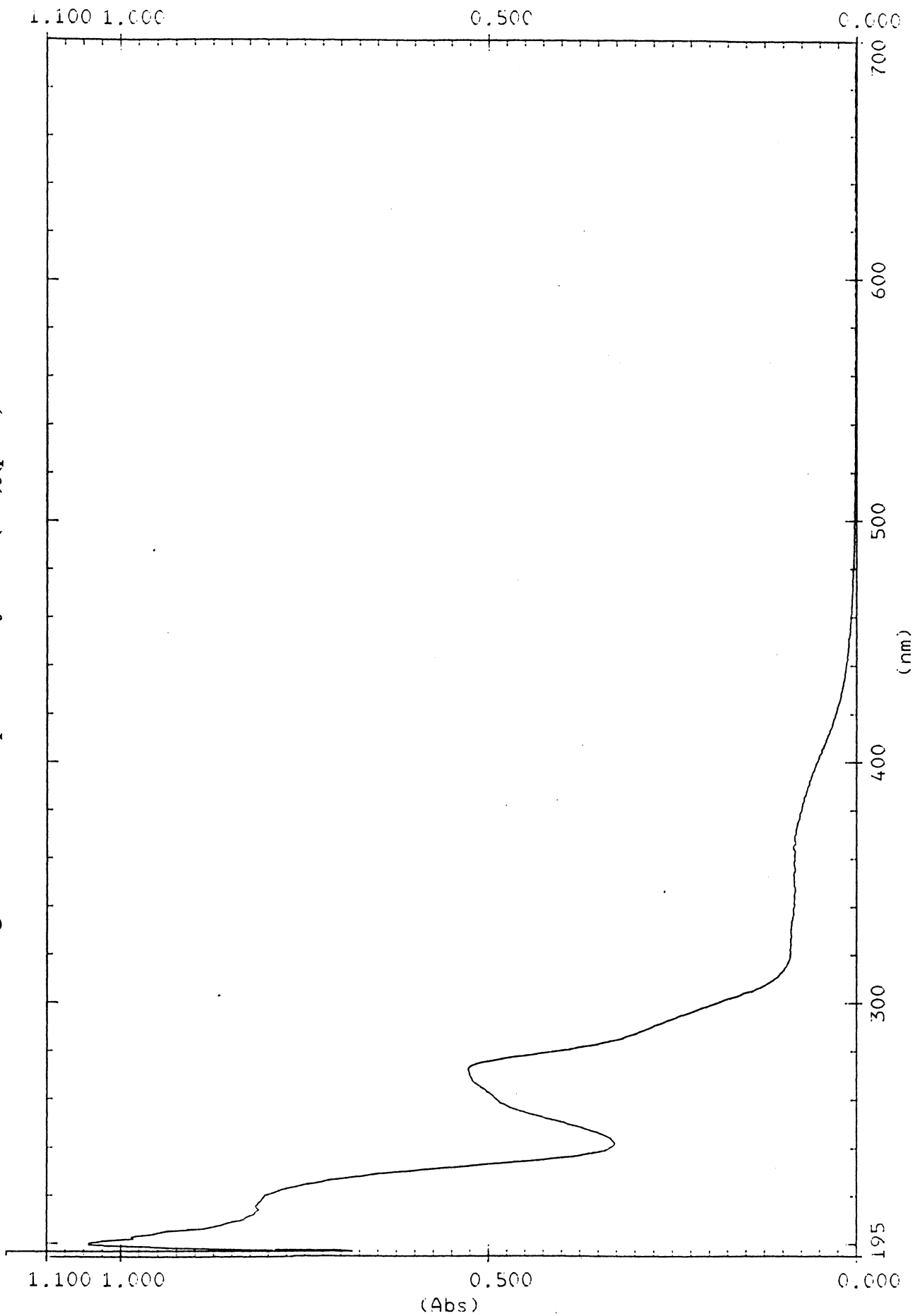


Fig. 3-42 UV-Vis spectrum of *fac*- $\text{Re}^{\text{I}}(\text{CO})_3(\text{phen-azo-p-phenol})\text{Cl}$

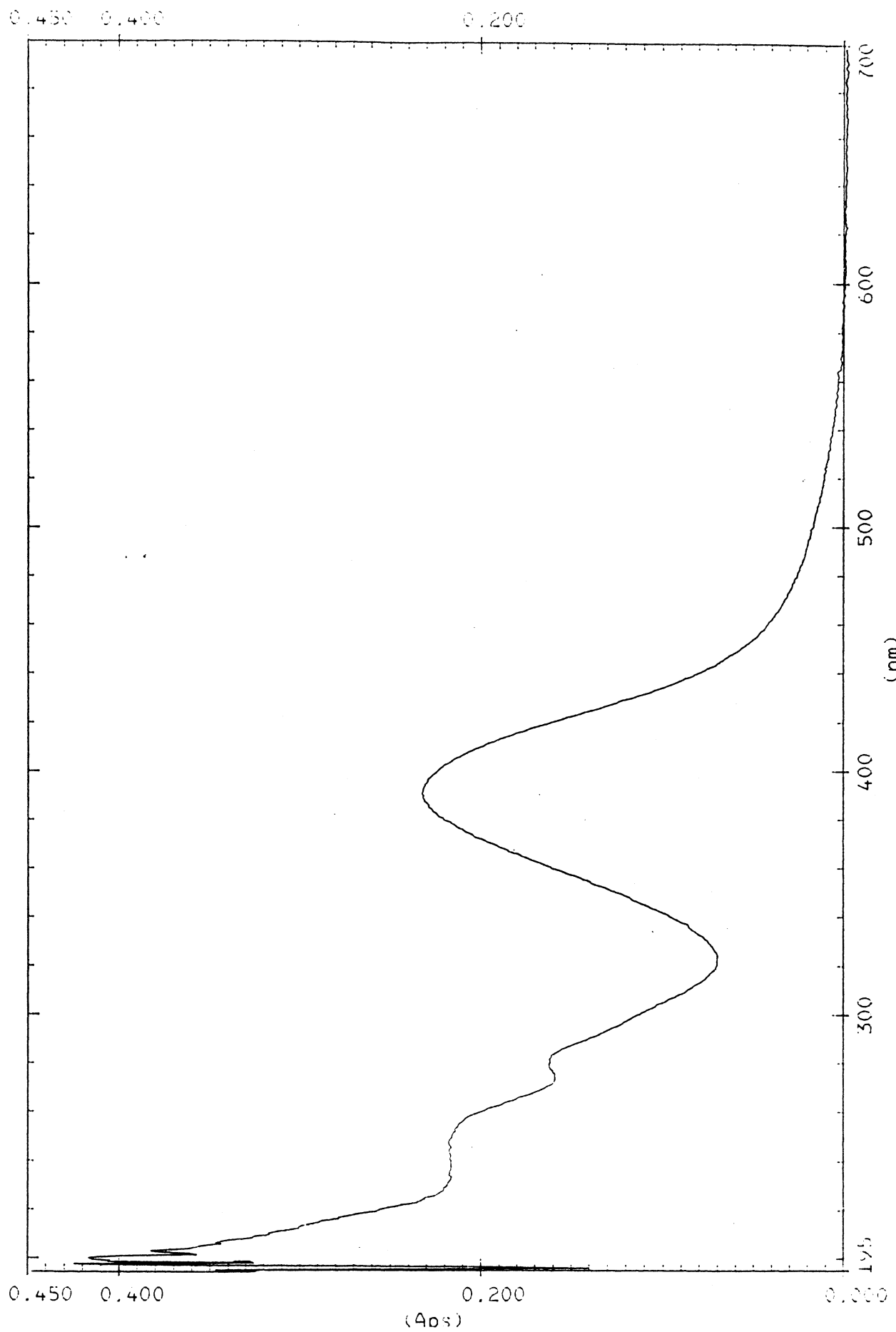


Fig. 3-43 Emission Spectrum of *fac*-Re^I(CO)₃(phen)Cl ($\lambda_{\text{excite}} = 365 \text{ nm}$)

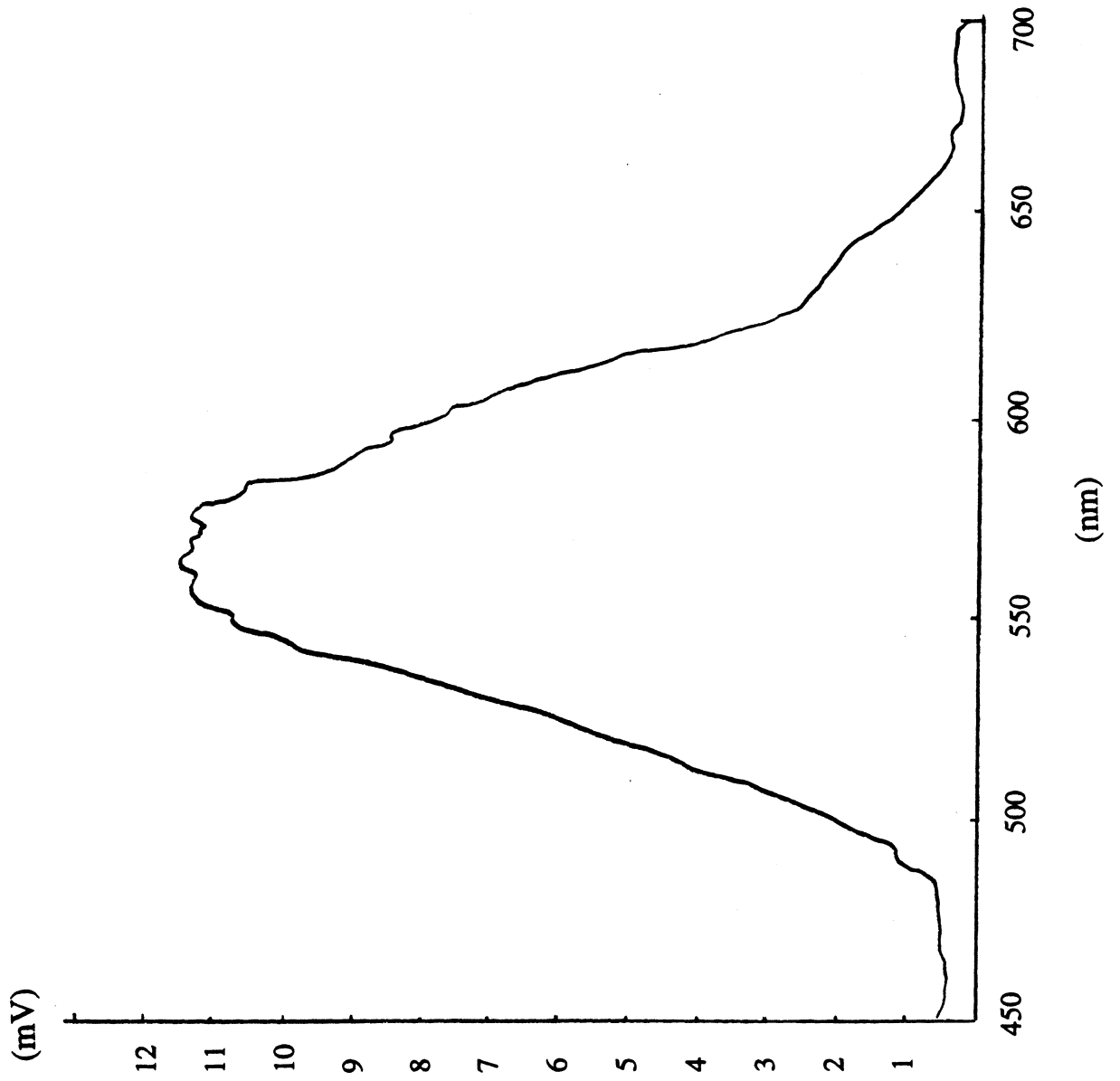
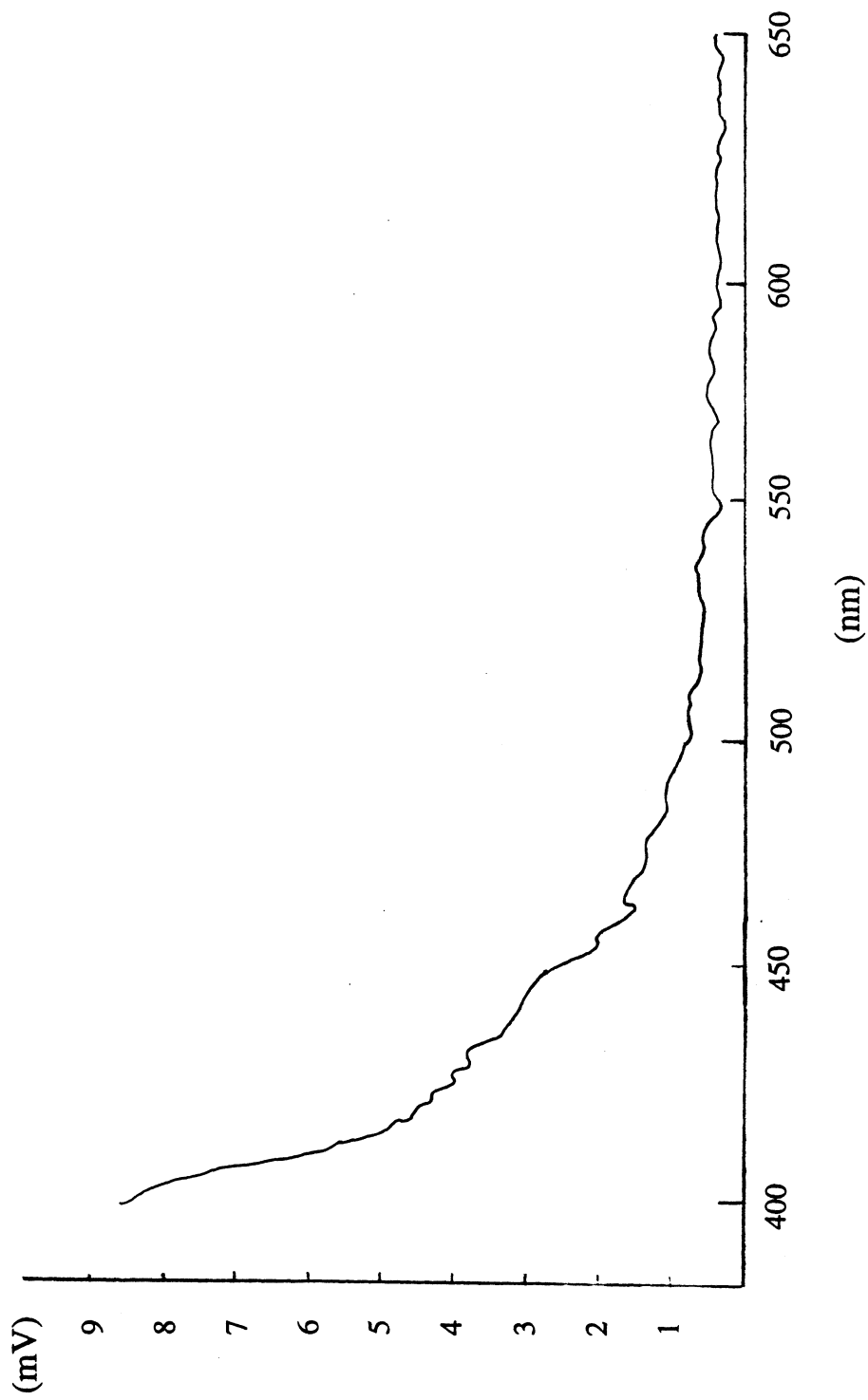


Fig. 3-44 Emission Spectrum of *fac*-Re^I(CO)₃(phen-azo-phenol)Cl ($\lambda_{\text{excite}} = 389 \text{ nm}$)



References:

1. Scandola, F.; Balzani, V. *J. Chem. Educ.* **1983**, *60*, 814.
2. Weller, A. *Pure Appl. Chem.* **1968**, *16*, 115.
3. Kavarnos, G.J.; Turro, N.J. *Chem. Rev.* **1986**, *86*, 401.
4. Balzani, V.; Moggi, L.; Manfrin, M.F.; Boletta, F.; Laurence, G.S. *Coord. Chem. Rev.* **1975**, *15*, 321.
5. Demas, J.N.; Adamson, A.W. *J. Amer. Chem. Soc.* **1973**, *95*, 5159.
6. Sutin, N.; Navon, G. *Inorg. Chem.* **1974**, *13*, 2976.
7. Creutz, C.; Sutin, N. *Proc. Natl. Acad. Sci., USA* **1975**, *72*, 2858.
8. Hawecker, J.; Lehn, J.M.; Ziessel, R. *J. Chem. Soc.* **1983**, 536.
9. Hawecker, J.; Lehn, J.M.; Ziessel, R. *Chem. Commun.* **1985**, 56.
10. Roffia, S.; Marcaccio, M.; Paradisi, C.; Paolucci, F.; Balzani, V.; Denti, G.; Serroni, S.; Campagna, S. *Inorg. Chem.* **1993**, *32*, 3003.
11. Turro, C.; Bossmann, S.H.; Leroi, G.E.; Barton, J.K.; Turro, N.J. *Inorg. Chem.* **1994**, *33*, 1344.
12. Holmlin, R.E.; Barton, J.K. *Inorg. Chem.* **1995**, *34*, 7.
13. Krotz, A.H.; Barton, J.K. *Inorg. Chem.* **1994**, *33*, 1940.
14. Kalyanasundaram, K. *Photochemistry of Polypyridine and Porphyrin Complexes*; Academic Press: London, 1992, and references therein.
15. Belser, P.; Von Zelewsky, A.; Juris, A.; Tucci, A.; Balzani, V. *Chem. Phys. Lett.* **1982**, *89*, 101.
16. Barigelletti, F.; Belser, P.; Von Zelewsky, A.; Balzani, V. *J. Phys. Chem.* **1985**, *89*, 3680.
17. a) Balzani, V.; Scandola, F. *Supramolecular Photochemistry*; Horwood: Chichester, 1990.
b) Balzani, V.; Sabbatini, N.; Scandola, F. *Chem. Rev.* **1986**, *86*, 319.
18. a) Ruminski, R.R.; Petersen, J.D. *Inorg. Chem.* **1982**, *21*, 3706.

- b) Sahai, R.; Rillema, D.P.; Shaver, R.; Van Wallendael, S.; Jackman, D.C.; Boldaji, M. *Inorg. Chem.* **1989**, *28*, 1022.
- c) Sai, R.; Morgan, L.; Rillema, P. *Inorg. Chem.* **1988**, *27*, 3495.
19. Anderson, P.A.; Strouse, G.F.; Treadway, J.A.; Keene, F.R.; Meyer, T.J. *Inorg. Chem.* **1994**, *33*, 3863.
20. Mabrouk, P.A.; Wrighton, M.S. *Inorg. Chem.* **1986**, *25*, 526.
21. a) Hanazaki, I.; Nagakura, S. *Inorg. Chem.* **1969**, *8*, 648.
 b) Gondo, Y., *J. Chem. Phys.* **1964**, *41*, 3928.
22. Kalyanasundaram, K.; Kiwi, J.; Grätzel, M. *Helv. Chim. Acta.* **1980**, *62*, 2720.
23. a) Weber, G.Z. *Phys. Chem.* **1962**, *218*, 204.
 b) Day, P.; Sander, N.J. *J. Chem. Soc. (A)*, **1967**, 1530.
24. Staal, L.H.; Stufkens, D.J.; Oskam, A. *Inorg. Chim. Acta* **1978**, *26*, 255.
25. Ernst, S.; Kaim, W. *Angew. Chem., Int. Ed. Engl.* **1985**, *24*, 430.
26. Nasielski-Hinkens, R.; Benedek-Vamous, M.; Maetens, D.; Nasielski, J. *J. Organomet. Chem.* **1981**, *217*, 179.
27. Hughes, E. D.; Ingold, C. K.; and Ridd, J. H. *J. Chem. Soc.* **1958**, 58.
28. Zollinger, H. *Color Chemistry*; VCH Publishers: Weinheim, 1987, and references therein.
29. Van Wallendael, S.; Shaver, R.J.; Rillema, D.P.; Yoblinski, B.J.; Stathis, M.; Guarr, T.F. *Inorg. Chem.* **1990**, *29*, 1761.
30. Yoblinski, B.J.; Stathis, M.; Guarr, T.F. *Inorg. Chem.* **1992**, *31*, 5.
31. Hart, H.; Craine, L.E. *Laboratory Manual-Organic Chemistry*; Houghton Mifflin Company: Boston, 1991; p. 228.
32. Dean, J.A. *Lange's Handbook of Chemistry*; McGraw-Hill Inc.: New York, 1992.
33. Saeva, F.D. *J. Org. Chem.* 1971, **24**, 3842.
34. Silverstein, R.M.; Bassler, G.C., Morrill, T.C., *Spectrometric Identification of Organic Compounds*; John Willey: New York, 1991.
35. Bellmann, L.T. *The Infra-Red Spectra of Complex Molecules*, John Willey: New York, 1954.

36. Black, K.J.; Huang, H.; Starks, L.; Olson, M.; McGuire, M.E. *Inorg. Chem.* **1993**, *32*, 5591.
37. Wrighton, M.; Morse, D.L. *J. Am. Chem. Soc.* **1974**, *96*, 998.
38. Bryant, G.M.; Fergusson, J.E.; Powell, K.J. *Aust. J. Chem.* **1971**, *24*, 257.
39. Smith, G.F.; Gagle, F.W. *J. Org. Chem.* **1947**, *12*, 781.
40. Reeves, R.L.; Kaiser, R.S.; Finley, K.T. *J. Chromatog.* **1970**, *47*, 217.
41. Zollinger, H. *Azo and Diazo Chemistry*; Interscience, New York, 1961, and references therein.
42. Tanner, C. *Spectrochim. Acta* **1959**, *15*, 20.
43. Wallendael, S.V.; Shaver, R.J.; Rillema, P.; Yoblinski, B.J.; Stathis, M.; Guarr, T.F. *Inorg. Chem.* **1990**, *29*, 1761.
44. Hadzi, D. *J. Chem. Soc.* **1956**, 2143.
45. Original 5-NO₂-phen preparation taken from: Amouyl, E.; Homso, A.J. *J. Chem. Soc. Dalton Trans.* **1990**, 1841.